Functional analysis of FLOWERING LOCUS T (FT)-interacting proteins in citrus

（カンキツにおける FLOWERING LOCUS T (FT)相互作用タンパク質の機能解析）

NAZMUL HASAN

(ナズムル　ハサン)

2023

Functional analysis of FLOWERING LOCUS T (FT)-interacting proteins in citrus

（カンキツにおける FLOWERING LOCUS T(FT)相互作用タンパク質の機能解析）

by

NAZMUL HASAN

(ナズムル　ハサン)

2023

A dissertation submitted in partial fulfillment of the requirements
for the degree of Doctor of Philosophy in Agricultural Science

The United Graduate School of Agricultural Sciences
Kagoshima University, Kagoshima
Saga University, Saga, Japan
September 2023

DECLARATION

A dissertation entitled "**Functional analysis of FLOWERING LOCUS T(FT)-interacting proteins in citrus**" submitted to the United Graduate School of Agricultural Sciences, Kagoshima University, Japan, prepared and submitted by **Nazmul Hasan** in partial fulfillment of the requirements for the degree of Doctor of Philosophy in Agricultural Science is hereby accepted on the recommendation of:

Dissertation evaluation committee members

(Dr. Nobuhiro Kotoda)
Professor
Laboratory of Fruit Science
Faculty of Agriculture
Saga University, Saga, Japan
(Major Advisory Supervisor)

(Dr. Masashi Yamamoto)
Professor
Laboratory of Fruit Science
Faculty of Agriculture
Kagoshima University, Kagoshima, Japan
(Vice Advisory Supervisor)

(Dr. Satoshi Watanabe)
Associate Professor
Laboratory of Plant Breeding and Genetics
Faculty of Agriculture
Saga University, Saga, Japan
(Vice Advisory Supervisor)

(Dr. Kanji Ishimaru)
Professor
Laboratory of Plant Metabolism Analysis
Faculty of Agriculture
Saga University, Saga, Japan
(Vice Advisory Supervisor)

(Dr. Sho Nishida)
Associate Professor
Laboratory of Plant Nutrition
Faculty of Agriculture
Saga University, Saga, Japan
(Vice Advisory Supervisor)

ABSTRACT

FLOWERING LOCUS T (FT) acts as a transmissible floral inducer and can interact with other transcription factors (TFs) throughout the flowering system in *Arabidopsis*. In this study, two putative citrus orthologs of *VASCULAR PLANT ONE-ZINC FINGER1* (*VOZ1*) and *VOZ2*, *CuVOZ1* and *CuVOZ2*, and two *FT*-like genes, *CuFT1* and *CuFT3*, were isolated from the Satsuma mandarin (*Citrus unshiu* Marc.) 'Aoshima'. Protein-protein interaction was confirmed between CuVOZs and CuFTs in the Y2H system. N-terminal 400 amino acids of CuVOZ1, consisting of three motifs: domain of unknown function 4749 (DUF4749), no apical meristem (NAM), and zinc coordination motif, were assumed to be involved in the CuVOZ1–CuFT1 and CuVOZ1–CuFT3 complexes. NAM and zinc coordination motifs were identified within the N-terminal 400 amino acids of CuVOZ2. Docking simulation suggested that three motifs in CuVOZ1 participated in the interaction of the CuVOZ1-CuFT1 complex. Only the zinc coordination motif region of CuVOZ1 was possibly involved in the interaction of CuVOZ1-CuFT3 complex. The same motif region in CuVOZ2 was involved in CuVOZ2-CuFT1 and CuVOZ2-CuFT3 complexes. The phosphatidylethanolamine-binding protein (PBP) motif in exon 4 of CuFTs was predicted to be crucial for the interaction between CuVOZs and CuFTs. The distance between the amino acid residues involved in docking was varied in CuVOZs-CuFTs complexes. The distances were predicted to be from 2.69 to 3.37 Å in CuVOZ1–CuFTs complexes and from 1.09 to 4.37 Å in CuVOZ2–CuFTs complexes, respectively, suggesting that the forces between CuVOZs and CuFTs in the CuVOZs–CuFTs complexes were weak Van der Waals forces. However, one associated pair (CuVOZ2 Ser200 – CuFT3 Pro113) suggested the formation of a hydrogen bond. Cys218, Cys223, Cys237, and His241 in CuVOZ1 and Cys216, Cys221, Cys235, and His239 in CuVOZ2 were suggested to bond with a Zn^{2+} in the Zn coordination motif region. Ectopic expression of *CuVOZ1* and *CuVOZ2* affected the morphology of transgenic *Arabidopsis*. Unlike 35SΩ:*CuVOZ1,* 35SΩ:*CuVOZ2* affected the flowering time, length of inflorescence, and the number of siliques in *Arabidopsis*. These results indicate that *CuVOZ1* might be involved in a trigger for early flowering and in the elongation and branching of the inflorescence. On the other hand, *CuVOZ2* might regulate both vegetative and reproductive development, act as a trigger for early flowering, and be involved in the elongation of inflorescence.

ABBREVIATIONS

Abbreviation	Elaboration
%	Percentage
°C	Degree Celsius
3-AT	3-amino-1,2,4-triazole
5FOA	5-fluoroorotic acid
aa	Amino acid
ANOVA	Analysis of variance
AP	APETALA
AtFT	*Arabidopsis thaliana FLOWERING LOCUS T*
AtVOZ	*Arabidopsis thaliana VASCULAR PLANT ONE-ZINC FINGER*
BLAST	Basic Local Alignment Search Tool
BFT	*BROTHER OF FT AND TFL*
bp	Base pair
cDNA	Complementary DNA
CEN	*CENTRORADIALIS*
C/I	Chloroform/Isoamyl alcohol (24:1, v/v)
CO	*CONSTANS*
CTAB	Cetyltrimethylammonium bromide
dATP	Deoxyadenosine triphosphate
DAI	Days after incubation
DNA	Deoxyribonucleic acid
E. coli.	*Escherichia coli*
ERK	Extracellular signal-regulated kinases
EtOH	Ethanol
FAOSTAT	The Food and Agriculture Organization Corporate Statistical Database
FLC	*FLOWERING LOCUS C*
FLM	*FLOWERING LOCUS M*
FT	*FLOWERING LOCUS T*
g	Gram
Ga3ox	*GIBBERELLIN 3-OXIDASE*
gDNA	Genomic deoxyribonucleic acid
HPLC	High-performance liquid chromatography
IPTG	Isopropyl-β-D-1-thiogalactopyranoside
K	× 1000
kD	Kilodalton
L	Liter
LB	Luria-Bertani
LFY	*LEAFY*
LD	Long day
MAPK	Mitogen-activated protein kinase
mg	Milligrams
min	Minutes
mL	Milliliter
MMT	Million metric tonne

Abbreviation	Elaboration
MFT	*MOTHER OF FT AND TFL1*
N-J	Neighbor-joining
NGS	Next generation sequencing
PCR	Polymerase chain reaction
P/C	Phenol/Chloroform/Isoamyl alcohol (25:24:1, v/v/v)
PEBP	Phosphatidylethanolamine-binding protein
PHYB	*PHYTOCHROME B*
PIF	*PHYTOCHROME INTERACTING FACTOR*
qRT-PCR	Quantitative RT-PCR
r.t.	Room temperature
RNA	Ribonucleic acid
RAM	Root apical meristem
RKIP-1	Raf-1 kinase inhibitory protein
rpm	Revolutions per minute
RT	Reverse-transcription
RT-PCR	Reverse-transcription polymerase chain reaction
SAM	Shoot apical meristem
SDS	Sodium dodecyl sulfate
SDW	Sterilized distilled water
SQ	Semi-quantitative
SVP	SHORT VEGETATIVE PHASE
Taq polymerase	Thermus aquaticus polymerase
TE	Tris EDTA
TFL1	*TERMINAL FLOWER 1*
TSF	*TWIN SISTER OFF*
USDA	United States Department of Agriculture
UV	Ultraviolet
µL	Microliter
µm	Micrometer
µM	Micromolar
VOZ	*VASCULAR PLANT ONE ZINC-FINGER*
Y2H	Yeast two-hybrid

LIST OF TABLES

LIST OF FIGURES

LIST OF CONTENTS

Chapter 1

General Introduction

1.1. General Introduction

Citrus is a commonly cultivated worldwide popular fruit. In 2022 the total citrus production, including oranges, mandarin, tangerine, grapefruits, lemons, and limes, was 102.9 million metric tonnes (MMT), whereas Japan alone produced 0.924 MMT of tangerines/mandarins (USDA, 2022). Perennial woody fruit trees have a very long juvenile period, ranging from five to 10 years for citrus, depending on the genetic background of the species. The long juvenile phase impairs The breeding, genetic studies, and production of citrus (Hackett, 2011; Krajewski and Rabe, 1995). Such juvenile nature hinders efficient breeding, and if the mechanism of shortening the juvenile period and flower bud formation progresses, it can be expected to be applied to accelerate the development of new cultivars and improve production efficiency.

Flowering in higher plants is controlled by various factors such as photoperiod and temperature. Vernalization can promote the flowering of auxotrophic plants that require exposure to low-temperature. Without this low-temperature treatment, flowering is significantly delayed (Wilkie et al., 2008). In *Arabidopsis thaliana*, five known flowering-promoting regulatory pathways are the photoperiod-dependent pathway, the autonomous pathway, the vernalization-dependent pathway, the gibberellin (GA)-dependent pathway, and the thermosensory pathway (Balasubramanian et al., 2006; Blázquez et al., 2003; Komeda, 2004; Lee et al., 2013; Levy and Dean, 1998; Lutz et al., 2017; Mouradov et al., 2002; Posé et al., 2013; Simpson and Dean, 2002; Sureshkumar et al., 2016; Wilkie et al., 2008)

The photoperiod-dependent pathway is related to the promotion of flowering under long-day conditions. The transcription factor (TF) CONSTANS (CO) is regulated by red photoreceptors (phytochrome) and blue photoreceptors (cryptochrome) via the biological clock, leading to transcriptional regulation. The autonomous and vernalization-dependent pathways

converge through the flowering suppressor gene *FLOWERING LOCUS C.* The gibberellin-dependent pathway comprises a group of genes involved in gibberellin synthesis and signal transduction. A temperature-dependent promotion pathway competitively interacts with *SHORT VEGETATIVE PHASE* (*SVP*) to affect flowering time in an antagonistic manner through the accumulation of two *FLOWERING LOCUS M* (*FLM*) splicing variants at different temperatures (Lee et al., 2013; Lutz et al., 2017; Posé et al., 2013; Sureshkumar et al., 2016). Although each of these pathways is independent, signals from these pathways might integrate to cause flowering.

The *TFL1/FT* family encodes a small, soluble, globular, mobile protein similar to phosphatidylethanolamine binding domain protein (PEBP) of approximately 23 kD (Kardailsky et al., 1999; Kobayashi et al., 1999). The Raf-1 kinase inhibitory protein (RKIP-1), a member of PEBP, is expressed in many mammalian tissues and inhibits the mitogen-activated protein kinase (MAPK) pathway by inhibiting the phosphorylation of ERK kinase (MEK). This kinase activates the extracellular signal-regulated kinases (ERK) by Raf1 (Trakul and Rosner, 2005). *FLOWERING LOCUS T* (*FT*), *TWIN SISTER OF FT* (*TSF*), *TERMINAL FLOWER 1* (*TFL1*), *MOTHER OF FT AND TFL1* (*MFT*), *BROTHER OF FT AND TFL1* (*BFT*) and *CENTRORADIALIS* (*CEN*) have been identified as members of the *TFL1/FT* family in *Arabidopsis*. *FT* is considered a flowering-promoting gene and is positively regulated by CO downstream of the photoperiod-dependent promoting pathway (An et al., 2004; Kardailsky et al., 1999; Kobayashi et al., 1999; Koornneef et al., 1991; Samach et al., 2000). Overexpression of *APETALA1* (*AP1*) or *LEAFY* (*LFY*) in *Arabidopsis* also promotes flowering (Mandel and Yanofsky, 1995; Weigel and Nilsson, 1995). *FT* mRNA is expressed in the leaf phloem, but only the protein translocates through the vascular bundle to the shoot apex. There, it forms a complex with the basic leucine zipper (bZIP) transcription factor FD to induce flowering (Abe et al., 2005; Andrés and Coupland, 2012; Jaeger and Wigge, 2007; Mathieu et al., 2007;

Notaguchi et al., 2008; Zeevaart, 2008). On the other hand, *TFL1* maintains the inflorescence meristem and delays flowering by suppressing *AP1* and *LFY* (Ratcliffe et al., 1999). In addition, *tfl1* mutants show phenotypes similar to those with overexpression of *FT* or *AP1* (Bradley et al., 1997; Kardailsky et al., 1999; Kobayashi et al., 1999; Shannon and Meeks-Wagner, 1993). Wheat *MFT* is involved in germination and the regulation of seed dormancy and is expressed in the scutellum and root sacs of seeds (Nakamura et al., 2011). In *Arabidopsis*, the *MFT*-deficient mutant does not delay flowering, but when overexpressed, it shows early flowering, suggesting that it also functions as a flowering-promoting gene (Yoo et al., 2004). Both *BFT* and *TFL1* have the function of delaying flowering, and *BFT* is expressed in axillary meristems and vascular bundles. Increased *BFT* expression suppresses the development of axillary inflorescence and delays the termination of primary inflorescence. On the other hand, low expression of *BFT* is thought to enhance axillary development and increase the number of axillary inflorescences. In addition, *BFT* expression is enhanced by abiotic stresses such as drought and salt, and it has been suggested that especially under salt stress, *BFT* competes with *FT* and *BFT* interacts with *FD* to delay flowering (Ryu et al., 2014; Yoo et al., 2010). *CEN* delays flowering in *Arabidopsis thaliana* and exhibits a phenotype similar to that of *TFL1*.

Since herbaceous, woody plants, evergreens, and deciduous trees have different life cycles, it is thought that the functions of the *TFL1/FT* family also differ. Studies in poplar trees have suggested a relationship between *FT* and dormancy, reporting a gradual but dramatic rise in *FT* expression during dormancy and a decline shortly after shoot emergence (Rinne et al., 2011). In the case of citrus, trifoliate oranges transfected with the *FT* homologous gene (*CiFT*) of mandarin orange flowered in less than a year (Endo et al., 2005). In addition, *CiFT* is expressed not only in leaves and stems but also in developed fruits, and the function of *CiFT* expressed in fruits has not been elucidated (Nishikawa et al., 2007). Introduction of apple *FT* (*MdFT*) or poplar *FT* homolog (*PnFT*) into *Arabidopsis* or apple showed early flowering

(Igasaki et al., 2008; Kotoda et al., 2010). On the other hand, the introduction of apple *TFL1* (*MdTFL1*) and *MdCEN* into *Arabidopsis* showed delayed flowering (Kotoda and Wada, 2005; Mimida et al., 2009), and the introduction of the *MdTFL1* into apple resulted in flowering within one year after acclimatization (Kotoda et al., 2006). In *Arabidopsis* transformants into which the *MdCEN* promoter region was introduced, promoter activity was confirmed in the meristems of the roots and leaves of young seedlings, and in the hypocotyls, suggesting that it is involved in meristematic development and branching (Mimida et al., 2009).

In recent years, the relationship between flowering and ascorbic acid has also been reported. Four ascorbate-deficient *Arabidopsis* mutants, *vtc1*, *vtc2*, *vtc3*, and *vtc4*, showed altered gene expression of photoperiod-dependent [*GIGANTIA*(*GI*)*, CO, FT*] and autonomous (*FLC*) pathways with an early flowering phenomenon (Kotchoni et al., 2009). The *VTC1* gene encodes the GDP-D-mannose pyrophosphorylase, and the *VTC4* gene encodes the L-Galactose-1-P phosphatase (Conklin et al., 1999, 2006; Laing et al., 2004). In addition, the *VTC2* gene has been identified as a GDP-L-galactose phosphorylase/L-galactose guanyltransferase (Laing et al., 2007; Linster et al., 2007; Smirnoff et al., 2007), but the *VTC3* gene has not yet been identified. Not contrary to the deletion, artificially increasing the ascorbic acid content of wild-type *Arabidopsis* delayed flowering (Kotchoni et al., 2009). In addition, it has been reported that the expression of *VTC1* increases when exposed to high-intensity light but hardly decreases when exposed to darkness (Yabuta et al., 2007).

There have already been reports of protein-protein interactions involving FT-like proteins with 14-3-3-like proteins and a bZIP transcription factor, SELF-PRUNING G-BOX (SPGB) (Taoka et al., 2011). FT and TSF alter florigen activity in the axillary buds to delay the floral transition of axillary meristem via interacting with BRANCHED1 (BRC1) but not TFL1 (Niwa et al., 2013). According to reports, FT-INTERACTING PROTEIN 1 (FTIP1)

interacts with FT in phloem companion cells, facilitating the FT protein movement from companion cells to sieve elements (Liu et al., 2012). The protein-protein interaction between SODIUM POTASSIUM ROOT DEFECTIVE 1 (NaKR1) and FT *in vivo* mediates leaf-to-shoot apices translocation of FT through the phloem stream (Zhu et al., 2016). Furthermore, FT and FD demonstrated stable interaction in the Y2H and bimolecular fluorescence complementation (BiFC) studies. At the shoot apical meristem (SAM), FT interacts with FD and promotes the transcription of floral meristem identification genes (Abe et al., 2005; Wigge et al., 2005). Apple VASCULAR PLANT ONE-ZINC FINGER (VOZ)-like family protein, MdVOZ1a, interacts with MdFT1 and MdFT2 in the Y2H system, and the protein is suggested to be involved in the development of reproductive organs (Mimida et al., 2011). The transcriptional regulation of *FT* is illustrated in Figs. 1-1 and 1-2.

VOZs (VOZ1 and VOZ2) have crucial roles in the flowering of *Arabidopsis* and abiotic stress-signaling pathways, as well as in the plant's reaction to drought, cold, heat, and salt stresses (Koguchi et al., 2017; Mitsuda et al., 2004; Nakai et al., 2013a; Prasad et al., 2018; Song et al., 2018). Two proteins act redundantly as positive regulators of plant responses to fungal or bacterial infection and heat stress but as negative regulators of cold and drought stress. The transcriptional activators VOZ1 and VOZ2 are members of the NAC family of subgroup VIII-2 and include a zinc finger motif (Jensen et al., 2010; Mitsuda et al., 2004). VOZs alter the function of the CO, thus contributing to the promotion of *FT* expression and photoperiodic flowering. Additionally, *FLC* is repressed by VOZs independently, and VOZs activate *FT* during flowering (Koguchi et al., 2017; Kumar et al., 2018; Nakai et al., 2013b, 2013a; Song et al., 2018; Yasui et al., 2012; Yasui and Kohchi, 2014).

Previous studies confirmed that VOZ homologs in apple interact with FT1 *in vivo* with a yeast two-hybrid (Y2H) system. The outline of Y2H is illustrated in fig. 1-3. The mechanism

by which the VOZs interact with FT and control flowering/fruiting is not well known in fruit trees like citrus. Therefore, two *VOZs* (*CuVOZ1* and *CuVOZ2*) and two *FTs* (*CuFT1* and *CuFT3*) genes were isolated from the Satsuma mandarin 'Aoshima' to authenticate the protein-protein interaction between CuVOZs with CuFTs by Y2H system. Furthermore, the characteristics of *CuVOZ1* were elucidated by using transgenic *Arabidopsis*, deletion mutants in the Y2H system, and docking simulation. The flow chart of the work procedure is illustrated in Fig. 1-4.

The objectives of the study were-

1. To identify the TF proteins that interact/bind with FTs in citrus using a Y2H system.
2. To elucidate the binding mechanism between FTs and VOZs.
3. To elucidate the molecular network of FT in Citrus.
4. To analyze the functions of FT interacting genes (*CuVOZ1* and *CuVOZ2*) with a transgenic experiment.

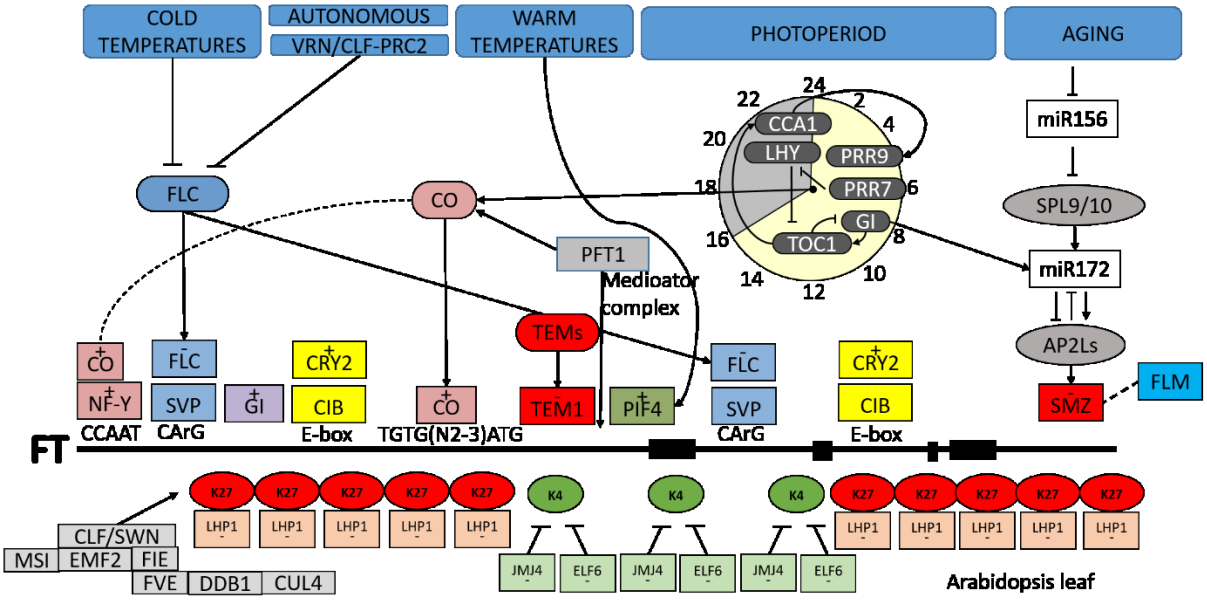

Fig. 1-1. Transcriptional regulation of FT in *Arabidopsis* leaf [reviewed by Pin and Nilsson (2012)]. *FT* expression is promoted by CO, CO/NF-Y complex, CRYPTOCHROME 2/CRYPTOCHROME-INTERACTING bHLH complex (CRY2/CIB), PHYTOCHROME INTERACTING FACTOR 4 (PIF4), GIGANTEA (GI) and mediator complex (Iñigo et al., 2012; Kumar et al., 2012; Liu et al., 2008; Sawa and Kay, 2011; Tiwari et al., 2010). FT expression is balanced by the repressive transcriptional activity of FLC/SVP, TEM1, and SMZ (Castillejo and Pelaz, 2008; Li et al., 2008; Mathieu et al., 2009). H3K27me3 (K27) deposition involving LHP1, CURLY LEAF (CLF)-containing polycomb repressive complex 2 (PRC2)-like complex and CUL4-DDB1FVE complex also regulates *FT* transcription (Adrian et al., 2010; Jiang et al., 2008; Pazhouhandeh et al., 2011). H3K4me3 (K4) is, in contrast to K27, an active mark that is negatively regulated by at least two K4 demethylases, JMJ4 and EARLY FLOWERING 6 (ELF6) (Jeong et al., 2009). An unknown WEREWOLF (WER) cofactor can stabilize FT mRNAs (Seo et al., 2011). Ovals and rectangles represent genes and proteins, respectively. '+' and '-' represent activating and repressing action.

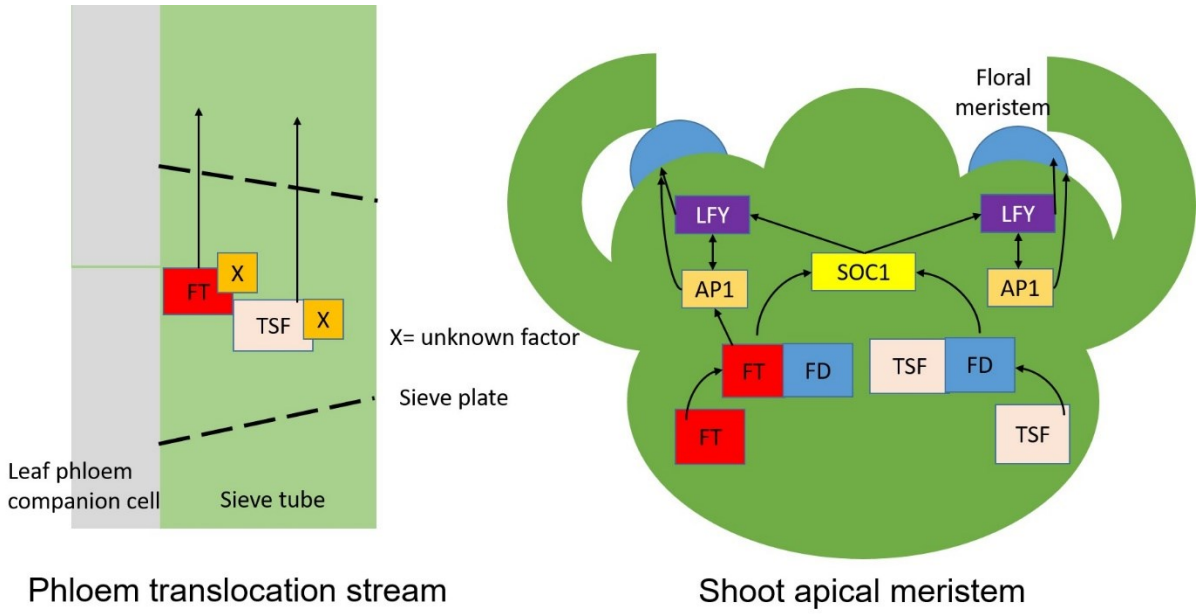

Fig. 1-2. Long-distance transport of FT toward the phloem up to shoot apical meristem. FT is unloaded from the phloem and transported to the apex, which probably involves cell-to-cell transport through plasmodesmata. The green area indicates a possible FT and TSF protein distribution gradient in the shoot apical meristem. Induction of SUPPRESSOR OF OVEREXPRESSION OF CONSTANS1 (SOC1) is the first detectable event in the inflorescence meristem. SOC1 depends on the presence of FT and the bZIP transcription factor FD. FT and FLOWERING LOCUS D (FD) interact physically, and the complex is directly involved in APETALA 1 (AP1) transcriptional activation. AP1 directly represses SOC1 in the floral meristem (Abe et al., 2005; Wigge et al., 2005). Ovals and rectangles represent genes and proteins, respectively. '+' and '-' represent activating and repressing action.

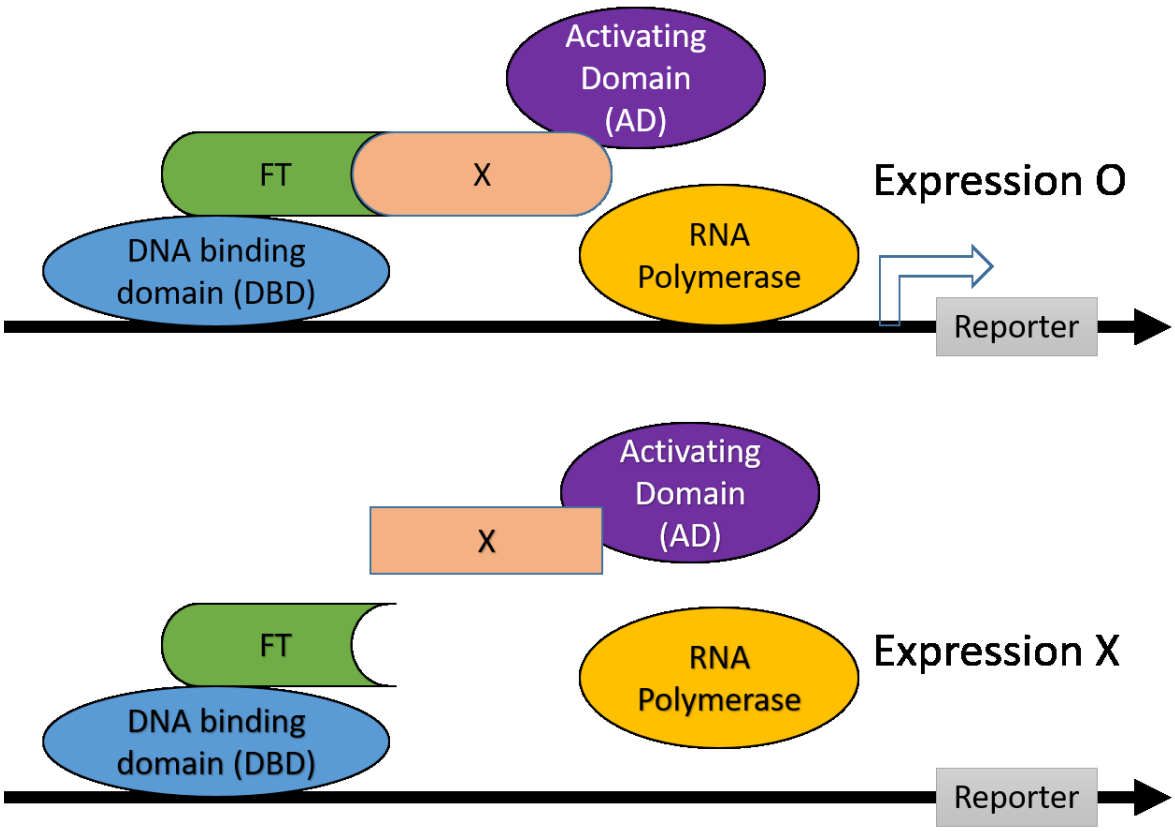

Fig. 1-3. A typical yeast two-hybrid system. *LacZ*, *HIS3*, or *URA3* are used as reporter genes in this system. The reporter genes are expressed if the target proteins interact with each other. Transformed yeast cells with positive protein-protein interaction exhibit indigo coloration in β-galactosidase assay due to the expression of *LacZ*. The yeast cells can survive in the synthetic defined (SD) media lacking histidine because of *HIS3*. The strength of the interaction is checked using 25 mM 3-Amino-1,2,4-triazole (3AT), a competitive inhibitor of imidazole glycerol-phosphate dehydratase at the 6th step of histidine production in the yeast cell. The positively interacted yeasts can survive in the SD media lacking uracil because of the *URA3* gene. The yeast cells are suppressed if 5-fluoro-2,6-dioxo-1,2,3,6-tetrahydro-4-pyrimidinecarboxylic acid (5FOA) is used. *URA3* encodes orotidine 5'-phosphate decarboxylase (ODCase). Active ODCase converts 5FOA into the toxic compound 5-fluorouracil, which is the cause of the suppression of interactive colonies.

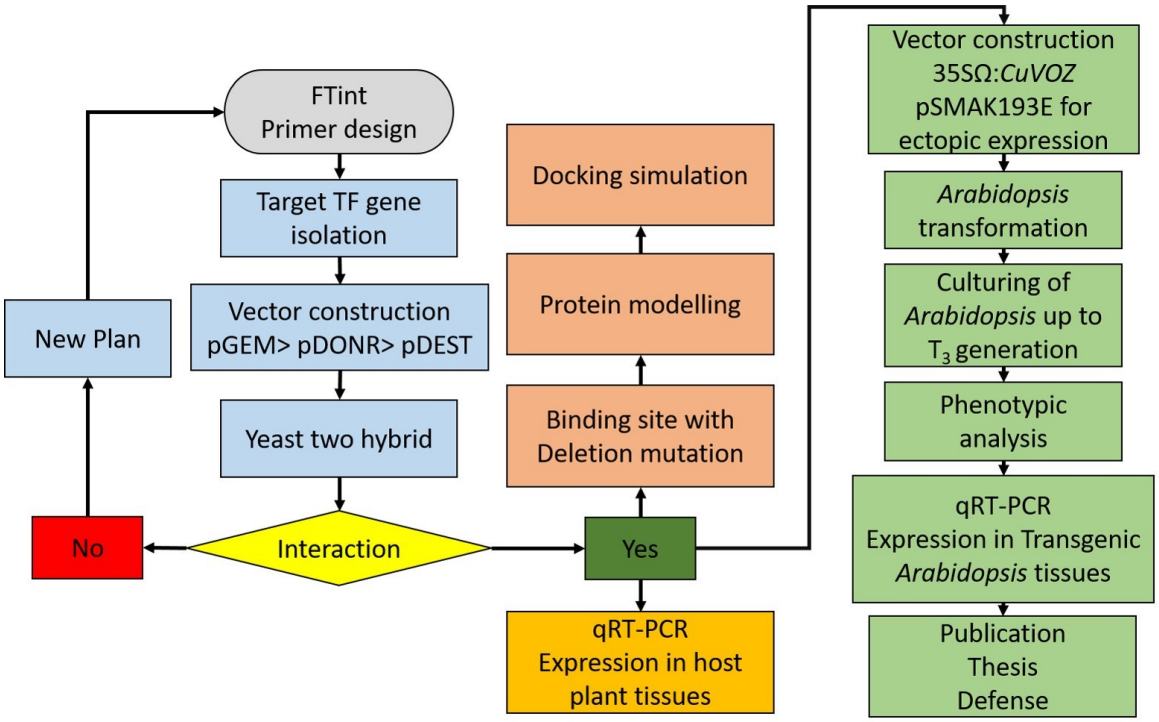

Fig. 1-4. Flow chart of the work procedures followed in the study.

Chapter 2

Citrus VASCULAR PLANT ONE-ZINC FINGER1 (VOZ1) interacts with CuFT1 and CuFT3, affecting flowering in transgenic *Arabidopsis*

2.1. Introduction

Citrus is an important commercial fruit crop with an annual production of 143.76 million tonnes worldwide (FAO, 2021). The crucial impairment in breeding, genetic studies, and production in citrus is the long juvenile phase, which usually lasts five to 10 years, depending on the genetic background of the species (Hackett, 1985; Krajewski and Rabe, 1995). The biennial-bearing habit is another problem in citriculture (Moss, 1971). Elucidation of the molecular mechanism during the transition from the juvenile to the adult phase and that from the vegetative to the reproductive phase would provide insight into the means to accelerate breeding and understanding biennial bearing, respectively.

Abundant experimental evidence from model plants such as *Arabidopsis* has suggested that *FLOWERING LOCUS T* (*FT*) acts as a floral integrator in photoperiod and vernalization pathways. FT encodes a small, globular protein similar to the phosphatidylethanolamine-binding protein (PEBP) and the Raf-1 kinase inhibitor protein (Kardailsky et al., 1999; Kobayashi et al., 1999) and acts as a transmissible floral inducer, such as florigen (Corbesier et al., 2007; Jaeger and Wigge, 2007; Lin et al., 2007; Mathieu et al., 2007; Notaguchi et al., 2008). Synthesis of FT is promoted by photoperiodic induction through the zinc finger protein, CONSTANS (CO), in companion cells of the leaf phloem at dusk (Andrés and Coupland, 2012; Koornneef et al., 1991; Lifschitz et al., 2006; Liu et al., 2013; Mathieu et al., 2007; Putterill and Varkonyi-Gasic, 2016; Samach et al., 2000; Wigge, 2011). FT then translocates into the sieve tube system, moves to the shoot apical meristem (SAM), and forms a complex with transcription factor (TF) proteins (Abe et al., 2005; An et al., 2004; Corbesier et al., 2007; Jaeger and Wigge, 2007; Lin et al., 2007; Tamaki et al., 2007; Wigge et al., 2005). The complex at the SAM induces expression of the downstream floral meristem identity genes, thereby promoting flowering (Ferrándiz et al., 2000; Mandel and Yanofsky, 1995; Weigel et al., 1992).

In the vernalization pathway, *FT* is repressed by the vernalization integrators of *FLOWERING LOCUS C* (*FLC*) and *LIKE HETEROCHROMATIN PROTEIN1* (*LHP1*)/*TERMINAL FLOWER2* (*TFL2*), a homolog of *HETEROCHROMATIN PROTEIN1* (*HP1*), without exposure to low temperature (Kotake et al., 2003; Michaels and Amasino, 1999; Takada and Goto, 2003). *TERMINAL FLOWER1* (*TFL1*), another member of the PEBP-like gene family, acts as a floral repressor (Bradley et al., 1997; Ohshima et al., 1997). Specific regions within the fourth exon of FT and TFL1 function as a potential ligand-binding pocket, and replacing these regions allows the opposite effects on flowering time (Ahn et al., 2006).

Interactions of FT-like proteins with the proteins that are analogous to 14-3-3 proteins and a bZIP transcription factor, SELF-PRUNING G-BOX (SPGB), have already been reported (Park et al., 2014; Taoka et al., 2011). BRANCHED1 (BRC1) interacts with FT and TSF but not with TFL1 and modulates florigen activity in the axillary buds to prevent premature floral transition of the axillary meristem (Niwa et al., 2013). An endoplasmic reticulum (ER) membrane protein, FT-INTERACTING PROTEIN 1 (FTIP1), interacts with FT in companion cells of the phloem and mediates FT protein movement from companion cells to sieve elements (Liu et al., 2012). SODIUM POTASSIUM ROOT DEFECTIVE 1 (NaKR1) interacts with FT *in vivo,* mediating FT translocation from leaves to shoot apices through the phloem stream (Zhu et al., 2016). Protein-protein interaction was reported between FT and FD in yeast two-hybrid (Y2H) system and in bimolecular fluorescent complementation (BiFC). At the SAM, FT interacts with FD to activate the transcription of floral meristem identity genes (Abe et al., 2005; Wigge et al., 2005). A previous study showed that a TF protein of the VASCULAR PLANT ONE-ZINC FINGER (VOZ)-like family from apple, MdVOZ1a, interacted with MdFT1 and MdFT2 in the Y2H system (Mimida et al., 2011), suggesting the involvement of MdVOZ1a in the development of reproductive organs.

VOZ1 and *VOZ2* have been noted for their involvement in flowering and abiotic stress-signaling pathways in *Arabidopsis* (Mitsuda et al., 2004). VOZs play essential roles in response to drought, cold, heat, and salinity (Koguchi et al., 2017; Nakai et al., 2013a; Prasad et al., 2018; Song et al., 2018). VOZ1 and VOZ2 proteins act as positive regulators of plant responses to biotic stress, such as fungal or bacterial infection, and abiotic stress, such as heat stress; on the other hand, they act as negative regulators of cold and drought stress. In addition, VOZs repress *FLC* independently and activate *FT* to promote flowering. Modulation of the function of the CO protein by VOZs also contributes to promoting FT expression and photoperiodic flowering in *Arabidopsis* (Koguchi et al., 2017; Kumar et al., 2018; Nakai et al., 2013a, 2013b; Song et al., 2018; Yasui et al., 2012; Yasui and Kohchi, 2014). VOZ1 and VOZ2 have a zinc finger motif and transcriptional activator activities and belong to the subgroup VIII-2 of the NAC family in plants (Jensen et al., 2010; Mitsuda et al., 2004).

The mechanism by which the VOZs interact with FT and regulate flowering/fruiting is not entirely understood in fruit trees, such as citrus. In this study, VOZ1 was focused because in a previous study showed that apple VOZ1 (MdVOZ1a) interacted with apple FTs (MdFT1 and MdFT2) in the Y2H system (Mimida et al. 2011). Therefore, one *VOZ* (*CuVOZ1*) and two *FT* (*CuFT1* and *CuFT3*) genes were isolated from the Satsuma mandarin ‘Aoshima’ to authenticate the protein-protein interaction between CuVOZ1 and CuFTs in the Y2H system. Further, the characteristics of *CuVOZ1* were elucidated by using transgenic *Arabidopsis*, deletion mutants in the Y2H system, and docking simulation.

2.2. Materials and Methods

2.2.1. Plant materials

Tissues of the Satsuma mandarin (*Citrus unshiu* Marc.) 'Aoshima' in its adult phase were collected in the experimental field of the Saga Prefectural Fruit Tree Experiment Station in the city of Ogi, Japan. Vegetative [apices (April), new leaves (April), old leaves (August), and stems with a node (August)] and reproductive [flower buds (April), young fruit (May), juice sacs (August and November), and peels (August and January)] tissues were collected in 2018. The juvenile vegetative tissues (roots, stems, leaves, and apices) were collected in August 2019 from 20-month-old seedlings grown at Saga University. Seeds of 'Aoshima' were collected in January 2020. The seed coats were removed from the cotyledons to accelerate germination and nurtured for ten days in dark conditions at 22°C in the incubator (SANYO Electric Co., Ltd., Osaka, Japan) on a sterilized moist filter paper enclosed by a glass petri dish. Sterile distilled water (SDW) was added to moisten the filter paper with the precaution of waterlogging. When the hypocotyl and radicle length grew 1 cm, those were transplanted to the soil and nurtured for several months inside the greenhouse. Before winter, in the last week of October, the seedlings were brought outside to mimic natural growth conditions. Nurturing for 20 months made the plants ready for collecting juvenile tissues.

Transgenic and wild-type (WT) *Arabidopsis thaliana* ecotype Columbia (Col-0) were grown under long-day (LD) conditions (16 h light/8 h dark, cool white fluorescent light, 72.36 μmol m^{-2} s^{-1}) in an incubator (Biotron; Nippon Medical and Chemical Instruments Co., Ltd., Tokyo, Japan) at 22°C. The whole plant was collected for RNA extraction. All collected tissues were immediately frozen with liquid nitrogen and preserved in a freezer at -70°C until further use.

2.2.2. Extraction of gDNA (CTAB)

The gDNA of 'Aoshima' was extracted from new leaves using the cetyltrimethylammonium bromide (CTAB) method. Isolation buffer (IB) 1 µl, 5 µL of 2-mercaptoethanol, and finely ground (in liquid nitrogen) leaf samples were taken in a 1.5 mL tube and tapped vigorously. The tube was kept on ice for 2-3 min and then centrifuged at 13K rpm for 4 min. The supernatant was discarded. Lysis buffer (LB) of 250 µl and 25 µl of 10% n-lauroylsarcosine were added, tapped, and rested for ten minutes. CTAB (2X) (275 µL) was added and incubated with a dry heat bath at 65°C for 10 min. The pressure of the tubes was released every 5 min. Chloroform/Isoamyl alcohol (C/I) 550 µl was added, tapped, and centrifuged at 13K rpm for 10 minutes. The supernatant was collected. This step was repeated two times. After that, 550 µl of isopropanol was added, tapped, and centrifuged at 6K rpm for 5 min. Then, the supernatant was discarded. The pellet was incubated at 37°C for 10 min and dissolved in 100 µl of SDW. The dissolved solution was treated with 1 µl of RNase (10 mg/mL) by incubating for 40-60 minutes at 37°C. The RNase was removed with 100 µl of Phenol/Chloroform (P/C), and the supernatant was collected and treated with 100 µl of C/I. The supernatant was taken in another tube. The pellet was found by adding 10 µl of Sodium acetate, 250 µl of 100% EtOH, and subsequent centrifugation at 13K rpm for 10 min. The supernatant was discarded, and the pellet was washed with 100 µl of 75% EtOH and centrifugation at 13K rpm for 5 min. The supernatant was discarded, the pellet was incubated at 37°C for 8-10 min, and dissolved in 100 µl of SDW. Extracted DNA was preserved at -20°C for future usage.

2.2.3. Extraction of Total RNA (CTAB)

Total RNAs were extracted from various juvenile and adult tissues of Satsuma mandarin 'Aoshima'. The list of tissues and the method of RNA extraction are presented in Table 2-1.

Total RNA was extracted by the CTAB method (Kotoda et al., 2000). CTAB (2×) of 700 μL and 0.5% 2-mercaptoethanol were taken in a 1.5 mL tube. Four tubes were prepared for one sample. The sample was ground in liquid nitrogen; a 0.15 g/tube sample was taken in the prepared tube and incubated at 65°C for 15 minutes. An equal volume of C/I was added, vortexed, and centrifuged at 14K rpm for 10 min at 10°C (Hybrid high-speed refrigerated centrifuge 6200; KUBOTA CORPORATION, Tokyo, Japan). The supernatant was taken to a new tube and treated with C/I one more time. After centrifugation, the supernatant was transferred to a new 1.5 mL tube; ¾ volume of isopropanol was added, left at room temperature for 10 min, and centrifuged. The pellet was dissolved in 100 μL of SDW, ¼ volume of 10 M lithium chloride was added, left at –30°C for 1-2 hours, and centrifuged. The supernatant was removed, and the pellet was dissolved in 100 μL of SDW. Four tubes were merged into one tube and proceeded as 400 μL/tube. An equal volume of P/C was added, vortexed, centrifuged, and the supernatant was transferred to a new 1.5 mL tube. The solution was treated with an equal volume of C/I, and the supernatant was collected in a new tube. Sodium acetate (3M) 1/10th volume and 2.5 volumes of 100% EtOH were added to the supernatant and mixed, and the mixture was kept at –30°C for 10 minutes, centrifuged, and the supernatant was discarded. The pellet was washed with 500 μL of 70% EtOH, centrifuged, and the supernatant was discarded. The pellet was incubated at 37°C for 10 minutes and dissolved in 100 μL of SDW.

SDW of 9 μL was taken to a new 1.5 mL tube and mixed with 1 μL of RNA, and the absorbance was measured with BioSpec-mini (SHIMADZU CORPORATION, Kyoto, Japan). GelRed (Biotium, Inc., Fremont, Calif., USA) of 1 μL, 6 μL of RNA Buffer, and 6 × Loading Buffer were mixed with three μL of the obtained RNA solution and heated at 65°C for 10 minutes, placed on ice for 5 minutes and electrophoresed using a gel for RNA migration to confirm the isolation of RNA. The concentration of RNA was adjusted to 200 ng·μL^{-1}.

2.2.4. RT reaction

RT reaction was performed using ReverTra Ace ® qPCR RT Master Mix FSQ-301 (TOYOBO). Total RNA (0.5µg) isolated from the new leaves of 'Aoshima' was used as a template. The composition of reagents is shown in Table 2-2. The RT products were preserved at -70°C for further usage.

2.2.5. Primer design and synthesis of complementary DNA

The primers for two flowering genes, *CuFT1* and *CuFT3,* used in this study were designed based on *Citrus clementina*. The TF genes were selected based on a previously reported list of TF [No. 1(MDP000029316)] interacting with MdFTs in apple (Mimida et al., 2011) and homologous to 'Aoshima' unshu. Sequence No. 1 was searched in *Citrus clementina* database v1.0 in Phytozome. Two different sequences for No. 1 (indicated as CuVOZ1 and CuVOZ2) were identified from the database. Primer sets were designed to isolate the genes based on *C. clementina* sequences for RT-PCR. The primer set for the isolation of target genes is presented in Table 2-3. The perfect temperature for amplification was identified with gradient temperature using gDNA as a template and subsequent nested PCR. RT products of 'Aoshima' leaves were used to amplify the cDNA of *FT* genes corresponding to *CuFT1*, *CuFT3,* and the TF gene *CuVOZ1* by PCR using KOD-Plus-Neo (TOYOBO). Amplification of the target region was checked with a 10 µL of PCR solution with different combinations of primers and a subsequent nested PCR. The working PCR product was produced with a 50 µL solution. The composition of mixtures during RT-PCR is given in Table 2-4.

2.2.6. Ethanol precipitation

The PCR product was taken in a 1.5 mL tube, and the volume increased to 100 µL with SDW. Glycogen (20 mg/ml) 1 µL was added. Sodium acetate ($NaCH_3COO$ 3M) $1/10^{th}$ volume

and 2.5 × volume of 100% EtOH was added, mixed with a seesaw movement, and then centrifuged at 14.5K rpm for 15 min. The supernatant was discarded, and the tube was dried up, keeping it upside-down on a paper towel. The pellet was washed with 500 µL of 70% EtOH and centrifuged at 14K rpm for 5 min. The supernatant was discarded, and the pellet was incubated at 37°C for 10 min. The pellet was dissolved in 40 µL of SDW.

2.2.7. Addition of nucleotide 'A'

The addition of dATP to the 3' end of the RT-PCR product was performed for TA cloning. For TA cloning, dATP was added to the 3' end of the RT-PCR product. The mixture for A attachment was added to the EtOH precipitated PCR product and incubated at 72°C for 20-30 minutes (Table 2-5).

2.2.8. TA cloning

pGEM®-T Easy Vectors (Promega Corporation, Madison, WI, USA) are linearized vectors containing T7 and SP6 RNA polymerase promoters flanking a multiple cloning region within the α-peptide coding region of the enzyme β-galactosidase with a single 3′-terminal thymidine at both ends. Insertional inactivation of the α-peptide allows the identification of recombinants by blue/white screening on indicator plates.

The agar plates are supplemented with a chromogenic substrate known as X-gal in order to screen for clones that contain recombinant DNA. When β-galactosidase is formed, it hydrolyzes X-gal to 5-bromo-4-chloroindoxyl, which then spontaneously dimerized to create an insoluble blue dye called 5,5'-dibromo-4,4'-dichloro-indigo. As a result, non-recombinant cell colonies look blue, while recombinant cell colonies appear white. This makes it simple to collect and cultivate the required transgenic colonies. For blue/white screening, X-gal is combined with isopropyl -D-1-thiogalactopyranoside (IPTG). IPTG stimulates the expression

of the lacZ gene and is a non-metabolizable analog of galactose. It is to mention that IPTG is not a substrate for -galactosidase; it is merely an inducer. A chromogenic substrate, such as X-gal, is necessary for visual screening.

Insert of 2.5 µL was added to 0.5 µL of vector and an equivalent amount of Ligation Mix (TAKARA BIO) on ice. The reaction mixture was incubated at 16°C for 30 minutes. Previously prepared 100 µL of *E. coli* DH5α competent cells thawed on the ice were added to the reaction solution, and the mixture was kept on ice for 15 minutes and then exposed to heat shock in a water bath (AS ONE) at precisely 42°C for 30 seconds and again returned on ice for 2 min. Super Optimal broth with Catabolite repression (SOC) medium of 500 µL was added and cultured in a bio shaker (TAITEC, M.BR-024) at 37°C for an hour.

A Luria-Bertani (LB) broth agar medium plate containing ampicillin (50 mg/L) was spread with 50 µL of X-gal (5-Bromo-4-chloro-3-indolyl-β-D-galactopyranoside) and 100 µL of Isopropyl-β-Dthiogalactopyranoside (IPTG) and dried up. The cultured cells were plated on the LB plate containing ampicillin, X-gal, and IPTG and incubated for 17 hours at 37°C. Clones of the formed colonies were checked the next day. The colonies were taken with the tip of a sterilized toothpick, suspended in 30 µL of SDW, and then boiled at 98°C for 10 minutes. The boiled product of 0.5 µL was added to the PCR reaction solution. Ex-Taq (TAKARA BIO) was used as a PCR enzyme. PCR was performed according to Table 2-6.

2.2.9. Plasmid extraction (alkaline-SDS method)

2.2.9.1. Liquid culture of selected clones

LB liquid media (2 mL) and specific antibiotics (2 µL) were taken in a test tube. The selected colony was taken with the tip of a sterilized toothpick and cultured overnight in a water bath shaker (TAITEC, PERSONAL-11) at 37°C. When the culture was ready, the culture was

transferred to a 2 mL Eppendorf tube and centrifuged at 13K rpm for 1 min. The supernatant was discarded, and the bacteria pellet was kept for plasmid extraction.

2.2.9.2. Plasmid extraction

The pellet was suspended with 100 µL of solution I [Two mg/ml lysozyme, 50 mM glucose, ten mM EDTA (or CDTA), 25 mM Tris-HCl (pH 8.0), Stirred until completely dissolved]; subsequently, 200 µL of 0.2 N NaOH + 1% SDS solution was added. The tube was kept on ice for 2-5 min. 150 µL of 3 M sodium acetate was added and mixed. After that, 450 µL of P/C was added, vortexed, and centrifuged at 14K rpm for 5 min at r.t. The supernatant was collected in another tube, and an equal volume of C/I was added, vortexed, and centrifuged again. The supernatant was collected in another tube. EtOH (100%) 1 mL was added and mixed by a seesaw move. After centrifugation for 10 min, the supernatant was discarded, and the pellet was washed with 500 µL of 70% EtOH for 2 min. The supernatant was discarded, and the pellet was incubated at 37°C for 8 minutes and then dissolved in 100 µL of SDW. The solution was treated with one µL of 10 $mg \cdot mL^{-1}$ RNase and incubated at 37°C for 1 hour. An equal amount of P/C was added, vortexed, and centrifuged at 13K rpm for 5 min. The supernatant was taken in a new tube. An equal volume of C/I was added, vortexed, centrifuged, and the supernatant was taken in a new tube. After that, $1/10^{th}$ volume of 3M sodium acetate and 2.5 volumes of 100 % EtOH were added, mixed with a seesaw move, and centrifuged at 13K rpm for 10 min. The supernatant was discarded, and the pellet was washed with 500 µL of 70% EtOH (13K rpm, 5 min). The supernatant was discarded, the pellet was incubated at 37°C for 8 min and then dissolved in 100 µL of SDW. The plasmid concentration was measured with a UV-VIS spectrophotometer (BioSpec-mini, SHIMADZU Corporation, Japan). The plasmid was preserved at -20°C for further usage.

2.2.9.3. Plasmid digestion by restriction enzyme

Restriction enzyme treatment was performed on the plasmid to confirm whether the target insert was inserted into the vector. *Apa*I and *Sac*I with L buffer were used to check the constructs of the pGEMT-Easy vector. The enzymatic reaction times were at least 3 hours at 37°C. The mixture of each restriction enzyme was electrophoresed on a 1% agarose gel.

2.2.10. Gel electrophoresis

One µl of reaction mixture was electrophoresed on a 1% agarose gel. Agarose powder 1% and 0.5 × TBE buffer solution was taken in a beaker and heated until the powder was dissolved. The mixture was poured onto a gel tray once it had cooled to around 60°C and submerged a comb in it. The gel was allowed to be set. The solidified gel was dipped in an electrophoresis tank filled with 0.5% TBE buffer. The samples (1 µL) were mixed with a loading buffer (1 µL) containing a tracking dye on a piece of parafilm. The tracking dye helps visualize the progress of the electrophoresis and helps ensure that the samples are loaded evenly. The electrophoresis was done at 100 volts for 30 minutes or 50 volts for 60 minutes. Different ladders of 1Kb, 100 BP, or λ50 were used to check nucleic acid concentration.

2.2.11. Big Dye sequencing of isolated plasmid

The target gene insertion was confirmed by the Big Dye sequence using the constructed plasmid. In order to perform the sequence, the extracted plasmid DNA was adjusted to a concentration of 400 ng·µL^{-1}. Samples were prepared with Big Dye (Thermo Fisher Scientific Inc., Waltham, MA, USA) according to Table 2-7. After completion, the reaction solution was treated with 2.5 µL of stop solution and centrifuged with 30 µL of 100 % EtOH at 3.5K rpm for 30 min. The supernatant was discarded carefully, and the almost invisible pellet was washed with 30 µL of 70% EtOH at the same speed for 15 min. The supernatant was discarded, the

pellet was incubated at 37°C, and then dissolved in 15 µL of HiDi Formamide. The sample was heat denatured at 96°C for 3 minutes and given a cold shock by immediately placed on ice for 5 min. The prepared sequencing products were sequenced with an Applied Biosystems 3130 Genetic Analyzer (Life Technologies Corporation, Carlsbad, Calif., USA). The primer sets used in gene cloning are listed in Table 2-3.

2.2.12. Sequence analysis of isolated plasmid

The data obtained by the Big Dye sequence is converted to Gene Studio™ Professional Edition ver 2.2.0.0 (http://www.genestudio.com) and BioEdit program ver. 7.7.0 (http://www.mbio.ncsu.edu/Bioedit/bioedit), the obtained sequences of *CuVOZ1* were not identical with the sequences deposited in the *C. clementine* genome database.

2.2.13. Renaming of isolated plasmids genes

The cDNA was amplified from the RT product by PCR using KOD Plus Neo (TOYOBO). The amplified PCR products were cloned into pGEM®-T Easy vectors (Promega, Madison, WI, USA) after attachment of the adenine nucleotide. The isolated genes were designated as *CuVOZ1* (acc. no. LC729264), *CuFT1* (accession no. LC729261), and *CuFT3* (acc. no. LC729263).

2.2.14. Phylogenetic analysis and comparison of amino acid sequences

Putative amino acid sequences were analyzed using ClustalX2 multiple-sequence alignment program ver. 2.0.5 (Jeanmougin et al., 1998) and the BioEdit program ver. 7.7.0 (Hall, 1999) with known genes from other plant species to clarify the phylogenetic relationship of the *VOZ1* gene in citrus. The tree was constructed using the neighbor-joining (N-J) method for the deduced amino acid sequences of the *VOZ* genes from *Arabidopsis* (AT1G28520 and AT2G42400), Satsuma mandarin (LC729264), Clementine [*Citrus clementina*

(Ciclev10015064m and Ciclev10015076m)], orange [*Citrus sinensis* (XP006467710 and XP006469061)], apple [*Malus* × *domestica* (MDP0000729316, MDP0000879912, and MDP0000296843)], and rice [*Oryza sativa* (LOC_Os01g54930 and LOC_Os05g43950)]. The accession numbers of deduced protein sequences of the TFL1/FT family from other species are AB161112 and AB458504 (apple), AB027504 and AT4G20370 (*Arabidopsis*), DQ871590 (grapevine, *Vitis vinifera*), AB106111, AB161109, and AB110009 (Lombardy poplar, *Populus nigra*), and AY186735 (tomato, *Solanum lycopersicum*). The phylogenetic tree for VOZ1 was displayed using the N-J plot with bootstrap values for 1000 trials in each branch.

2.2.15. Yeast two-hybrid (Y2H)

2.2.15.1. Yeast Strain

Yeast (*Saccharomyces cerevisiae*) MaV203 strain served as the host strain for the bait and prey plasmids in the Y2H system. MaV203 contains a single copy of the three reporter genes (*HIS*3, *URA*3, and *lac*Z). These are stably integrated at different loci in the yeast genome. The genotype of MaV203 is (MATα, *leu*2-3,112, *trp*1-901, *his*3Δ200, *ade*2-101, *gal*4Δ, *gal*80Δ, *SPAL*10*::URA*3, *GAL*1::*lac*Z, *HIS*3UAS GAL1*::HIS*3*@LYS*2, *can*1^{R}, *cyh*2^{R}) (Vidal, 1997).

2.2.15.2. Vector construction for yeast two-hybrid assay

2.2.15.2.1 BP recombination reaction

Following the manufacturer's protocol, *att*B flanked PCR products for the entire coding regions of *CuFTs* (*CuFT1* and *CuFT3*) and *CuVOZ1,* or the truncated region of *CuVOZ1*, were produced with *att*B primers. *att*B-PCR products were purified. *att*B-flanked PCR products were introduced into a pDONR221 vector (Invitrogen, Life Technologies Corp.) in-frame as a

donor vector. The process required a BP recombination reaction with an *att*P containing pDONR221 vector and a catalyst BP clonase enzyme mix (Invitrogen, Life Technologies Corp.). After performing the BP recombination reaction, the entry clone was transformed into DH5α. Successful clones were selected from LB/kanamycin plates.

2.2.15.2.2. LR recombination reaction

LR recombination reaction was performed to generate the expression clones. This reaction occurred between an *att*L containing entry clone and an *att*R containing destination vector. LR recombination reaction was catalyzed by an LR clonase enzyme mix (Invitrogen).

2.2.15.2.2.1. Construction of Gal4-AD prey plasmid (LR recombination reaction)

pDEST™22 vector was used to introduce the gene of interest to construct the prey plasmid. It has the sequence encoding the GAL4 activation domain (AD) fused to the nuclear localization signal from SV40 large T antigen for fusion to the prey gene of interest (Invitrogen). This vector contains a chloramphenicol resistance gene (Cm^R), a *ccd*B gene, and a gentamicin resistance gene. The gene of interest replaced the Cm^R and *ccdB* gene regions, and the *att*R sites were converted to *att*B sites by LR recombination reaction. Gentamicin resistance permitted the selection of the plasmid in DH5α. Thus, the gene of interest was fused in frame with AD flanked by *att*B sites in the destination vector backbone.

Each entry clone was introduced into a pDEST22 ($ampicillin^R$) to construct the expression vector with the GAL4 activation domain (GAL4 AD). The constructs for GAL4 AD (prey) were designated as CuFT1 (AD), CuFT3 (AD), and CuVOZ1 (AD), and the truncated version of CuVOZ1 was designated as CuVOZ1N1 (AD) (1–100aa), CuVOZ1DelN1 (AD) (101–485aa), CuVOZ1N2 (AD) (1–200aa), CuVOZ1N3 (AD) (1–300aa) and CuVOZ1N4 (AD) (1–400aa).

2.2.15.2.2.2. Construction of Gal4-BD bait plasmids (LR recombination reaction)

pDEST™32 vector was used to introduce the gene of interest to construct the bait plasmid. The sequence encodes the GAL4 DNA binding domain (DBD) for fusion to the gene of interest. The vector contains a chloramphenicol resistance gene (Cm^R), a *ccd*B gene, and an ampicillin resistance gene. The gene of interest replaced the Cm^R and *ccd*B gene regions, and the *att*R sites were converted to *att*B sites by an LR recombination reaction. Ampicillin resistance allowed the selection of plasmid in DH5α. The gene of interest was fused in the frame with the DBD flanked by *att*B sites in the vector.

Each entry clone was introduced into a pDEST32 ($gentamicin^R$) to construct the expression vector with the GAL4 DNA-binding domain (GAL4 DBD). The constructs for GAL4 DBD (bait) were designated as CuFT1 (BD), CuFT3 (BD), and CuVOZ1 (BD).

2.2.15.3. Transformation of Yeast

MaV203 was transformed with several combinations of bait [CuFTs (BD) and CuVOZ1 (BD)] and prey [CuFTs (AD), CuVOZ1 (AD), CuVOZ1N1 (AD), CuVOZ1DelN1 (AD), CuVOZ1N2 (AD), CuVOZ1N3 (AD), and CuVOZ1N4 (AD)] plasmids according to the lithium method (Gietz and Woods, 2002).

To make single transformant, MaV203 yeast was cultured overnight. YPD media (20 ml) was taken in a 50 ml Erlenmeyer flask. About one loop of cultured yeast was mixed in YPD media and cultured overnight at 30°C with shaking at 200 rpm. The yeast culture was taken in a 50 ml tube and then centrifuged at 3K rpm for 5 minutes. The supernatant was discarded, and the pellet was dissolved in 10 ml SDW with vigorous tapping and then centrifuged the same way again. The pellet was taken, dissolved in 3 ml 0.1 M lithium acetate, and incubated at 30 °C in the water bath without shaking for 15 minutes. After 15 min, the incubated yeast was

taken out and centrifuged at 3K rpm for 5 min. The supernatant was discarded, keeping the pellet. One loop from the pellet was taken and mixed with the transformation mixture (DW - 25 µL, 50% PEG – 240 µL, 1M lithium Acetate - 36 µL, 2mg/ml carrier DNA - 50 µL, 10X TE - 4 µL). plasmid (0.5 µg) to the corresponding 1.5 ml tube and vortexed to mix properly. Then, the tubes were incubated at 30°C for 25 min (dry without shaking). Then again, the tubes were incubated in a water bath at 42°C for 30 min. The tubes were tapped every 15 minutes during incubation. After incubation, the tubes were centrifuged at 12K rpm for 10-12 seconds, the supernatant was discarded, and the pellet was dissolved in 500 µL of 1X TE. This process was repeated three times. The last time, the pellet was mixed with 100 µL of 1X TE and plated on dropout media. the media plates were incubated at 30°C for two days

2.2.15.4. HIS3, URA3 and LacZ assays

Single AD yeast transformants were screened on a selective agar medium with a minimal synthetic defined (SD) base and –L dropout (DO) supplement (Clontech Laboratories Inc., Mountain View, CA, USA) containing 2% glucose as a carbon source and single BD transformants were screened on SD –W media. Co-transformed yeast with AD and BD constructs were selected on SD –L/–W media. Co-transformed yeasts were incubated on SD –L/–W/–H media to confirm the induction of the *HIS3* gene and the protein-protein interaction. To prevent self-activation of the *HIS3* reporter gene, 25 mM of 3-amino-1,2,4-triazole (3-AT), a *HIS3* inhibitor, was added to the media. The yeasts with the same combination were grown on SD –L/–W/–U media to confirm the activity of the *URA3* reporter gene. To select against positive interactions, 0.2% 5-fluoroorotic acid (5FOA) was used. All of the yeasts were grown at 30°C for 48 h. CuVOZ1–CuFT protein-protein interactions were also confirmed via the colony filter lift assay according to protocols described in the Invitrogen ProQuest™ Two-Hybrid System kit (Breeden and Nasmith 1985).

Imidazoleglycerol-phosphate dehydratase, an enzyme that catalyzes the sixth stage of histidine synthesis in yeast cells, is produced by the HIS3 gene. Imidazoleglycerol-phosphate dehydratase is inhibited by the nonselective systemic triazole herbicide 3-Amino-1,2,4-triazole (3-AT). Using 3-AT on yeast cell cultures needs a plasmid carrying *HIS3* to make histidine. The survival of the yeast cell is dependent on enhanced *HIS3* expression in dropout media.

Orotidine 5'-phosphate decarboxylase (ODCase), an enzyme that catalyzes one process in the production of pyrimidine ribonucleotides (a building block of RNA), is encoded by the gene *URA3*. Cell growth is inhibited when ODCase activity is lost unless uracil or uridine is supplied to the medium. The *URA3* gene restores ODCase function in yeast, enabling growth on medium without uracil or uridine supplements and enabling selection for yeast containing the gene. As opposed to this, if 5-FOA (5-Fluoroorotic acid) is introduced to the medium, the active ODCase will convert it into the poisonous substance (5-fluorouracil, a suicide inhibitor), which results in cell death and enables selection against yeast expressing the gene in URA3 assay.

X-gal is an analog of lactose. The yeast enzyme β-galactosidase (*LacZ*) hydrolyzes X-gal, breaking the β-glycosidic link in D-lactose. When X-gal is broken down by β-galactosidase, galactose and 1-bromo-4-chloro-3-hydroxyindole-1 are produced. The latter then spontaneously dimerizes and is oxidized to produce 5,5'-dibromo-4,4'-dichloro-indigo-2, a blue insoluble compound. Since X-gal itself is colorless, a test for the presence of active galactosidase is performed by looking for the presence of a blue-colored product in colony filter lift assay.

2.2.16. Vector construction and Arabidopsis transformation

The coding region of *CuVOZ1* was amplified by PCR to construct a binary vector for plant transformation. The oligonucleotide primers are listed in Table 2-3. The amplified

product was digested with *Xba*I and *Kpn*I and cloned into the corresponding restriction enzyme site of the 35SΩ/pSMAK193E plant-transformation vector (Kotoda et al., 2010). The Ω sequence responsible for enhancing translation was placed after the promoter sequence of cauliflower mosaic virus 35S (Gallie and Walbot 1992). Wild-type *Arabidopsis* was transformed with *Agrobacterium tumefaciens* EHA101 using the floral-dip method (Clough and Bent, 1998). Kanamycin-resistant transgenic seedlings were transplanted from the plate to moistened soil (vermiculite: perlite = 1:1) at the two-leaf stage and then grown in a growth chamber (Nippon Medical and Chemical Instruments Co., Ltd.) at 22°C under LD conditions. WT and transgenic plants with a pSMAK251 empty vector (indicated as PSM251) were used as controls. Morphological and expression analyses were performed on the third-generation (T_3) transgenic plants. The number of days to bolting and flowering, number of rosette leaves and cauline leaves at flowering, and numbers of adventitious flower buds, branches, siliques, and nodes were counted. The length of the first inflorescence was measured at flowering and 40 days after incubation (DAI). Whole plants of the transgenic lines and controls were collected at 40 DAI for qRT-PCR analysis.

2.2.17. Expression analysis in the Satsuma mandarin 'Aoshima' and transgenic Arabidopsis

One microgram of RNA was used to synthesize the first-strand cDNA in 20 μL of a reaction mixture using ReverTra Ace® qPCR RT Master Mix (TOYOBO). Expression analysis of *CuVOZ1*, *CuFT1*, and *CuFT3* was carried out with qRT-PCR. One microliter of the first-strand cDNA was used as a template in a total volume of 12.5 μL using SYBR® Green RealTime PCR Master Mix (TOYOBO). The qRT-PCR was performed using LightCycler® 96 System (Roche Diagnostics, Mannheim, Germany) as follows: 95°C for 1 min, 40 cycles of 95°C for 15 s and 60°C for 1 min for *CuVOZ1*, *CuActin*, and *AtTUB*. For *CuFTs*, the thermal-cycle program was 95°C for 1 min and 40 cycles of 95°C for 5 s, 60°C for 10 s, and 72°C for

15 s. Three technical replicates were maintained for each analysis. *CuActin* was used as a reference gene to normalize the transcript levels of *CuVOZ1*, *CuFT1*, and *CuFT3* (Kotoda et al., 2016). *AtTUB4* was used as a reference gene to normalize the transcript levels of *CuVOZ1* in transgenic *Arabidopsis*. The primer sets used in the experiment are listed in Table 2-3.

2.2.18. Docking simulation

Predictions of the three-dimensional (3D) structure of the proteins and protein-protein interaction were simulated based on the cDNA sequences of *CuVOZ1*, *CuFT1*, and *CuFT3* to better understand the results obtained in the Y2H assays. The protein modeling and interaction were predicted in AlphaFold2_advanced.ipynb (Jumper et al., 2021), a Web-based iPython Notebook service for interactive coding supported by Google. Visualizations of protein models and prediction of docking regions were observed via ChimeraX ver. 1.5 (Pettersen et al., 2021). At the AlphaFold2_advanced.ipynb window, there is an option to enter the amino acid sequence to fold. To specify intra-protein chain breaks, "/" is used. To specify inter-protein chain breaks for modeling protein-protein hetero-complexes, ":" was used in between two amino acid sequences. For example, sequence AC/DE:FGH was modeled as polypeptides: AC, DE and FGH. A separate multiple sequence alignment (MSA) was generated for ACDE and FGH. Then in the 'Runtime' option, "Run all" was selected. The program then searched the sequence in the protein database. The protein models were predicted by how well each residue was covered by similar sequences in the MSA. The models were then ranked by the average predicted local distance difference test (plDDT). The top five models were visible in the UCSF ChimeraX molecular visualization application (Pettersen et al., 2021). In ChimeraX, the possible docking regions with relative positions were visualized from the protein complexes.

2.2.19. Statistical analysis

Data on the number of days to bolting and flowering; the numbers of leaves, lateral flower buds, nodes, and siliques; and the length of the first inflorescence and internode were analyzed using one-way ANOVA, and the differences were analyzed using Tukey's honestly significant difference (HSD) test. Statistical analyses were performed at a significance level of $P < 0.05$ using RStudio v.1.2.5089 (RStudio Team, 2020).

2.3. Results

2.3.1. Isolation of CuVOZ1, CuFT1, and CuFT3 from the Satsuma mandarin 'Aoshima'

The cDNA of *CuVOZ1* was isolated from the Satsuma mandarin 'Aoshima' to investigate the function of *CuVOZ1.* The *CuVOZ1* gene consisted of four exons of 231, 147, 523, and 557 base pairs (bp) encoding a putative protein of 485 amino acids, which was also confirmed by next generation sequencing (NGS) of the 'Aoshima' genome (Fig. 2-1A). A phylogenetic analysis using the putative amino acid sequences corresponding to *VOZ* genes from apple, *Arabidopsis*, citrus (Satsuma mandarin, Clementine, and sweet orange), and rice was performed to understand the evolutionary relationship among those genes. Neighbor-joining distance analysis revealed that CuVOZ1 groups with the VOZ1 of Clementine, sweet orange, apple, and *Arabidopsis* (Fig. 2-1B).

The multiple-sequence alignment showed that the transcription factor isolated in this study, *CuVOZ1*, was homologous to the *Arabidopsis* VOZ family genes. The sequence of CuVOZ1 is 100% identical to CcVOZ1 and 99.38% identical to CsVOZ1 at the amino acid level. The motif search tool using the Pfam database showed that the amino acid sequence of CuVOZ1 contains two conserved regions. An N-terminal basic helix–loop–helix region was identified as a domain of the unknown function (DUF4749) (28–99 aa), and a C-terminal beta pleated sheet was found to have no apical meristem (NAM) (284–380 aa) motif region (Finn et al., 2016) (Fig. 2-2A, green regions). In Satsuma mandarin, there were three *FT* homologs (*CiFT1*, *CiFT2*, and *CiFT3*) reported by Nishikawa et al. (2007), but *CiFT1* and *CiFT2* appeared to be encoded by the same gene, meaning that these two genes were allelic (Samach 2013). Therefore, *CuFT2* corresponding to *CiFT2* was excluded from analysis in this study. Each *CuFT1* and *CuFT3,* consisting of four exons of 201, 63, 42, and 225 bp, has a sequence of 177 amino acids. The multiple-sequence alignment of the putative amino acid sequences

from the TFL1/FT family of different plant species showed that CuFT1 and CuFT3 share 169 identical residues. These two proteins are 95.48% identical to each other. One motif, named the phosphatidylethanolamine-binding protein (PBP) region, was identified in the sequence of CuFT1 (63–160 aa) and CuFT3 (52–160 aa) (Fig. 2-2B, green region).

2.3.2. Interactions of CuVOZ1 with CuFT1 or CuFT3 in a Y2H system

A Y2H system with full-length CuFTs as bait and CuVOZ1 as prey, and vice versa, was used to investigate the protein-protein interaction between them. Auxotrophy assays for *HIS3* and *URA3* reporter genes, a sensitivity test for 5FOA, and an X-gal filter assay for the *LacZ* reporter gene were performed using the yeast transformants harboring a pair of bait and prey plasmids, CuFT1 (AD)/CuVOZ1 (BD), CuFT1 (BD)/ CuVOZ1 (AD), CuFT3 (AD)/CuVOZ1 (BD), and CuFT3 (BD)/CuVOZ1 (AD) to confirm whether CuVOZ1 could interact with CuFT1 or CuFT3. As a result, the activities of *HIS3* and *LacZ* were detected in yeast cells with all combinations analyzed (Fig. 2-3, upper panel). All the yeast constructs co-transformed with AD and BD plasmids grew on –L/–W/–H + 25 mM 3-AT media, confirming induction of the *HIS3* reporter gene in the His auxotrophy assays. Growth induction of CuFT1 (AD)/CuVOZ1 (BD) and CuFT3 (AD)/CuVOZ1 (BD) constructs on an SD –L/–W/–U media plate in the Ura auxotrophy assay and growth inhibition of all constructs on an SD –L/–W + 5FOA media plate in the 5FOA sensitivity assay confirmed the activity of the *URA3* reporter gene. However, CuFT1 (BD)/CuVOZ1 (AD) and CuFT3 (BD)/CuVOZ1 (AD) constructs did not show growth induction on the SD –L/–W/–U media plate. The indigo coloration in the X-gal filter assay confirmed the activity of the *LacZ* reporter gene. The growth inhibition of all the BD constructs tested on –W or –L/–H media plates and the colony filter lift assay showed that no single construct was self-activated (Fig. 2-3, lower panel).

2.3.3. Expression patterns of CuVOZ1, CuFT1, and CuFT3

Tissue-specific expression patterns of *CuVOZ1, CuFT1,* and *CuFT3* were examined using qRT–PCR analyses. *CuVOZ1* was expressed in various vegetative and reproductive tissues (Fig. 2-4A). Expression of *CuVOZ1* was relatively high in shoot apices, stems with a node, and leaves at both juvenile and adult stages and in flower buds. However, *CuVOZ1* was expressed lower in juice sacs in the reproductive tissues. *CuFT1* was expressed highly in the early stage of juice sac development in August and in the later stage of peels in November (Fig. 2-4B). However, slight expression was detected in seeds (November), old leaves (August), and juice sacs in November. *CuFT3* was expressed in peels (November), shoot apices (April), and old leaves (August) at the adult stage and roots (August) at the juvenile stage, with a lower expression in other tissues (Fig. 2-4C).

2.3.4. Analysis of CuVOZ1 in transgenic Arabidopsis

The construct of 35SΩ:*CuVOZ1* (Fig. 2-5A) was introduced into wild-type *Arabidopsis* to elucidate the possible role of *CuVOZ1* in *Arabidopsis*. About 30 independent transgenic lines were obtained. The T_3 transgenic plants were grown in an incubator under LD conditions, and five independent lines (n = 14) were phenotyped together with controls (Fig. 2-5B). In the transgenic plants with 35SΩ:*CuVOZ1*, the appearance of adventitious flower buds was observed (Fig. 2-5C). In addition to the phenotypic analyses, the transgene expression in five independent *Arabidopsis* lines was confirmed via qRT-PCR. All transgenic lines with 35SΩ:*CuVOZ1* expressed the transgene. Among them, lines 1 and 2 showed higher expression, followed by lines 4, 3, and 6 in decreasing order (Fig. 2-5D). Several parameters were taken into consideration to analyze the characteristics of transgenic *Arabidopsis.* 35SΩ:*CuVOZ1* induced early flowering in all transgenic lines compared to the WT and PSM251, an empty vector control (Figs. 2-5B and 2-6A). The inflorescence was significantly elongated (Fig. 2-

6B). A particular type of adventitious flower buds was observed on the main stem with enhanced elongation in transgenic lines (Figs. 2-5C and 2-6C). The adventitious flower buds without cauline leaves appeared from the side of the upper main stem (inflorescence) of transgenic plants after the oldest flower formation, whereas lateral flowers naturally occurred acropetally after the oldest flower formation in the controls. These adventitious flower buds never opened but were fertile because they developed siliques. The number of branches, siliques, and nodes was high (Fig. 2-6D-F), whereas the length of internodes was shorter in transgenic lines (Fig. 2-6G). The number of rosette leaves was significantly higher in lines 4 and 6 at flowering time (Fig. 2-6H). The number of cauline leaves was significantly higher in lines 2, 3 and 4 at flowering time (Fig. 2-6I). The lines with a higher expression of each transgene showed a phenotype of significantly early flowering, long inflorescence, and more lateral flower buds (Fig. 2-5D).

2.3.5 Identification of binding regions using a Y2H system

A series of truncated CuVOZ1 proteins was fused to the GAL4 activation domain (GAL4 AD) further to verify the interaction region between CuVOZ1 and CuFT1 (Fig. 2-7A) and between CuVOZ1 and CuFT3 (Fig. 2-7B). The series of truncations was constructed by gradual deletion of the C terminal region [(N1, 1–100aa), (N2, 1–200aa), (N3, 1–300aa), and (N4, 1–400aa)] or deletion of the N terminal region [DelN1, 101–485aa]. In Y2H assays, constructs of the CuVOZ1 truncation series (AD)/CuFTs (BD) showed inhibited growth in the SD –L/–W/–H + 25 mM 3-AT media and less blue coloration in the X-gal assay except for the CuVOZ1N4 (AD)/CuFT (BD) construct. The CuVOZ1N4 (AD)/CuFT (BD) construct showed normal growth in the SD –L/–W/–H + 25 mM 3-AT media and indigo coloration in the X-gal assay similar to that of the full-length CuVOZ1 (AD)/CuFT (BD) construct. These observations indicated that CuFTs showed little interaction with C-terminal truncations of CuVOZ1 [(N1,

1–100aa), (N2, 1–200aa), and (N3, 1–300aa)] and an N-terminal truncation of CuVOZ1 (DelN1, 101–485aa) on the SD –L/–W/–H + 25 mM 3-AT media plate and the X-gal assay but showed a strong interaction with CuVOZ1N4 region, which consisted of 1–400 aa in the N-terminal (Fig. 2-7).

2.3.6 Docking simulation by AlphaFold

A deep-learning neural network was applied to predict possible docking regions to understand how CuVOZ1 and CuFTs interact. Predicted structures of these proteins were generated using the AlphaFold2_advanced.ipynb notebook. This Google-supported notebook used artificial intelligence to query several protein sequence databases, construct a multiple sequence alignment, and model the protein complex structure. The docking regions were predicted by AlphaFold and displayed with ChimeraX (Fig. 2-8). The predicted amino acid residues associated with the interaction between CuVOZ1 and CuFT1 in the CuVOZ1-CuFT1 complex were as follows: His56, Arg60, Tyr182, Pro204, Ile206, Asp222, Pro224, Arg225, Gln227, Ser238, Phe240, Leu244, Leu257, Arg258, Pro259, and Leu308 in CuVOZ1 (Figs. 2-2A, 2-8A and 2-8D) and Leu128, Gln131, Tyr134, Pro136, Gly137, Trp138, Gln140, Asn141, Asp146, Glu149, Leu150, Tyr 151, and Asn152 in CuFT1 (Figs. 2-2B, 2-8A and 2-8D). The predicted amino acid residues associated with the interaction between CuVOZ1 and CuFT3 in the CuVOZ1-CuFT3 complex were as follows: Tyr202, Leu203, Arg225, Phe240, Arg258, Pro259, and Gly260 in CuVOZ1 (Figs. 2-2A, 2-8B and 2-8D) and Ser100, Phe101, Gln103, Asn107, Gly137, and Trp138 in CuFT3 (Figs. 2-2B, 2-8B and 2-8D).

The protein-protein interaction between CuVOZ1 and AtFT was simulated in the same procedure to understand how CuVOZ1 functions in the transgenic *Arabidopsis*. The predicted amino acid residues associated with the interaction between CuVOZ1 and AtFT in the CuVOZ1-AtFT complex were as follows: Pro204, Ile206, Cys207, Pro209, Arg225, Phe240

and Gly260 in CuVOZ1 (Fig. 2-2A, 2-8C and 2-8D) and Gln49, Asn103, Glu104, Ile105, Cys107, Glu109, Asn110, Thr114 and Trp138 in AtFT (Fig. 2-2B, 2-8C and 2-8D).

The common amino acid residues that participated in docking in three protein-protein complexes were Arg225 and Phe240 in CuVOZ1 and Trp138 in FTs (Figs. 2-2 and 2-8). Two of the predicted amino acid residues of CuVOZ1 involved in docking in the CuVOZ1–CuFT1 complex were in the first exon, 15 were in the third exon, and one was in the fourth exon. In the CuVOZ1-CuFT3 and CuVOZ1-AtFT complexes, all the predicted amino acids of CuVOZ1 involved in docking were in the third exon. For CuFT1, all the amino acids involved in docking in both protein complexes were predicted in the fourth exon. For CuFT3, two amino acids involved in docking were predicted in the third exon, and four amino acids were predicted in the fourth exon. In AtFT, one predicted amino acid involved in docking was found in the first exon and eight in the fourth exon.

2.4. Discussion

The genomic DNA of *CuVOZ1* was comprised of four exons, and the exon-intron structure was similar between *CuVOZ1* and *AtVOZ1* in the coding sequence (Fig. 2-1A). Citrus VOZ1s, including CuVOZ1, clustered with the same clade of AtVOZ1 and MdVOZ1, suggesting that they function in citrus as AtVOZ1 and MdVOZ1 (Fig. 2-1B). A motif search revealed that the VOZ family had a NAM (PF02365) motif, which is indicated to have a role in determining the positions of meristems and primordia in the latter half of each protein in common (Fig. 2-2A; Sauer et al., 1996). On the other hand, a characteristic feature of VOZ1 derived from citrus was highlighted by a motif named DUF4749 (PF15936), which is functionally uncharacterized (Fig. 2-2A; Finn et al., 2016).

The previous study demonstrated for the first time that a VOZ1-like protein (MdVOZ1a) interacted with FT-like proteins (MdFT1 and MdFT2) in apple by using the Y2H system (Mimida et al., 2011). CuVOZ1 in Satsuma mandarin clustered closely with MdVOZ1 (MdVOZ1a) in apple, prompting us to investigate the protein-protein interaction between CuVOZ1 and two CuFTs with the Y2H system. As a result, strong positive interactions were confirmed in yeast cells with the combinations of CuFT1 (AD)/CuVOZ1 (BD) and CuFT3 (AD)/CuVOZ1 (BD), with weaker ones in the opposite combinations of AD and BD (Fig. 2-3, upper panel). The N-terminal region of each protein close to a fused domain might be affected by swapping the AD and BD because molecular forces involved in protein-protein interaction include steric forces that play significant roles in modifying the protein microstructure and functional properties (Wang et al., 2019).

CuVOZ1 strongly interacted with CuFT1 and CuFT3 in the Y2H assays. Therefore, the expression pattern of each gene was investigated to clarify the expression domains in common between CuVOZ1 and CuFT1 and between CuVOZ1 and CuFT3. The expression analysis

revealed that *CuVOZ1* was expressed in all tissues of Satsuma mandarin, whereas *CuFT1* was expressed exclusively in juice sacs (August) and peels (November), where both genes were expressed (Fig. 2-4A, B). It has been noted that cells of citrus peels contain very large vacuoles (Pérez and Garrido, 1985). The zinc-finger transcription factor, AtVOZ1, was first identified as a vacuolar H^+-pyrophosphatase (V-PPase) promoter-binding protein via the yeast one-hybrid (Y1H) system, and *AtVOZ1* was expressed in vascular bundles of various tissues, such as roots, shoots, leaves, flowers, and siliques, which are likely to correspond to citrus fruit (Mitsuda et al., 2004). In Japanese pear, V-PPase was expressed in the vacuole membrane in young fruit and acted as a vacuolar proton pump (Shiratake et al., 1997). In apple and citrus, *MdFT2* and *CiFT1* were expressed abundantly in young fruit, respectively, suggesting the involvement of *FT*-like genes in fruit development (Kotoda et al., 2010; Nishikawa et al., 2007). In addition, *SFT* in tomato regulates the termination of symptomatic meristems and leaf structures, suggesting that the *FT*-like gene is not only a promoter of flower induction but also a general systemic regulator of plant growth (Shalit et al., 2009). Ectopic expression of the rice *Hd3a* gene in potatoes induces tubers under LD conditions (Navarro et al., 2011). Considering these facts, the protein complex of CuVOZ1–CuFT1 might modify the activity of V-PPase and/or the function of FT and play an additional role in fruit development and ripening.

In contrast, *CuFT3* was expressed relatively highly in peels (November), shoot apices (April), and old leaves (August) in the adult phase and roots (November) in the juvenile phase, where *CuVOZ1* was also expressed (Fig. 2-4A, C). Among the flowering genes, *PHYTOCHROME A* (*PHYA*) and *CRYPTOCHROME2* (*CRY2*) in the long-day pathway; *LUMINIDEPENDENS* (*LD*), *FLOWERING LOCUS D* (*FLD*), *VERNALIZATION-INSENSITIVE 3* (*VIN3*), *VERNALIZATION* (*VRN*), *FLC*, *FRIGIDA* (*FRI*), and *AGAMOUS-LIKE 24* (*AGL24*) in the autonomous/vernalization pathways; and some flowering repressor

genes, such as *PHYTOCHROME B* (*PHYB*), *TFL2*, *MADS AFFECTING FLOWERING 1* (*MAF1*), and *SHORT VEGETATIVE PHASE* (*SVP*), are highly expressed in both the SAM and the root apical meristem (RAM) (Bernier and Périlleux, 2005). In apple, *TFL1*-like (*MdTFL1* and *MdTFL1a*) and *CEN*-like (*MdCENa*) genes, which function as flowering repressors, are expressed preferentially in roots as well as the SAM (Kotoda et al., 2006; Kotoda and Wada et al., 2005; Mimida et al., 2009). Based on these results, CuVOZ1 might affect flower induction via *CuFT3* in the SAM and leaves. The function of the CuVOZ1–CuFT1 complex in roots and peels also needs to be clarified in future studies.

Previous studies on transgenic *Arabidopsis* overexpressing *AtVOZ2* showed that *AtVOZ2* confers biotic stress tolerance but impairs abiotic stress tolerance (Koguchi et al., 2017; Nakai et al., 2013a). In contrast, loss-of-function mutations in both *AtVOZ1* and *AtVOZ2* increased cold and drought stress tolerance and hypersensitivity to salt stress, decreasing biotic stress resistance in *Arabidopsis* (Nakai et al., 2013b; Prasad et al., 2018). To date, no study on transgenic *Arabidopsis* overexpressing *AtVOZ1* has been conducted. In this study, the transgenic *Arabidopsis* ectopically expressing *CuVOZ1* showed early bolting and flowering with an elongated stem and fertile adventitious flower buds (Figs. 2-5B, C and 2-6A–C). On the other hand, the ectopic expression of apple *MdVOZ1a* induces the elongation of flower stalks like that of *CuVOZ1*, but the transgenic *Arabidopsis* is sterile (Mimida et al., 2011). The difference in the phenotype between 35SΩ:*CuVOZ1* and 35SΩ:*MdVOZ1a* transgenic lines might be due to the additional amino acid sequence or adaptin-binding motif in the N-terminal of MdVOZ1a (Fig. 2-2A; Finn et al., 2016). The role of *AtVOZ*s in flowering, with regard to *CO*, *FLC*, *MAF*, and *PHYB*, was previously explained in the studies conducted with a double mutant (*voz1 voz2*) in *Arabidopsis* (Celesnik et al., 2013; Kumar et al., 2018; Yasui et al., 2012). The early flowering phenotype of 35SΩ:*CuVOZ1* transgenic lines might be a result of the

interaction with *FT* or the downregulation of *FLC* and/or the stabilization of *CO* in transgenic *Arabidopsis* because *AtVOZ1* suppresses *FLC* and acts together with *CO* by interacting physically to control flowering (Kumar et al., 2018; Yasui et al., 2014). Recent studies showed that *OPEN STOMATA 1* (*SlOST1*) mediated phosphorylation of SlVOZ1 is important for the stability of the protein under drought conditions in tomato. Phosphorylated SlVOZ1 binds directly to the promoter region of *SFT* to activate early flowering under drought conditions (Chong et al., 2022). It has long been known that under drought conditions, citrus, such as Satsuma mandarin and lemon, was induced to flower (Spiegel-Roy and Goldschmidt, 1996; Suzuki et al., 1967). The number of flowers, flowering nodes, and flowers per node was increased under high water stress and drought conditions in Satsuma mandarin (Inoue, 1989). In this phenomenon, stabilized *CuVOZ1* might function as one of the triggers for the inductive flowering. CuVOZ1 might also be involved in the elongation and branching of the stem because 35SΩ:*CuVOZ1* transgenic lines had phenotypes showing elongated inflorescence and an increased number of nodes and branches (Fig. 2-6B, D, F).

As an ectopic expression of *CuVOZ1* conferred traits such as early flowering and elongation of the inflorescence on transgenic *Arabidopsis*, the interaction between the truncated CuVOZ1 and full-length CuFT1/CuFT3 was investigated in yeast to further identify binding regions. The Y2H assays showed that N-terminal 400 amino acids were important for the protein-protein interaction between CuVOZ1 and CuFT1 (Fig. 2-7A) and between CuVOZ1 and CuFT3 (Fig. 2-7B). Based on the results for each truncated protein of CuVOZ1, it was suggested that both the region from the 1st to 100th amino acid and the one from the 301st to 400th amino acid were required at least for the interaction. Interestingly, the first and second regions corresponded to the DUF4749 and NAM motifs, respectively (Fig. 2-2A).

In addition to the Y2H assays, a simulation with AlphaFold was performed to predict several models of CuVOZ1–CuFT1 and CuVOZ1–CuFT3 complexes and to validate the results of the Y2H assays (Fig. 2-8). The simulation predicting CuVOZ1-AtFT binding was also performed to confirm the interaction between CuVOZ1 and AtFT in transgenic *Arabidopsis* (Figure 8). Two amino acid residues, His56 and Arg60, in the DUF4749 motif region and one amino acid residue, Leu308, in the NAM motif region of CuVOZ1 were involved in docking CuFT1 as suggested in the Y2H assays. In contrast, no amino acid residues were found in these two motif regions involved in docking between CuVOZ1 and CuFT3. The other residues involved in binding were found between the 182nd and 259th amino acids. The amino acid residues involved in binding between CuVOZ1 and AtFT were also found in the same region. The difference in the position of associated amino acids between CuFT1 and CuFT3 might be explained by the difference in their 3D structures, leading to the functional divergence of CuFT1 and CuFT3. Mitsuda et al. (2004) showed that the third exon of *AtVOZ1* and *AtVOZ2* contained the zinc-coordinating motif and the basic region that functions as the DNA-binding and dimerization of VOZ family proteins. The zinc coordination motif was also found in the third exon of CuVOZ1 (Fig. 2-2A). This binding region in CuVOZ1 was common in the complexes of CuVOZ1-CuFT1, CuVOZ1-CuFT or CuVOZ1-AtFT (Fig. 2-2A). The amino acid residues of CuFTs or AtFT involved in the interactions were found in the PBP motif region, specifically in the fourth exon (Fig. 2-2B). The distance between the residues was predicted to be 2.69–3.37 Å, suggesting that the forces between CuVOZ1 and CuFTs in the CuVOZ1–CuFT complexes or between CuVOZ1 and AtFT in CuVO1–AtFT complex were weak Van der Waals forces. In the fourth exon of FT orthologs, a highly conserved 14-amino acid segment (segment B, LGRQTVYAPGWRQN) forms an external loop, which is considered to form the ligand-binding site together with the adjacent segment C (Ahn et al.,

2006). Eight of 13, two of six, and one of nine residues associated with docking were localized in segment B for CuFT1, CuFT3, and AtFT, respectively (Fig. 2-2B). Taken together, this indicates that CuVOZ1 might interact with the region, including/around segments B and C of CuFTs, to function as a complex.

2.5. Conclusion

The protein-protein interaction between CuVOZ1 and CuFTs was confirmed via the Y2H system, and the truncation experiment suggested that the N-terminal region of CuVOZ1 from the 1st to 400th amino acid would be essential for the interaction. Moreover, the nature of binding between two proteins was predicted with a docking simulation. The 35SΩ:*CuVOZ1* transgenic *Arabidopsis* suggested that *CuVOZ1* might act as one of the triggers for early flowering and might also be involved in the elongation and branching of the inflorescence. However, it is still unclear how these proteins exhibit interaction *in vivo* and how CuVOZ1–CuFT complexes function in citrus. The response of CuVOZ1–CuFT complexes to environmental stresses and/or phytohormones in relation to flowering remains to be studied further, in addition to the BiFC and/or immunoprecipitation assays.

Table 2-1. List of Satsuma mandarin ('Aoshima') tissues used in Quantitative real-time RT-PCR and method of RNA extraction

	Tissues	Time of sample collection	Method
	Seed	November 2019	Modified CTAB
Juvenile phase	Root	20 months old seedlings. August 2019	CTAB
	Stem		
	Leaf		
	Apices		
Adult phase	Stem with lateral bud	August 2018	
	New leaf	April 2018	
	Old leaf	August 2018	
	Apices	April 2018	
	Flower bud	April (Before anthesis) 2014	
	Young fruit	May 2018	
	Juice sac	August 2018 and November 2018	Phenol-SDS
	Peel	August 2018 and January 2018	
Arabidopsis thaliana	Whole plant	30^{th} day and 40^{th} day July 2018	CTAB

Table 2-2. RT-PCR composition for cDNA synthesis

Reagents	μL
SDW	8
4 × DN master mix (with gDNA remover)	4
Template RNA (250 ng/μL)	4
Incubate at 37°C for 5 minutes	
5 × RT master mix II	4
Total volume	20

PCR condition (1 cycle)	
Temperature °C	Min
37	15
50	5
98	5
4	hold

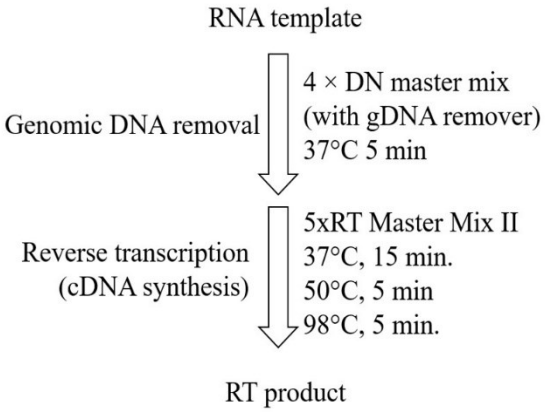

Table 2-3. Primer sets used in gene cloning, Y2H, quantitative real-time RT-PCR analysis, and vector construction.

Primer	Oligonucleotide (5′ → 3′)
Gene cloning	
Ciclev10015064m_F2	GGTTCTGAATTGTAGGTGTATC
Ciclev10015064m_R3	CATATTCATTGAAGCTTCTTTGA
CuFT1_F1	GTGCTTAGTGTTGTTGAGTG
CuFT1_R	ATCAAATTAAGCATGTATGG
CuFT3_F1	CAACAAAATTTCATCACTTGAATAGTC
CuFT3_R	TTGATATCAAATTAAGCATGTAC
*att*B primers	
VOZ1attB_F	acaagtttgtacaaaaaagcaggcttcATGGTGGGCAAGGGTGCGAA
VOZ1attB_R	accactttgtacaagaaagctgggtcTTACGTCAGGTAATACTCAC
CuVOZ1attB_DN1F	acaagtttgtacaaaaaagcaggcttcACTAGCACTTTAACTGCACC
CuVOZ1attB_N1R	accactttgtacaagaaagctgggtcTTAAGCATCATCTTCCTCCT
CuVOZ1attB_N2R	accactttgtacaagaaagctgggtcTTAAGAAATCTGTTGCATGG
CuVOZ1attB_N3R	accactttgtacaagaaagctgggtcTTAAGGAGCATTCCATGGAG
CuVOZ1attB_N4R	accactttgtacaagaaagctgggtcTTATTTCCCATCAACAAGCT
CuFT1&2_Y2H_F	aaaaagcaggcttcATGTCTAGCAGGGAGAGA
CuFT1&2_Y2H_R	agaaagctgggtcCATCGTCTGACAGGCCT
CuFT3_Y2H_F2	acaaaaaagcaggcttcATGTCTAGCAGGGACAGA
CuFT3_Y2H_R2	accactttgtacaagaaagctgggtcCATCGTGTCATAGTCCTTC
qRT-PCR	
qPCR_CuVOZ1_F	CAACTCAGCTTCTCACAAGC
qPCR_CuVOZ1_R	GCTCTCCTTCCTGGCAAATT
CuFT1&2_F (391>408)	CAGACTGTTTATGCACCA
CuFT1&2_R (520<537)	GGATCATCGTCTGACAGG
CuFT3_F (391>408)	CAGACTGTTTATGCACCG
CuFT3_R (520<537)	GGATCATCGTGTCATAGT
CuActin (-86>-66)	GAGCGATAGAGAGAATCGACA
CuActin (-1<19)	TATCCTCAGCATCGGCCATT
AtTUB4-F	TTCATATCCAAGGCGGTCAATGTGG
AtTUB4-R	CGAGCTTGAGGGTACGGAAACAG
Vector construction	
VOZ1_XbaI_F	AAAtctagaATGGTGGGCAAGGGTGCGAA
VOZ1_KpnI_R	AAAggtaccTTACGTCAGGTAATACTCAC

The thermal cycle program for qRT-PCR was as follows: 95˚C for 1 min, followed by 40 cycles at 95˚C for 15 s, 60˚C for 60 s for *CuVOZ1*, *CuActin,* and *AtTUB4*. The thermal program for *CuFT1* and *CuFT3* was as follows: 95˚C for 1 min, followed by 40 cycles at 95˚C for 5 s, 60˚C for 10 s, and 72˚C for 15 s. The site of *att*B or restriction enzymes used for vector construction is indicated with the characters in lowercase.

Table 2-4 Composition of RT-PCR mixture to produce PCR product and PCR conditions (for 10 μL)

Reagents	Volume (μL)
SDW	6.4
KOD-Plus-Neo Buffer	1
dNTP	1
MgSO4	0.6
Sense primer (10 pmol/ μL)	0.3
Anti-sense primer (10 pmol/ μL)	0.3
KOD-Plus-Neo	0.2
RT-Product	0.5

PCR condition (2-step PCR):

Cycle	Temperature (°C)	Time (min)
1	94	2
2-40	98	10s
	68	1-2 (depending on length)
99	10	Overnight

PCR condition (3-step PCR):

Cycle	Temperature (°C)	Time (min)
1	94	2
	98	10s
2-40	55	30s
	68	1-2 (depending on length)
99	10	Overnight

Table 2-5. Reagent composition for A attachment

Reagents	Volume (μL)
10 × Reaction Buffer	5
2 mM dNTP mix	4
10 mM dATP	1
Prime Taq DNA Polymerase 5U/μL	0.1
Total	10.1

Table 2-6. PCR reaction mixture and temperature schedule for clone check (for 1 sample)

Reagents	Volume (μL)
SDW	10.25
10 × Reaction Buffer	1.25
dNTP	1
Sense primer (10 pmol/ μL)	0.25
Anti-sense primer (10 pmol/ μL)	0.25
Prime Taq DNA Polymerase 5U/μL	0.025
Boiled product	0.5
Total	13.5

PCR condition

Cycle	Temperature (°C)	Time (min)
1	94	2
	94	15s
2-35	55	15s
	72	1:30 (depending on length)
99	10	Overnight

Table 2-7 Reagent composition and temperature schedule for sequencing reaction

	No of samples				
Reagents (μL)	1	4	8	16	32
SDW	6.25	25	50	100	200
5 X Buffer	1.5	6	12	24	48
Big Dye	0.5	2	4	8	16
Plasmid DNA	1	-	-	-	-
Primer	1	-	-	-	-

PCR condition

Cycle	**Temperature (°C)**	**Time (min)**
1	96	30s
	96	10s
2-35	50	5s
	60	4
99	10	Overnight

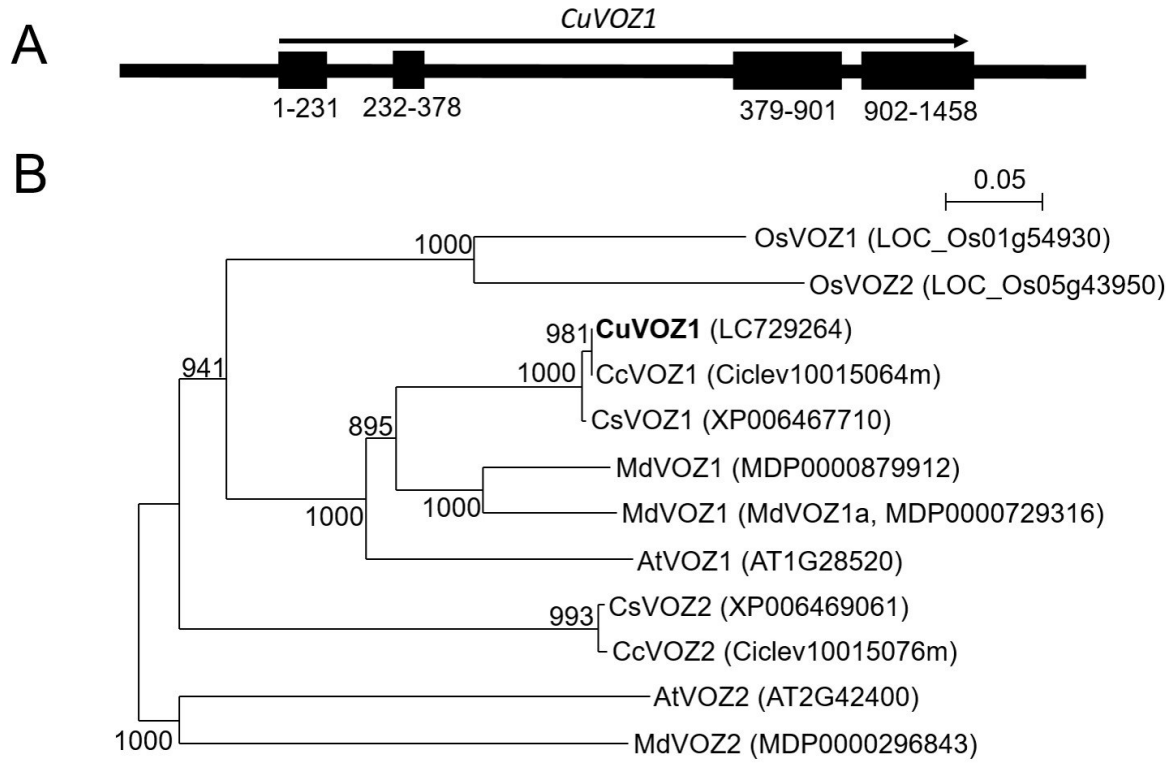

Fig. 2-1. Genomic organization of *CuVOZ1* and relationship of the predicted VOZ family protein between Satsuma mandarin 'Aoshima' and other plant species. (A) Schematic representation of the genomic organization of *CuVOZ1*. The numbers appearing below the exon region are based on the position of the cDNA sequence of *CuVOZ1*. (B) Relationship of the predicted VOZ family proteins between Satsuma mandarin and other plant species. The phylogenetic tree of VOZ family proteins of apple, *Arabidopsis*, citrus, and rice is shown. The amino acid sequences of *Arabidopsis* VOZ family proteins were obtained from TAIR, and others were obtained from the phytozome and Genome Database for Rosaceae (GDR). Numbers along branches are bootstrap values (1000 replicates). The unit for the scale bars displays branch lengths (0.05 substitutions/site).

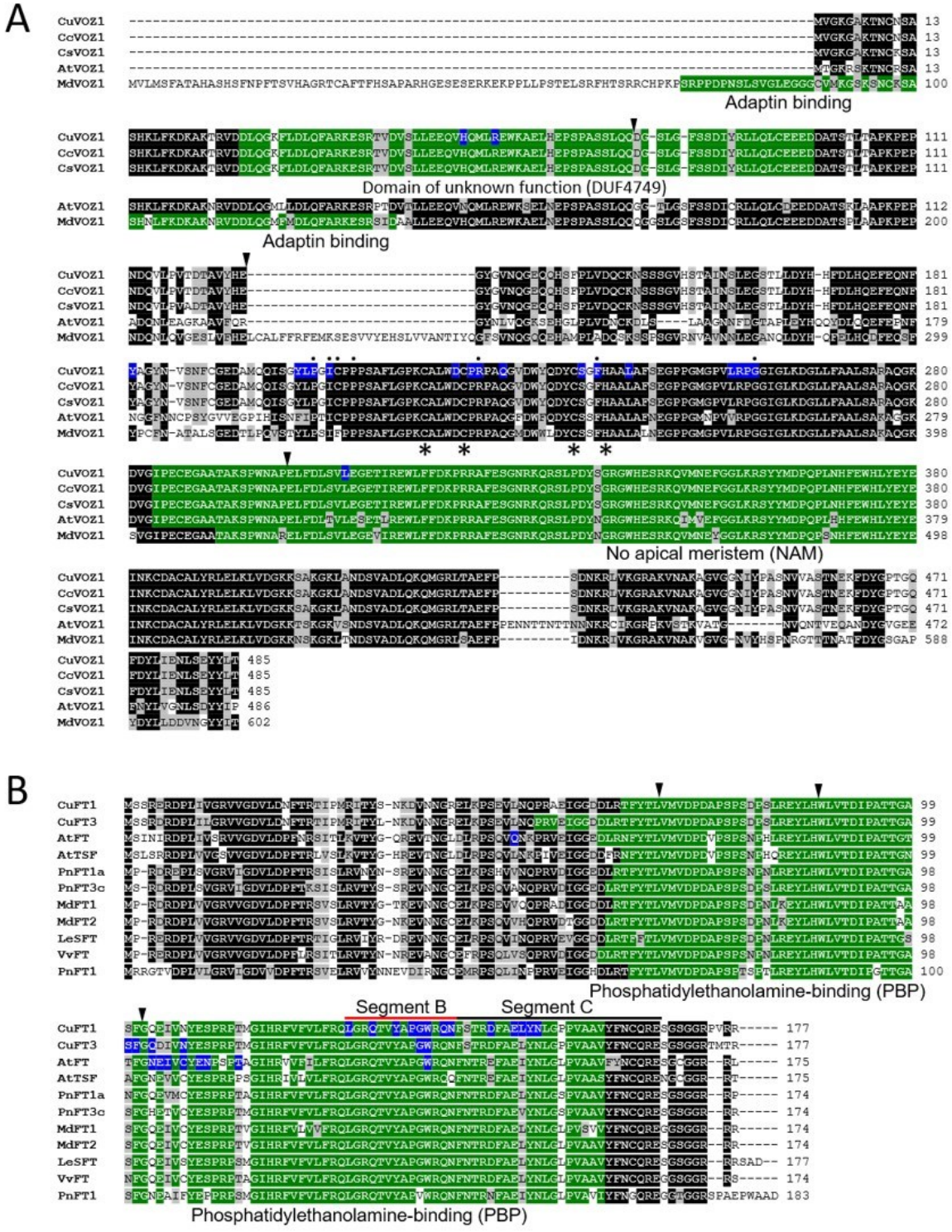

Fig. 2-2. Comparison of the deduced protein sequences of VOZ1 or FT in several plant species. (A) The deduced protein sequence of CuVOZ1 with those of the VOZ1 family proteins from apple, *Arabidopsis*, and citrus (Clementine and sweet orange). The proteins and accession numbers of each gene are CuVOZ1 (Satsuma mandarin, LC729264), MdVOZ1 (apple,

MDP0000729316), AtVOZ1 (*Arabidopsis*, AT1G28520), CcVOZ1 (Clementine, Ciclev10015064m), CsVOZ1 (sweet orange, XP006467710). (B) The deduced protein sequences of CuFT1 and CuFT3 with those of the TFL1/FT family from apple, *Arabidopsis*, grapevine, Lombardy poplar, and tomato. The proteins and accession numbers of each gene are as follows: CuFT1 (Satsuma mandarin, LC729261), CuFT3 (Satsuma mandarin, LC729263), MdFT1 (apple, AB161112), MdFT2 (apple, AB458504), AtFT (*Arabidopsis*, AB027504), AtTSF (*Arabidopsis*, AT4G20370), VvFT (grapevine, DQ871590), PnFT1 (Lombardy poplar, AB106111), PnFT1a (Lombardy poplar, AB161109), PnFT3c (Lombardy poplar, AB110009), and LeSFT (tomato, AY186735). Putative amino acid sequences were aligned using the ClustalX2 multiple-sequence alignment program ver.2.0.5 (Jeanmougin et al., 1998). Amino acids in black and gray are identical and similar, respectively. The gaps indicated by dashes are attributed to the lack of amino acids. The triangles show the intron positions. The green area shows the predicted motif regions. Asterisks represent conserved residues possibly forming a functional zinc-coordinating motif (Mitsuda et al., 2004). Amino acids in blue are in the predicted docking regions when the CuVOZ1 interacts with CuFTs. Amino acids with black dots on the top are associated with the predicted docking regions when the AtFT interacts with CuVOZ1. Red and black lines on the fourth exon of FT family proteins indicate segments B and C regions, respectively, as defined by Ahn et al. (2006).

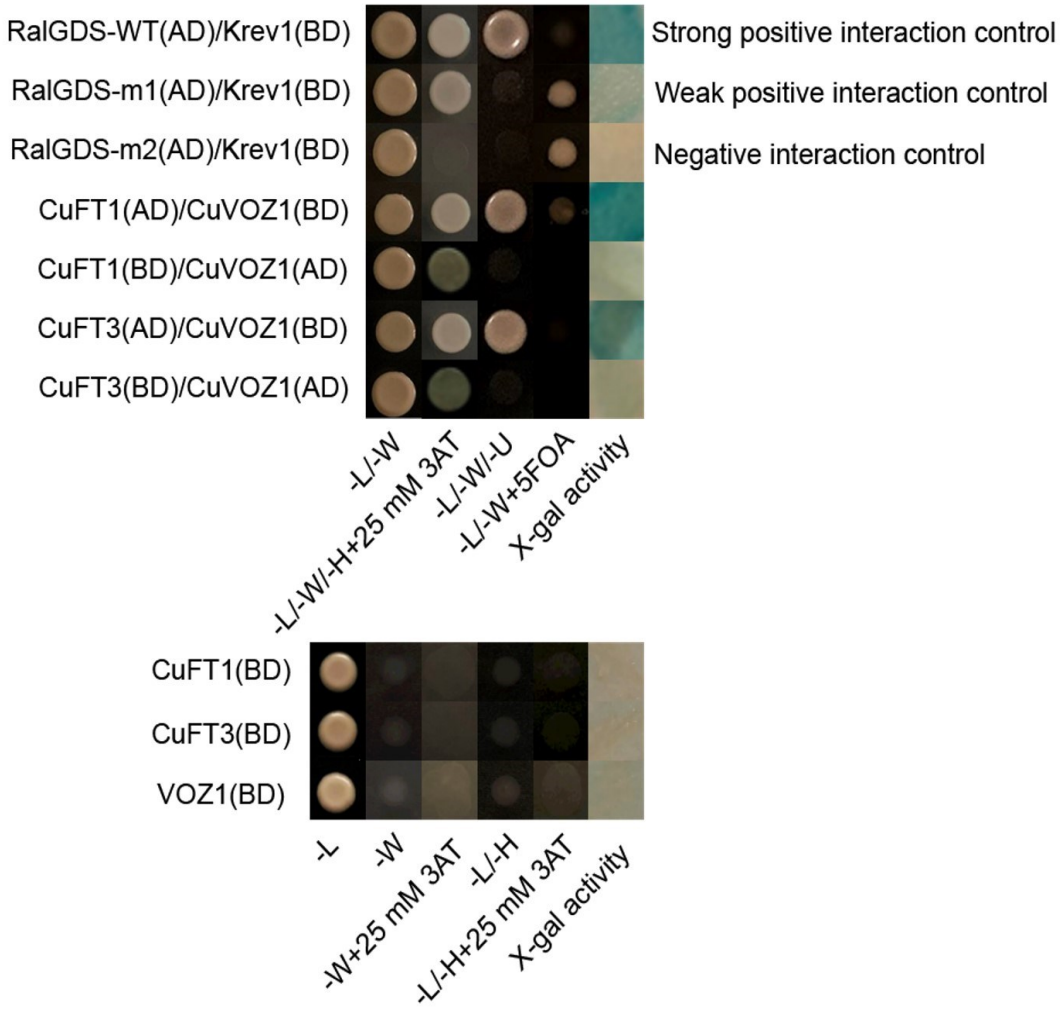

Fig. 2-3. Interactions of CuVOZ1 with CuFTs detected in the yeast two-hybrid system.

Yeast competent cell MaV203 was transformed with a pair of bait and prey plasmids, CuFTs(AD)/CuVOZ1(BD) and CuVOZ1(AD)/CuFTs(BD), using the lithium method. The transformants were grown at 30°C for 48 h. The selection test for the *HIS3* reporter gene of yeast transformants was performed on a selective agar medium with a minimal SD base and –L/–W/–H DO supplement containing 25 mM 3-amino-1,2,4-triazole (3-AT) and 2% glucose. The selection test for the *URA3* reporter gene was performed on SD –L/–W/–Ura DO supplement containing 0.2% 5-fluoroorotic acid (5FOA). A subsequent X-gal (5-bromo-4-chloro-3-indolyl-β-D-galactopyranoside) filter lift assay for ß-galactosidase activity was performed using yeast transformant cells to test with the *LacZ* reporter gene. No effect of self-activation was detected in the constructed vectors (lower panel). The RalGDS-WT(AD)/Krev1(BD) construct was used as a strong positive interaction control, the RalGDS-m1(AD)/Krev1(BD) construct as a weak positive interaction control, and the RalGDS-m2(AD)/Krev1(BD) construct as a negative interaction control.

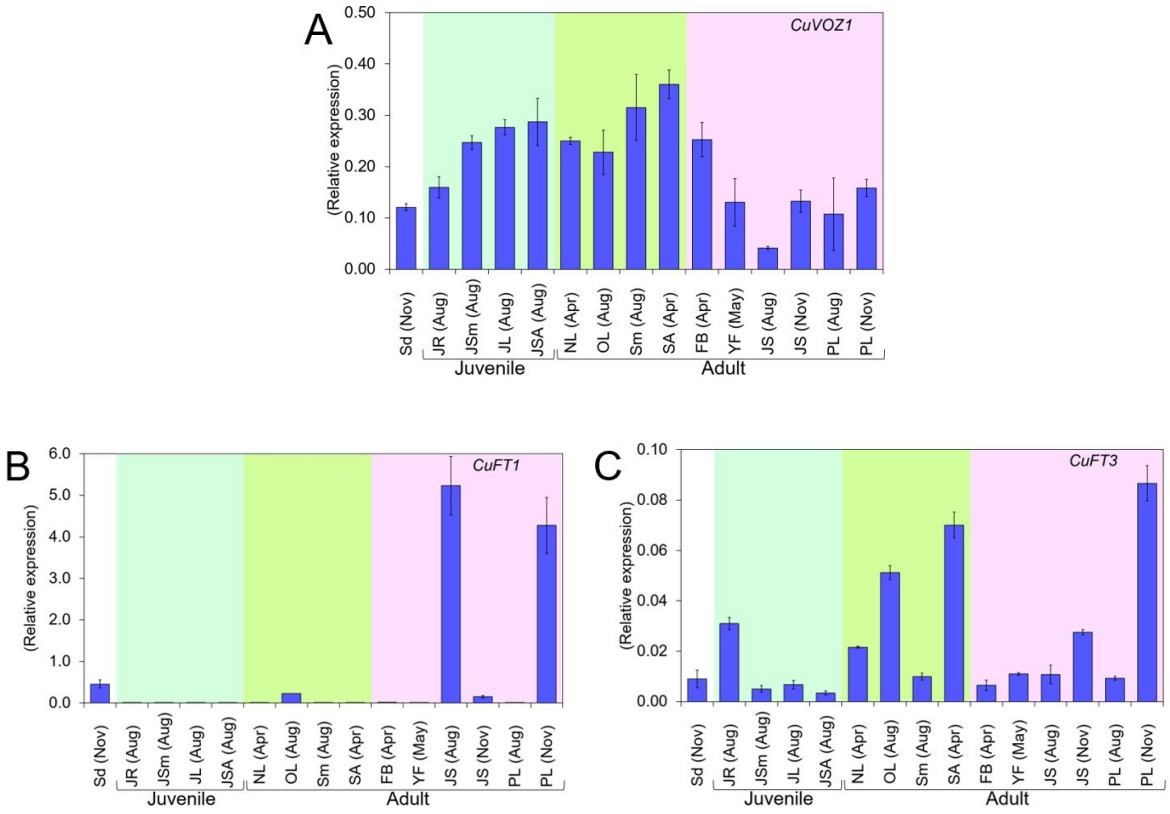

Fig. 2-4. Expression patterns of *CuVOZ1* (A), *CuFT1* (B), and *CuFT3* (C) in various tissues in the Satsuma mandarin 'Aoshima' indicated by quantitative real-time RT–PCR. The samples (left to right) are as follows: seeds (Sd), juvenile roots (JR), Juvenile stems (JSm), leaves from the juvenile plant (JL), and juvenile shoot apices (JSA) of 1-year-old seedlings in the juvenile phase; new leaves (NL), old leaves (OL), stems (Sm) and shoot apices (SA) in the adult phase; flower buds (FB), young fruit (YF), juice sacs (JS) and peels (PL) in the adult reproductive phase. Expression levels were normalized by a citrus actin gene (*CuActin*). Values are means ± SD of results from three technical replicates. A column without an error bar indicates that the standard deviation fell within the symbol.

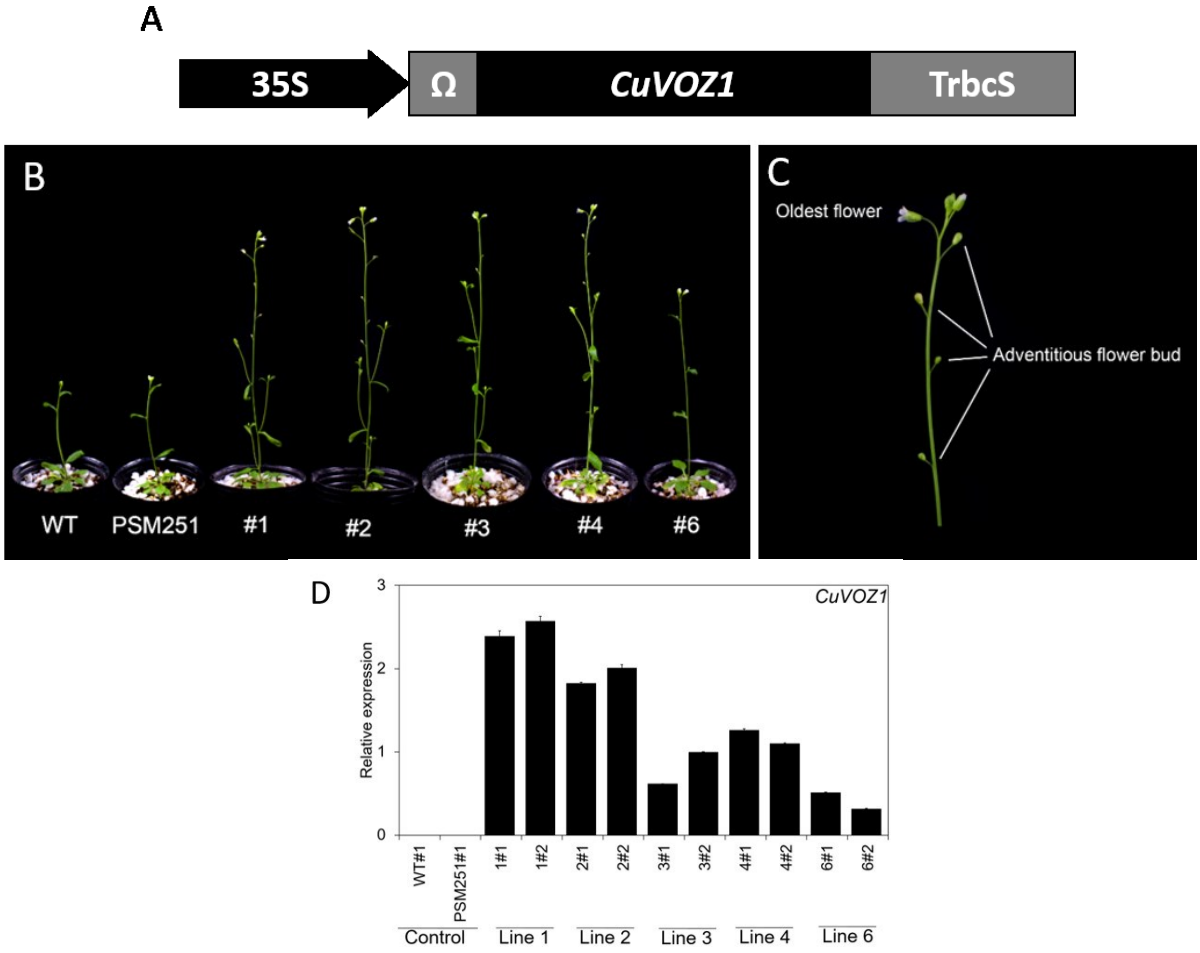

Fig. 2-5. Production of transgenic *Arabidopsis* with *CuVOZ1*. (A) Schematic representation of constructed transformation vector. 35S, promoter region of cauliflower mosaic virus 35S; Ω, Ω sequence responsible for enhancing translation (Gallie and Walbot 1992); TrbcS, 3′ region of *Arabidopsis* rbcS-2B gene. (B) Typical phenotypes of transgenic *Arabidopsis* with *CuVOZ1* at flowering time in a growth chamber under LD conditions. (C) The appearance of an adventitious flower bud in the inflorescence of transgenic *Arabidopsis* with *CuVOZ1*. (D) Expression analysis for transgenes in whole plants of transgenic *Arabidopsis*. The photo was taken on the 22nd day after the start of incubation. Samples for the expression analysis of *CuVOZ1* in transgenic lines were collected 40 days after incubation. WT (wild-type) and PSM251 (transgenic with an empty vector) were used as controls. Levels of detected amplicons were normalized by reference to *AtTUB4*. Values are means ± SD of the results from three technical replicates per line.

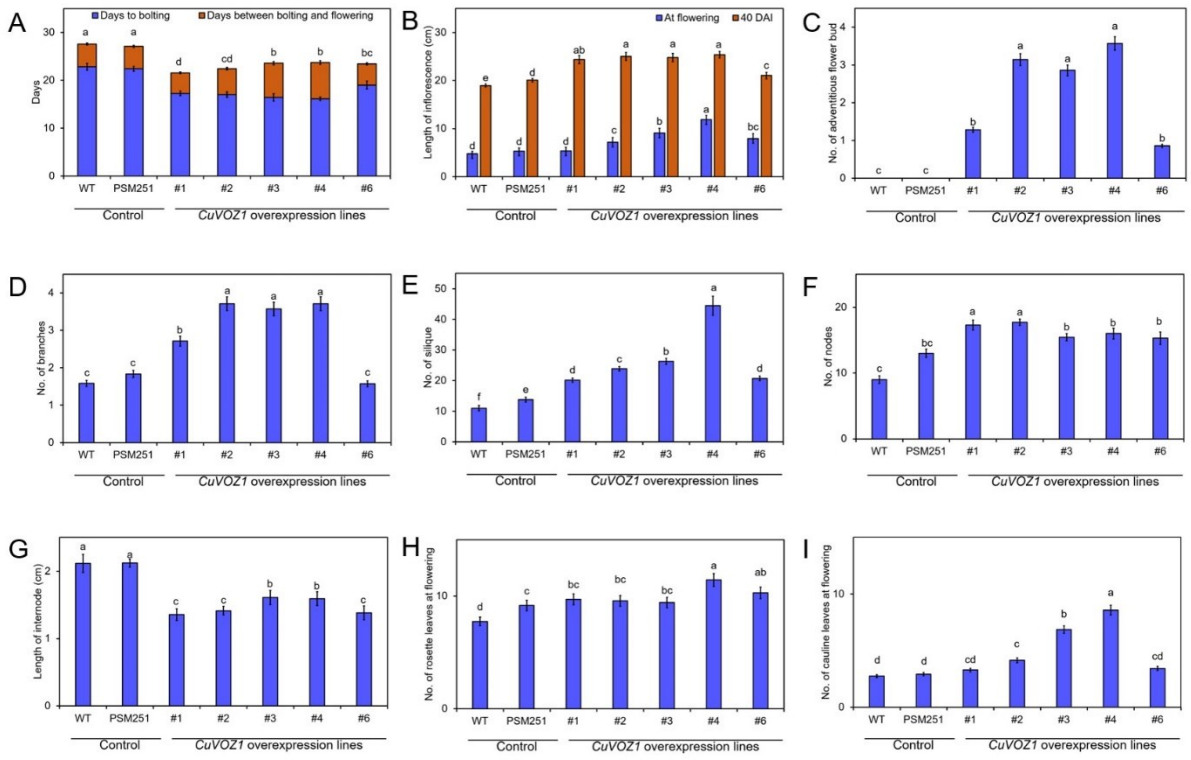

Fig. 2-6. Characteristics of transgenic *Arabidopsis* lines ectopically expressing *CuVOZ1*.
(A) Days to bolting and flowering, (B) length of the first inflorescence, (C) no. of the particular type of lateral flowers, (D) no. of branches, (E) no. of siliques, (F) no. of nodes, (G) length of internodes, (H) no. of rosette leaves, and (I) no. of cauline leaves. The transgenic plants in the third generation (T_3) and the controls were grown under LD conditions. Days to bolting and flowering were counted from the first day of incubation. All the transgenic plants showed early bolting and flowering. The length of the primary inflorescences was measured at flowering and on the 40th day of incubation. The particular types of lateral flowers were counted. The rosette and cauline leaves were counted on the day of the first flowering. Different letters at the top of each bar indicate significant differences among the lines, contrasted by Tukey's honestly significant difference (HSD) test ($P < 0.05$).

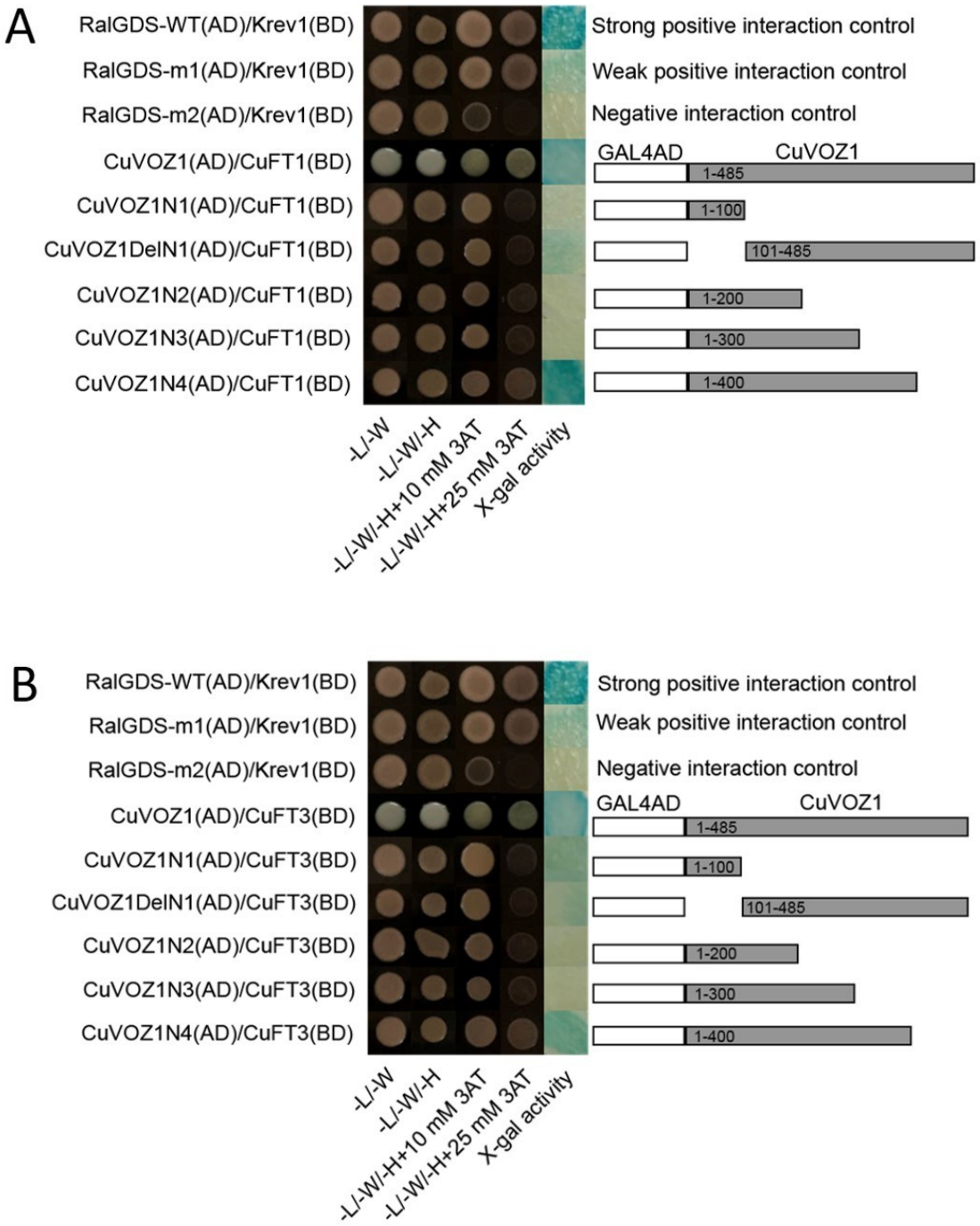

Fig. 2-7. The interaction between the truncated CuVOZ1 and full-length CuFT1 (A) and CuFT3 (B) in yeast. The left panel shows the growth of the transformed yeast cells on SD –L/–W, SD –L/–W/–H, SD –L/–W/–H +10 mM 3-AT, and SD –L/–W/–H +25 mM 3-AT media and a filter assay for β-galactosidase activity of the transformants grown on SD –L/–W/–H media. The right panel illustrates the full-length or truncated version of CuVOZ1 (N1–4, DelN1). The experimental procedure was the same as explained in Figure 3.

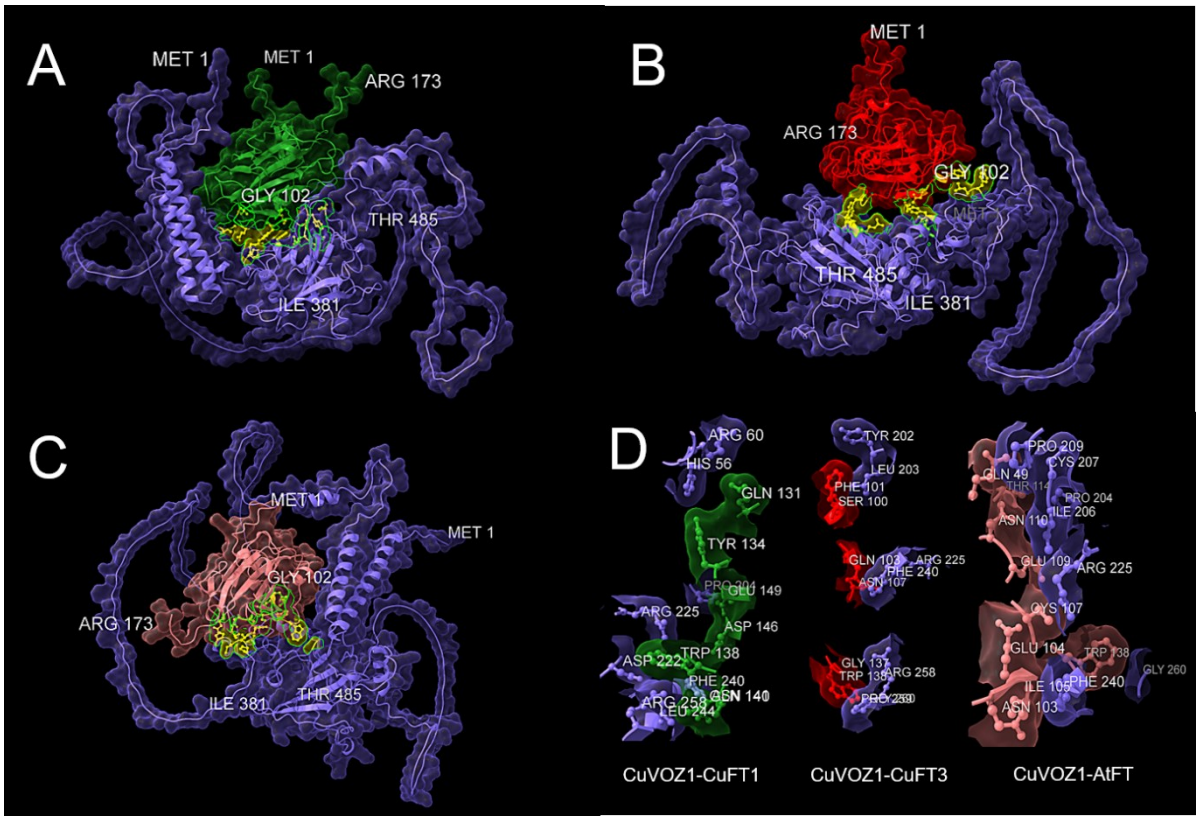

Fig. 2-8. Predicted protein-protein interaction between CuVOZ1 and CuFT1, CuVOZ1 and CuFT3, and CuVOZ1 and AtFT.

(A) Purple and green areas indicate CuVOZ1 and CuFT1, respectively. (B) Purple and red areas indicate CuVOZ1 and CuFT3, respectively. (C) Purple and pink areas indicate CuVOZ1 and AtFT, respectively. (D) Magnified docking regions in the three protein complexes. Some amino acids are hidden behind the 3D structures. The yellow areas in the middle of the three protein complexes indicate possible docking regions. MET1, ILE381, and THR485 for CuVOZ1 and MET1, GLY102, and ARG173 for FTs are displayed for confirmation of the relative position among the complexes. The prediction was calculated with AlphaFold2.ipnyb (Jumper et al. 2021) and visualized with ChimeraX ver. 1.5 (Pettersen et al., 2021).

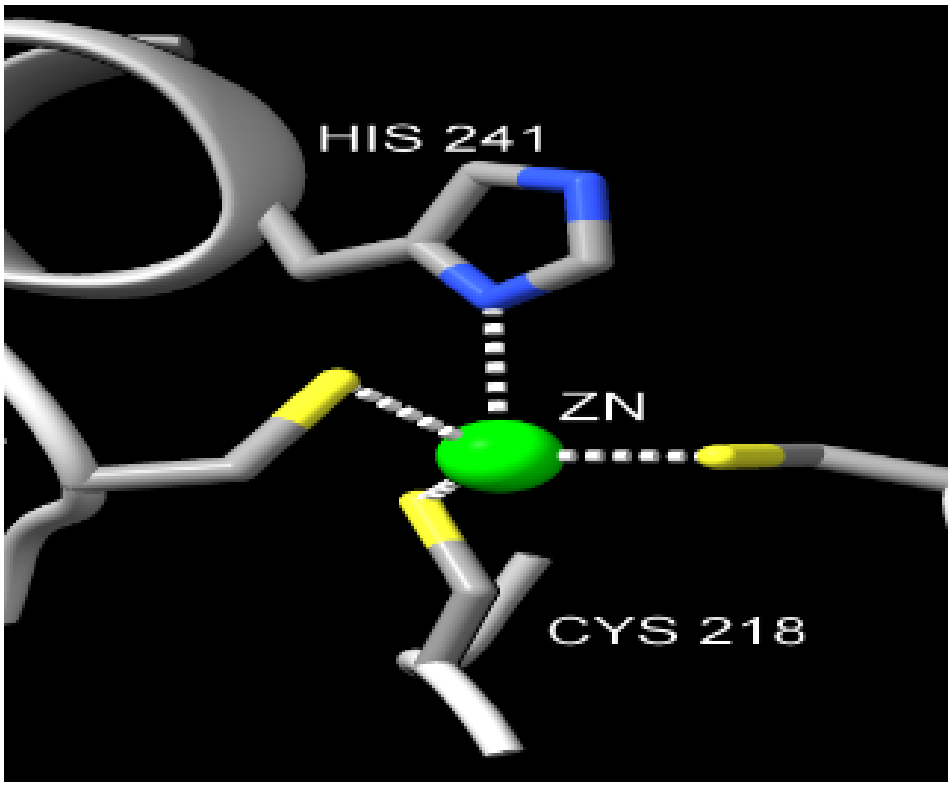

Fig. 2-9. The predicted Zn^{2+} binding site in CuVOZ1 protein.

The prediction of protein-protein interaction was calculated with AlphaFold.ipnyb (Jumper et al., 2021) and visualized with ChimeraX v1.5 (Pettersen et al., 2021). The prediction of the Zn^{2+} binding site was predicted with a metal ion-binding site prediction and modeling server (MIB2) (Lu et al., 2012).

Chapter 3

Molecular characterization of Satsuma mandarin (*Citrus unshiu* Marc.) VASCULAR PLANT ONE-ZINC FINGER2 (CuVOZ2) interacting with CuFT1 and CuFT3

3.1. Introduction

Citrus accounts for a significant portion of commercially cultivated fruit crops around the globe. The selection of ideal commercial and cultural traits in citrus through traditional breeding methods is time-consuming. A long juvenile period of five to ten years hinders the conventional breeding, heredity improvement, genetic studies, and production of citrus depending on the species (Albrigo et al., 2019; Krajewski and Rabe, 1995). The molecular mechanism during the transition from the juvenile vegetative to the adult reproductive phase, which would provide insight into the means of citrus-breeding acceleration, has yet to be elucidated.

In a typical flowering model, *FLOWERING LOCUS T* (*FT*), an integrator of photoperiod and vernalization pathways, acts as a transmissible floral inducer, such as florigen, during the transition from the vegetative to the reproductive phase in *Arabidopsis* (Corbesier et al., 2007; Jaeger and Wigge, 2007; Lin et al., 2007; Mathieu et al., 2007; Notaguchi et al., 2008). In the companion cells of leaves at dusk, FT is induced by photoperiodic signals through CONSTANS (CO) (Andrés and Coupland, 2012; Koornneef et al., 1991; Liu et al., 2013; Mathieu et al., 2007; Putterill and Varkonyi-Gasic, 2016; Samach et al., 2000; Wigge, 2011). Induced FT then translocates to the shoot apical meristem (SAM) through the sieve tube system and forms a complex with transcription factors (TFs), inducing expression of the floral meristem identity genes and promoting flowering (Abe et al., 2005; An et al., 2004; Corbesier et al., 2007; Jaeger and Wigge, 2007; Lin et al., 2007; Tamaki et al., 2007; Wigge et al., 2005). *TERMINAL FLOWER1* (*TFL1*), another member of the PEBP-like gene family, acts as a floral repressor (Bradley et al., 1997; Ohshima et al., 1997). Both FT and TFL1 contain a potential ligand-binding pocket region within the fourth exon. Ahn et al. (2006) demonstrated that the fourth exon, especially segments B and C in that region, plays a critical role in determining the function of TFL1 or FT in *Arabidopsis*. Previous study demonstrated a protein–protein

interaction of MdVOZ1a, apple VASCULAR PLANT ONE-ZINC FINGER (VOZ) 1, a member of the NAC family subgroup VIII-2 TF, with MdFT1 and MdFT2 (MdFTs), two apple FT proteins, in the Y2H system, suggesting the possible involvement of MdVOZ1a in leaf and fruit development through the binding with MdFTs (Mimida et al., 2011).

VOZ is a multifunctional gene regulating various biological processes, such as flower induction and development, pathogen defense, and abiotic stress responses (Li et al., 2020). VOZ transcription factors are present exclusively in higher plants, including vascular plants (Mitsuda et al., 2004). In *Arabidopsis,* VOZ1 and VOZ2 have a zinc-finger motif and transcriptional activator activities (Jensen et al., 2010; Mitsuda et al., 2004). Despite the differences in the lengths of the amino acid sequences, molecular weights, and sequence similarities between AtVOZ1 and AtVOZ2, they are redundantly involved in flowering, positively regulated in response to heat stress, salinity stress, and fungal or bacterial infections, and negatively regulated in response to cold and drought stress (Koguchi et al., 2017a; Mitsuda et al., 2004; Nakai et al., 2013a; Prasad et al., 2018; Song et al., 2018). *AtVOZ1* is especially expressed in the phloem, but *AtVOZ2* is abundantly expressed in *Arabidopsis* roots. *OsVOZ1* acts as a negative regulator in rice, but *OsVOZ2* functions as a positive regulator to resist the fungal pathogen *Magnaporthe oryzae* (Wang et al., 2021). In addition, *VOZ*s repress a floral repressor, *FLOWERING LOCUS C* (*FLC*), independently and activate *FT* to promote flowering. Modulation of the function of the CO protein by VOZs also contributes to promoting *FT* expression and photoperiodic flowering in *Arabidopsis* (Koguchi et al., 2017a; Kumar et al., 2018; Nakai et al., 2013b, 2013a; Song et al., 2018; Yasui et al., 2012; Yasui and Kohchi, 2014). Previous reports suggest that VOZ transcription factors play crucial roles in regulating plant growth and development and have important application values in the genetic improvement of stress resistance in crops.

However, in woody plants, the mechanism of protein–protein interaction between VOZs and FT and further regulation of flowering/fruiting have yet to be investigated. In addition to the protein–protein interaction between MdVOZ1a and MdFTs (Mimida et al., 2011), the interaction between citrus CuVOZ1 and CuFTs (CuFT1 and CuFT3) in the Y2H system was recently reported (Hasan et al., 2023). Therefore, in this study, the protein–protein interactions between the other VOZ (CuVOZ2) from the Satsuma mandarin 'Aoshima' and CuFTs were elucidated with some methods of Y2H, deletion mutation and docking simulation. The characterization of *CuVOZ2* was also performed using transgenic *Arabidopsis*.

3.2. Materials and Methods

3.2.1. Plant materials

The adult vegetative [apices (April), new leaves (April), old leaves (August), and stems with a node (August)] and reproductive [flower buds (April), young fruit (May), juice sacs (August and November), and peels (August and January)] tissues of the Satsuma mandarin (*Citrus unshiu* Marc.) 'Aoshima' were collected in 2018 from the Saga Prefectural Fruit Tree Experiment Station in Ogi, Japan. The juvenile vegetative tissues (roots, stems, leaves, and apices) were collected in August 2019 from 20-month-old seedlings grown at Saga University. Seeds of 'Aoshima' were collected in January 2020. Transgenic *Arabidopsis* plants were grown under long-day (LD) conditions in an incubator (Biotron; Nippon Medical and Chemical Instruments Co., Ltd., Tokyo, Japan). All collected tissues/plants were immediately frozen with liquid nitrogen and preserved in a freezer at -70°C until RNA extraction.

3.2.2. Isolation of CuVOZ2 from the Satsuma mandarin 'Aoshima'

Total RNA was extracted from tissues using the cetyltrimethylammonium bromide (CTAB) method (Kotoda et al., 2000). A reverse transcription (RT) reaction was performed using ReverTra Ace® qPCR RT Master Mix FSQ-301 (TOYOBO Co., Ltd., Osaka, Japan) with the extracted RNA from new leaves. The cDNA was amplified from the RT product by polymerase chain reaction (PCR) using KOD Plus Neo (TOYOBO). After attachment of the adenine nucleotide, the amplified PCR products were cloned into pGEM®-T Easy vectors (Promega, Madison, WI, USA). Several clones were sequenced and confirmed using an ABI PRISM 3130xl Genetic Analyzer (Life Technologies, Carlsbad, CA, USA). The isolated genes were designated as *CuVOZ2* (acc. no. LC729265). The oligonucleotide primer sets used in gene cloning are listed in Table 3-1.

3.2.3. Phylogenetic analysis and comparison of amino acid sequences

Putative amino acid sequences were analyzed using the ClustalX2 multiple-sequence alignment program ver. 2.0.5 (Jeanmougin et al., 1998) and the BioEdit program ver. 7.2.5 (Hall, 1999) with known genes from other plant species to clarify the phylogenetic relationship of the *VOZ2* gene in citrus. A phylogenetic tree was produced by the neighbor-joining (N-J) method for the deduced amino acid sequences of *VOZ* genes from apple [*Malus* × *domestica* (MDP0000729316, MDP0000879912, and MDP0000296843)], *Arabidopsis* (AT1G28520 and AT2G42400), Clementine [*Citrus clementina* (Ciclev10015064m and Ciclev10015076m)], maidenhair fern [*Adiantum capillus-veneris* (KAI5077272)], Lombardy poplar [*Populus nigra* (Potri.004G050900 and Potri.019G092800)], rice [*Oryza sativa* (LOC_Os01g54930 and LOC_Os05g43950)], Satsuma mandarin (LC729264 and LC729265), and sweet orange [*Citrus sinensis* (XP006467710 and XP006469061)]. The deduced proteins of the TFL1/FT family from plant species used in the amino acid comparison are MdFT1 (AB161112) and MdFT2 (AB458504) in apple; AtFT (AT1G65480) and AtTSF (AT4G20370) in *Arabidopsis*; VvFT (DQ871590) in grapevine (*Vitis vinifera*); PnFT1 (AB106111), PnFT1b (AB161109), and PnFT3c (AB110009) in Lombardy poplar; CuFT1 (LC729261) and CuFT3 (LC729263) in Satsuma mandarin; and LeSFT (AY186735) in tomato (*Solanum lycopersicum*). The phylogenetic tree for VOZ2 was displayed using the N-J plot with bootstrap values for 1000 trials in each branch.

3.2.4. Yeast two-hybrid (Y2H) assay

The *att*B-flanked PCR products for the entire coding regions of *CuVOZ2* or *CuFTs* (*CuFT1* and *CuFT3*) or the truncated region of *CuVOZ2* were introduced into a pDONR221 vector (Invitrogen, Life Technologies Corp., Carlsbad, CA, USA) in-frame as a donor vector.

Each entry clone was introduced into a pDEST22 (ampicillin^{R}) to construct the expression vector with the GAL4 activation domain (GAL4 AD) (prey). The constructs were designated as CuVOZ2 (AD), CuFT1 (AD) and CuFT3 (AD). The truncations were constructed by gradual deletion of the C-terminal region or deletion of the N-terminal region. The truncated version of CuVOZ2 was designated as CuVOZ2N1 (AD) (1 –100aa), CuVOZ2DelN1 (AD) (101–485aa), CuVOZ2N2 (AD) (1–200aa), CuVOZ2N3 (AD) (1–300aa) and CuVOZ2N4 (AD) (1–400aa). Similarly, the constructs produced with pDEST32 (gentamicin^{R}) for GAL4 DBD (bait) were designated as CuVOZ2 (BD), CuFT1 (BD) and CuFT3 (BD). Yeast (*Saccharomyces cerevisiae*) strain MaV203 (MATα, *leu*2-3,112, *trp*1-901, *his*3Δ200, *ade*2-101, *gal*4Δ, *ga*l80Δ, *SPAL*10::*URA*3, *GAL*1::*lac*Z, *HIS*3$_{\text{UAS GAL1}}$::*HIS*3@*LYS*2, *can*1^{R}, *cyh*2^{R}) (Vidal, 1997) was transformed with several combinations of AD and BD plasmids according to the lithium method (Gietz and Woods, 2002). Single AD yeast transformants were screened on a selective agar medium with a minimal synthetic defined (SD) base with a –L dropout (DO) supplement (Clontech Laboratories Inc., Mountain View, CA, USA) containing 2% glucose. Single BD transformants were screened on SD –W media. Yeast co-transformed with AD and BD constructs was selected on SD –L/–W media. Co-transformed yeasts were incubated on SD –L/–W/–H media to confirm induction of the *HIS3* gene and the protein–protein interaction. To prevent self-activation of the *HIS3* reporter gene, 25 mM of 3-amino-1,2,4-triazole (3-AT), a *HIS3* inhibitor, was added to the media. The yeasts with the same combination were grown on SD –L/–W/–U media to confirm the activity of the *URA3* reporter gene. For selection against positive interactions, 0.2% 5-fluoroorotic acid (5FOA) was used. All the yeasts were grown at 30°C for 48 h. The protein–protein interactions between CuVOZ2 and CuFTs were also confirmed by the colony filter lift assay.

3.2.5. Docking simulation

The three-dimensional (3D) structure of the proteins and the protein–protein interaction were simulated based on the cDNA sequences of *CuVOZ2*, *CuFT1*, and *CuFT3* to better understand the results obtained in the Y2H system. A deep-learning neural network was applied to predict possible docking regions to understand how CuVOZ2 and CuFTs interact. The protein modeling and interaction were predicted in AlphaFold2_advanced.ipynb (Jumper et al., 2021), a Web-based iPython Notebook service for interactive coding supported by Google. The artificial intelligence predicted and constructed models of protein–protein complex structures using several protein sequence databases and multiple-sequence alignment. The metal ion-binding site was predicted with the help of the Metal Ion-Binding site prediction and modeling server (MIB2) (Lu et al., 2012). Visualizations of protein models and predictions of docking regions were created using ChimeraX ver. 1.5 (Pettersen et al., 2021).

3.2.6. Vector construction and Arabidopsis transformation

The oligonucleotide primers of VOZ2_XbaI_F and VOZ2_KpnI_R (Table 1) were used to amplify the coding region of *CuVOZ2* to construct a binary vector for plant transformation. The amplified product was digested with *Xba*I and *Kpn*I and cloned into the corresponding restriction enzyme sites of the 35SΩ/pSMAK193E plant-transformation vector (Kotoda et al., 2010). The floral-dip method (Bent and Clough, 1998; Clough and Bent, 1998) was used to transform wild-type *Arabidopsis* with *Agrobacterium tumefaciens* EHA101. Kanamycin-resistant transgenic seedlings were transplanted from the plate to moistened soil (vermiculite: perlite = 1:1) at the two-leaf stage and incubated in a growth chamber (Biotron; Nippon Medical and Chemical Instruments Co., Ltd.) at 22°C under long-day (LD) conditions (16 h photoperiod; cool white fluorescent light, 72.36 $\mu mol \cdot m^{-2} \cdot s^{-1}$). Transgenic plants with an empty vector of pSMAK251 (indicated as PSM251) were used as the control. Morphological and

expression analyses were performed on the third-generation (T_3) transgenic plants. The number of days to bolting and flowering was tracked. Rosette and cauline leaves were counted at flowering time. The length of the first inflorescence was measured at flowering and 40 days after incubation (DAI). The branches, siliques, and nodes were also counted at 40 DAI. An entire transgenic or control plant was collected for qRT-PCR analysis.

3.2.7. Expression analysis in the Satsuma mandarin 'Aoshima' and transgenic Arabidopsis

Expression analysis of *CuVOZ2* was carried out via qRT-PCR. One microgram of RNA was used to synthesize the first-strand cDNA in 20 μL of a reaction mixture using a ReverTra Ace® qPCR RT Master Mix (TOYOBO). One microliter of the first-strand cDNA was used as a template in SYBR® Green RealTime PCR Master Mix (TOYOBO) for a total volume of 12.5 μL. The qRT-PCR was performed using a LightCycler® 96 System (Roche Diagnostics, Mannheim, Germany) as follows: 95°C for 1 min, 40 cycles of 95°C for 15 s and 60°C for 1 min for *CuVOZ2*, *CuActin*, and *AtTUB*. Three technical replicates were maintained for each analysis. *CuActin* was used as a reference gene to normalize the transcript levels of *CuVOZ2* (Kotoda et al., 2016). *AtTUB4* was used as a reference gene to normalize the transcript levels of *CuVOZ2* in transgenic *Arabidopsis*. The primer sets used in the experiment are listed in Table 3-1.

3.2.8. Statistical analysis

Data on the number of days to bolting and flowering; the numbers of leaves, nodes, and siliques; and the length of the first inflorescence were analyzed using one-way ANOVA, and the multiple comparison was done by Tukey's honestly significant difference (HSD) test. Statistical analyses were performed at a significance level of $P < 0.05$ using RStudio v.1.2.5089 (RStudio Team, 2020).

3.3. Results

3.3.1. Isolation of CuVOZ2 from the Satsuma mandarin 'Aoshima'

The cDNA of *CuVOZ2* was isolated from the Satsuma mandarin 'Aoshima' to investigate the function of *CuVOZ2.* The *CuVOZ2* gene consisted of four exons of 225, 156, 514, and 557 base pairs (bp) encoding a putative protein of 483 amino acids, which was also confirmed by next-generation sequencing (NGS) of the 'Aoshima' genome (Fig. 3-1A). The length of the coding sequence was 1452 bp. A phylogenetic analysis using the putative amino acid sequences corresponding to *VOZ* genes from apple, *Arabidopsis*, citrus (Satsuma mandarin, Clementine, and sweet orange), maidenhair fern, poplar, and rice was performed to understand the evolutionary relationship among those genes. The phylogenetic tree revealed that CuVOZ2 was closely clustered with the VOZ2 of Clementine and sweet orange and with the same clade as AtVOZ2, MdVOZ2, and PtVOZ2 (Fig. 3-1B).

The sequence of CuVOZ2 was 100% identical to that of CcVOZ2, 99.17% identical to that of CsVOZ2 and 53.86% identical to that of previously isolated CuVOZ1 (LC729264) at the amino acid level. The motif search tool using the Pfam database showed that the amino acid sequence of CuVOZ2 contains a C-terminal beta pleated sheet identified as a no apical meristem (NAM) (289–388aa) motif (Finn et al., 2016) (Fig. 3-2A, green regions). One motif, named the phosphoethanolamine-binding protein (PBP), was identified in the latter region in the sequence of TFL1/FT family proteins, including CuFT1 (LC729261) and CuFT3 (LC729262). The similarities between CuVOZ1 and AtVOZ1 and between CuVOZ1 and AtVOZ2 were 79% and 54%. similarities between CuVOZ2 and AtVOZ1 and between CuVOZ2 and AtVOZ2 were 61% and 57%, respectively.

3.3.2. Expression pattern of CuVOZ2

The tissue-specific expression pattern of *CuVOZ2* was examined using qRT-PCR. *CuVOZ2* was expressed in various tissues, as shown in Fig. 3-3. The expression was relatively high in shoot apices in both the juvenile and adult phases and in stems in the juvenile phase. However, the expression was lower in the reproductive tissues, such as juice sacs and peels in November. The expression was moderate in other tissues at the vegetative and reproductive stages.

3.3.3. Interactions of CuVOZ2 with CuFT1 or CuFT3 in the Y2H system

Auxotrophy assays for *HIS3* and *URA3* reporter genes, sensitivity tests for 5FOA, and X-gal filter lift assays for the *LacZ* reporter gene were performed using the yeast transformants harboring a pair of bait and prey plasmids [CuFT1 (AD)/CuVOZ2 (BD), CuFT1 (BD)/ CuVOZ2 (AD), CuFT3 (AD)/CuVOZ2 (BD), and CuFT3 (BD)/CuVOZ2 (AD)] to investigate the protein–protein interactions in the Y2H system. All the yeast constructs that grew on SD–L/–W/–H + 25 mM 3-AT showed the induction of the *HIS3* reporter gene in the His auxotrophy assays (Fig. 3-4A). Growth induction of the yeasts containing CuFT1 (AD)/CuVOZ2 (BD) and CuFT3 (AD)/CuVOZ2 (BD) constructs on an SD –L/–W/–U media plate in the Ura auxotrophy assay and growth inhibition of all constructs on an SD –L/–W + 5FOA media plate in the 5FOA sensitivity assay confirmed the activity of the *URA3* reporter gene. However, the yeasts containing CuVOZ2 (AD)/CuFT1 (BD) and CuVOZ2 (AD)/CuFT3 (BD) constructs did not show growth induction on the SD –L/–W/–U media plate. The indigo coloration in the X-gal filter assay confirmed the activity of the *LacZ* reporter gene. The growth inhibition of all the BD constructs tested on SD–W or SD–L/–H media plates and the colony filter lift assay showed that any single constructs were not self-activated (Fig. 3-4B).

3.3.4. Identification of binding regions using the Y2H system

A series of truncated CuVOZ2 proteins were fused with the GAL4 activation domain (GAL4 AD) to identify the region of interaction between CuVOZ2 and CuFT1 (Fig. 3-4C) and between CuVOZ2 and CuFT3 (Fig. 3-4D). In Y2H assays, constructs of the CuVOZ2 truncation series (AD)/CuFTs (BD) showed inhibited growth in the SD –L/–W/–H + 25 mM 3-AT media and less blue coloration in the X-gal assay except for the CuVOZ2N4 (AD)/CuFT (BD) constructs. Both the CuVOZ2N4 (AD)/CuFT1 (BD) and CuVOZ2N4 (AD)/CuFT3 (BD) constructs showed normal growth in the SD –L/–W/–H + 25 mM 3-AT media, and the indigo coloration in the X-gal assay was similar to that of the full-length CuVOZ2 (AD)/CuFT (BD) constructs. These observations indicated that CuFTs showed little interaction with C-terminal truncations of CuVOZ2 [(N1, 1–100aa), (N2, 1–200aa), and (N3, 1–300aa)] and an N-terminal truncation of CuVOZ2 (DelN1, 101–485aa) on the SD –L/–W/–H + 25 mM 3-AT media plate and X-gal assay but showed an apparent interaction with the CuVOZ2N4 region, which consisted of 1–400aa in the N-terminal region (Fig. 3-4C and D).

3.3.5. Docking simulation

The predicted amino acid residues associated with the interaction between CuVOZ2 and CuFT1 in the CuVOZ2-CuFT1 complex were as follows: Pro198, Asn199, Leu201, Ile203, His205, Arg223, Ser236, Phe238, Arg255, and Pro256 in CuVOZ2 (Fig. 3-2A and 3-5A) and Arg62, Ser100, Phe101, Gln103, Glu104, Asn107, Arg130, Gln131, Tyr134, Gly137 and Trp138 in CuFT1 (Fig. 3-2B and 3-5A). The predicted amino acid residues associated with the interaction between CuVOZ2 and CuFT3 in the CuVOZ2-CuFT3 complex were as follows: Ser200, Leu201, Pro202, Ile203, His205, and Phe235 in CuVOZ2 (Fig. 3-2A and 3-5B) and Pro75, Asp79, Ser80, Leu81, Pro113, Thr114, Met115, and Gln140 in CuFT3 (Fig. 3-2B and 3-5B). The common amino acid residues associated with docking in both complexes were

Leu201, Ile203, His205, and Phe238 in CuVOZ2 (Fig. 3-2A). No common amino acid residues involved in docking were found for CuFTs. All the predicted amino acid residues of CuVOZ2 involved in docking in the CuVOZ2–CuFT complexes were in the third exon. In the CuVOZ2–CuFT3 complex, one hydrogen bond was observed between the Ser200 of CuVOZ2 and the Pro113 of CuFT3 (Fig. 3-2 and 3-5C). The Zn^{2+} ion binding site for CuVOZ2 was predicted in the third exon, bonded by Cys216, Cys221, Cys235, and His241 (Fig. 3-5D).

3.3.6. Analysis of CuVOZ2 in transgenic Arabidopsis

The constitutive expression construct of 35SΩ:*CuVOZ2* (Fig. 3-6A) was introduced into wild-type *Arabidopsis* to elucidate the possible role of *CuVOZ2* in transgenic *Arabidopsis* using the heterologous system. About 30 independent transgenic lines were obtained. The T_3 transgenic plants were grown in an incubator under LD conditions, and five independent lines (n = 14) were phenotyped together with the controls (Fig. 3-6B). In addition to the phenotypic analyses, the transgene expression in five independent lines was confirmed via qRT-PCR. All transgenic lines with 35SΩ:*CuVOZ2* expressed the transgene. Among the transgenic plants, lines 2 and 9 showed higher expression as compared to lines 1, 4, and 10 (Fig. 3-6C). Several parameters were taken into consideration to analyze the characteristics of transgenic *Arabidopsis.* 35SΩ:*CuVOZ2* induced early flowering in all transgenic lines (Fig. 3-6B and 3-7A). The inflorescence was significantly elongated at flowering in lines 1, 9, and 10 and 40 DAI in lines 2 and 9 (Fig. 3-7B). The number of branches in line 1 was higher, whereas that of line 10 was significantly lower. The number of siliques in lines 1, 2, 4, and 9 was significantly higher. There was no significant difference in the number of nodes for transgenic lines 1, 2, and 3 (Fig. 3-7E), whereas the length of internodes in transgenic lines 2 and 10 was significantly higher (Fig. 3-7F). The number of rosette or cauline leaves did not show a significant difference at flowering time except in one line (Fig. 3-7G, H). The lines with a

higher expression of the transgene showed a phenotype of significantly early flowering and long inflorescence (Fig. 3-6C and 3-7A, B).

3.4. Discussion

Although Jensen et al. (2010) classified VOZ as a member of the NAC family subgroup VIII-2, Gao et al. (2018) classified VOZ genes as an independent gene family. In the VOZ family, 635 members have been identified in 166 plant species and listed in PlantTFDB, a plant TF database (Jin et al. 2017; Tian et al. 2020). The exon/intron structural diversity plays a crucial role in the evolution of plant gene families (Long et al., 1995; Xu et al., 2012). Similarly to *AtVOZ2*, the genomic DNA of *CuVOZ2* was comprised of four exons and three introns in the coding regions (Fig. 3-1A).

A phylogenetic tree based on the deduced amino acid sequences was constructed to evaluate the evolutionary relationships of 17 putative *VOZ* genes from different species, including the isolated *CuVOZ2* gene from the Satsuma mandarin. The phylogenetic tree revealed that CuVOZ2 was closely clustered with the VOZ2 of the Clementine and sweet orange and with the same clade as AtVOZ2, although the similarities between CuVOZ2 and AtVOZ1 and between CuVOZ2 and AtVOZ2 were 61% and 57%, respectively. Interestingly, CuVOZ2 seems to be more closely related to VOZ2 proteins of dicots rather than to those of monocots such as rice (Fig. 3-1B). These results indicated that CuVOZ2 might have functioned like AtVOZ2 (Fig. 3-1B). The differentiation of VOZ transcription factors seems to have occurred after the divergence of monocotyledons and dicotyledons (Shi et al., 2022).

Different VOZ family members contained highly conserved domains that might be closely related to their identical or similar regulatory functions (Koguchi et al., 2017b). No apical meristem (NAM) motif (PF02365) was identified in the VOZ family genes during the motif search (Fig. 3-2A). The NAM motif in CuVOZ2 might play a role in determining the position of the meristem and primordia. On the other hand, CuVOZ2 did not have a DUF4749

(PF15936) motif (Finn et al., 2016), the characteristic feature of CuVOZ1 (LC729264) (Fig. 3-2A).

CuVOZ2 was expressed in various tissues of the Satsuma mandarin (Fig. 3-3). The expression was higher in vegetative tissues (especially juvenile and adult shoot apices and the juvenile stem) than in reproductive tissues. According to the report of Nishikawa et al. (2007), *CiFT1*, corresponding to *CuFT1*, was expressed exclusively in juice sacs and peels, and *CiFT3*, corresponding to *CuFT3*, was expressed in vegetative tissues, such as the adult stem and leaves. *CuVOZ2* was also expressed in tissues where *CiFT1* and/or *CiFT3* were expressed (Fig. 3-3). *AtVOZ2*, coding a vacuolar H^+-pyrophosphatase (V-PPase) promoter-binding protein, is expressed in roots, shoots, leaves, flowers, siliques, and suspension cultures in *Arabidopsis* (Mitsuda et al., 2004). The expression pattern of *CuVOZ2* was similar to that of *AtVOZ2* in that both genes were expressed preferentially in roots, shoots, flower buds, and siliques/fruit. AtVOZ1 and AtVOZ2 act as positive regulators of plant flowering by modulating and interacting with CONSTANS (CO), and they are able to bind to the *cis*-acting region of the *A. thaliana* V-PPase gene (*AVP1*), which regulates auxin-mediated organ development and enhances NaCl and drought tolerance (Gaxiola et al., 2001; Kumar et al., 2018; Li et al., 2005; Prasad et al., 2018; Yasui and Kohchi, 2014). The *AVP1* expression was increased by the upregulation of *VOZ1* in the transgenic soybean (Han et al., 2021), assuming that the VOZ2–FT protein complex may affect the activity of V-PPase and/or the function of FT and play an additional role in flower/fruit development and ripening.

MdVOZ1a from the apple was reported for the first time to interact with MdFT1 and MdFT2 in a Y2H system (Mimida et al., 2011). In this study, CuVOZ2 from the Satsuma mandarin also exhibited protein–protein interaction with CuFTs in the Y2H system (Fig. 3-4A). Strong positive interactions were confirmed in yeast cells with the combinations of CuFT1 (AD)/CuVOZ2 (BD) and CuFT3 (AD)/CuVOZ2 (BD). Swapping AD and BD could alter the

steric force between the proteins and affect the N-terminal region (Wang et al., 2019); hence, the opposite combination of AD and BD may have shown weak interaction in the Y2H system. The binding region between two proteins was investigated using a truncation series of CuVOZ2 as AD and full-length CuFTs as BD constructs. The truncated construct containing N-terminal 400 amino acids of CuVOZ2 showed a detectable protein–protein interaction between CuVOZ2 and CuFTs (Fig. 3-4C, D). Based on the results of the truncation series, it was suggested that the region of the 1st to 400th amino acid of CuVOZ2 was required, at least for the successful interaction.

Besides the Y2H, simulations predicting 3D models of CuVOZ2–CuFT1 and CuVOZ2–CuFT3 complexes were performed to validate the results of the Y2H assay (Fig. 3-5A, B). Ten amino acid residues in the third exon of CuVOZ2 were involved in docking with CuFT1, and six amino acid residues in the same region were involved in docking with CuFT3 in the CuVOZ2–CuFT1 and CuVOZ2–CuFT3 complexes, respectively (Fig. 3-2A). No amino acid residues were found in NAM motif regions involved in docking in CuVOZ2–CuFT1 and CuVOZ2–CuFT3 complexes. Four amino acids involved in binding with CuFTs, Leu201, Ile203, His205, and Phe238, were common in the third exon of CuVOZ1. The difference in the position of associated amino acids between CuFT1 and CuFT3 might be explained by the difference in their 3D structures, leading to the functional divergence of CuFT1 and CuFT3. The AtVOZ proteins have two distinct conserved regions: N-terminal Domain A, including a stretch of amino acids, and a C-terminal Domain B, also known as the VOZ domain. The third exon of AtVOZ1 and AtVOZ2 contains the zinc-coordination motif with three conserved cysteines and one histidine residue that is required for the DNA-binding and dimerization of VOZ family proteins (Mitsuda et al., 2004). The zinc-finger motif of CuVOZ2 was found to be responsible for interaction with CuFTs (Fig. 3-2A and 3-5D). A single zinc finger possesses four amino acids at positions −1, 2, 3, and 6 of the α-helix that participate in hydrogen-bond

interactions with three to four nucleic acids within the major groove of the DNA (Wolfe et al., 2000). A hydrogen bond was identified in the protein complex of CuVOZ2–CuFT3 between CuVOZ2 Ser200 and CuFT3 Pro113 with a distance of 2.96 Å (Fig. 3-5C). The Zn^{2+} stabilizes the fold by binding with four amino acid residues, Cys216, Cys221, Cys235, and His239, with predicted molecular distances of 2.11-2.63 Å (Fig. 3-5D).

The amino acid residues of CuFTs involved in the interactions were found in the PBP motif region. The distance between the residues was predicted to be 1.09–4.37 Å, suggesting that the interaction forces between CuVOZ2 and CuFT1 in the CuVOZ1–CuFT1 complex were weak Van der Waals forces. The interaction force between CuVOZ2 and CuFT3 in the CuVOZ2–CuFT3 complex was predicted to be due to a weak Van der Waals force and a hydrogen bond with a minimum distance of 2.96 Å (Fig. 3-2 and 3-5C). Unlike the CuVOZ1–CuFT complex, where a hydrogen bond was not found (Hasan et al., 2023), the residues in the CuVOZ2–CuFT complex were not confined to the fourth exon of CuFTs. In CuFT1, one amino acid residue was found to be involved in docking in the first exon, two in the third exon, and eight in the fourth exon. However, five and six residues were found in the second and the fourth exons, respectively, in CuFT3 (Fig. 3-2B). A highly conserved 14-amino acid segment (Fig. 3-2B; segment B, LGRQTVYAPGWRQN) in the fourth exon of FT orthologs forms an external loop, considered to form the ligand-binding site together with the adjacent segment C (Ahn et al., 2006). Five of 11 and one of 11 residues associated with docking were localized in segment B for CuFT1 and CuFT3, respectively, indicating that CuVOZ2 may interact with the region of segment B of CuFTs to function as a complex. The simulation of interaction between CuVOZ2 and AtFT suggested that CuVOZ2 might interact with both segments B and C of AtFT (Fig. 3-2 and 3-8) to function as a complex in transgenic *Arabidopsis*.

The transgenic *Arabidopsis* ectopically expressing *CuVOZ2* showed early bolting and flowering with an elongated stem with fertile flowers (Fig. 3-6B and 3-7A). On the other hand,

the ectopic expression of apple *MdVOZ1a* induces the elongation of flower stalks like that of *CuVOZ1* (Hasan et al., 2023), but the flower of transgenic *Arabidopsis* is sterile (Mimida et al., 2011). The difference in the phenotype between 35SΩ:*CuVOZ2* and 35SΩ:*CuVOZ1* transgenic lines might be due to the additional amino acid sequence or DUF-4749 motif in the N-terminal region and NAM motif in the C-terminal region of CuVOZ1. The role of *AtVOZ*s in flowering, concerning *CO*, *FLC*, *MAF*, and *PHYTOCHROME B* (*PHYB*), was previously explained in the studies conducted with a double mutant (*voz1 voz2*) in *Arabidopsis* (Celesnik et al., 2013; Kumar et al., 2018; Yasui et al., 2012). The early flowering phenotype of 35SΩ:*CuVOZ2* transgenic lines might result from the alteration of *FT* expression because CuVOZ2 showed protein–protein interaction with AtFT in simulation (Fig. 3-8). *AtVOZ1* and *AtVOZ2* suppress *FLC* and act together with *CO* by interacting physically to control flowering (Kumar et al., 2018; Yasui et al., 2014). The downregulation of *FLC* and/or the stabilization of *CO* in transgenic *Arabidopsis* could be another reason for early flowering. *VOZ1* genes in the soybean showed a significant alteration in expression levels in response to dehydration and salt stress treatments, whereas *VOZ2* genes showed a weak change (Li et al., 2020). Light is a key environmental factor affecting flowering time (Zeevaart, 1976). The presence of *cis*-acting binding elements, such as LTR, MYB, MBS, ABRE, the CGTCA motif, and the W-box, including a light-related element, Box-4, was reported in the promoter region of *VOZ1/2* from soybeans (*Glycine max* and *Glycine soja*) and tef (*Eragrostis tef*) (Luo et al., 2020; Mulat and Sinha, 2021; Rehman et al., 2021). These studies indicate that *VOZ* TFs might be required to regulate flower induction through some factors, such as abiotic stresses and light. There is a possibility that the stabilized *CuVOZ2* functions as one of the triggers inducing flowering, elongation of the stem, and an increase in the number of nodes and siliques with a consistent result of expression analysis (Fig. 3- 6C and 3-7B, D, E).

The VOZs were also shown to have a function in seed germination. A recent study showed that PHYTOCHROME INTERACTING FACTOR1 (PIF1) induces the expression of *AtVOZ1* and *AtVOZ2* in the dark (Luo et al., 2020). Although both AtVOZ1 and AtVOZ2 were reported to interact with PHYB and promote flowering (Yasui et al., 2012), AtVOZ2 was found to bind to the promoter of a GA biosynthetic gene, *GIBBERELLIN 3-OXIDASE1* (*GA3ox1*), *in vitro* and *in vivo* and directly repressed *GA3ox1* expression in *Arabidopsis,* thereby negatively regulating *PHYB*-mediated seed germination (Luo et al., 2020). The *ga3ox1 Arabidopsis* mutant had a semi-dwarf phenotype (Mitchum et al., 2006), opposite to the phenotype of 35SΩ:*CuVOZ2*. It can be assumed that *CuVOZ2* did not repress but increased active GAs in transgenic *Arabidopsis*. The relationship between GA biosynthesis and *CuVOZ2* remains to be studied.

3.5. Conclusion

The protein–protein interactions between CuVOZ2 and CuFTs were confirmed in this study through a Y2H system. The N-terminal 1st to 400th region of CuVOZ2 was suggested via a truncation experiment to be necessary for the interaction with CuFTs. Furthermore, the 3D structures of the proteins, the nature of interactions, the specific residues involved in docking, and the Zn^{2+} binding site were predicted by virtual simulations. Interestingly, the amino acid residues associated with binding were not precisely the same between CuFT1 and CuFT3. It was assumed from the transgenic experiment that *CuVOZ2* might trigger the early flowering and elongation of inflorescence. These findings would provide us with an understanding not only of the function of *CuVOZ2* but also of the functional divergence of *CuFT1* and *CuFT3* in citrus. The relationship between the protein complexes and the phytohormones, such as ABA and GA, and the response of the protein complexes to environmental stimuli and/or stresses remains to be studied further.

Table 3-1. Primer sets used in gene cloning, Y2H, quantitative real-time RT-PCR analysis, and vector construction.

Primer	Oligonucleotide (5′ → 3′)
Gene cloning	
Ciclev10015076m_F3	TAGGAATCGGAGTAGAAGGG
Ciclev10015076m_R2	TGGTAAATTTGACGAGTTTCTGC
*att*B primers	
VOZ2attB_F	acaagtttgtacaaaaaagcaggcttcATGCAGAGTGGTTCAAAGAG
VOZ2attB_R	accactttgtacaagaaagctgggtcTCAATACTTGTGATAATAGT
CuVOZ2attB_DN1F	acaagtttgtacaaaaaagcaggcttcAGTCCATTAGCTGGATTTGC
CuVOZ2attB_N1R	accactttgtacaagaaagctgggtcTCAGGTGGCATCGTCTTGCT
CuVOZ2attB_N2R	accactttgtacaagaaagctgggtcTCAACTATTGGGTCCAATAT
CuVOZ2attB_N3R	accactttgtacaagaaagctgggtcTCATAGCTCTGTAGCATTCC
CuVOZ2attB_N4R	accactttgtacaagaaagctgggtcTCAACTCTTCTTCTCACTGG
Semi-qRT-PCR/ qRT-PCR	
qPCR_CuVOZ2_F (28>46)	GCATCTGCATCCCACCAGT
qPCR_CuVOZ2_R (105<124)	CCTCCTTCCTAGCAACTCTA
CuActin (-86>-66)	GAGCGATAGAGAGAATCGACA
CuActin (-1<19)	TATCCTCAGCATCGGCCATT
AtTUB4-F	TTCATATCCAAGGCGGTCAATGTGG
AtTUB4-R	CGAGCTTGAGGGTACGGAAACAG
Vector construction	
VOZ2_XbaI_F	AAAtctagaATGCAGAGTGGTTCAAAGAG
VOZ2_SacI_R	AAAgagctcTCAATACTTGTGATAATAGT

The thermal cycle program for qRT-PCR was as follows: 95˚C for 1 min, followed by 40 cycles at 95˚C for 15 s, 60˚C for 60 s for *CuVOZ2*, *CuActin,* and *AtTUB4*. The site of *att*B or restriction enzymes used for vector construction is indicated with the characters in lowercase.

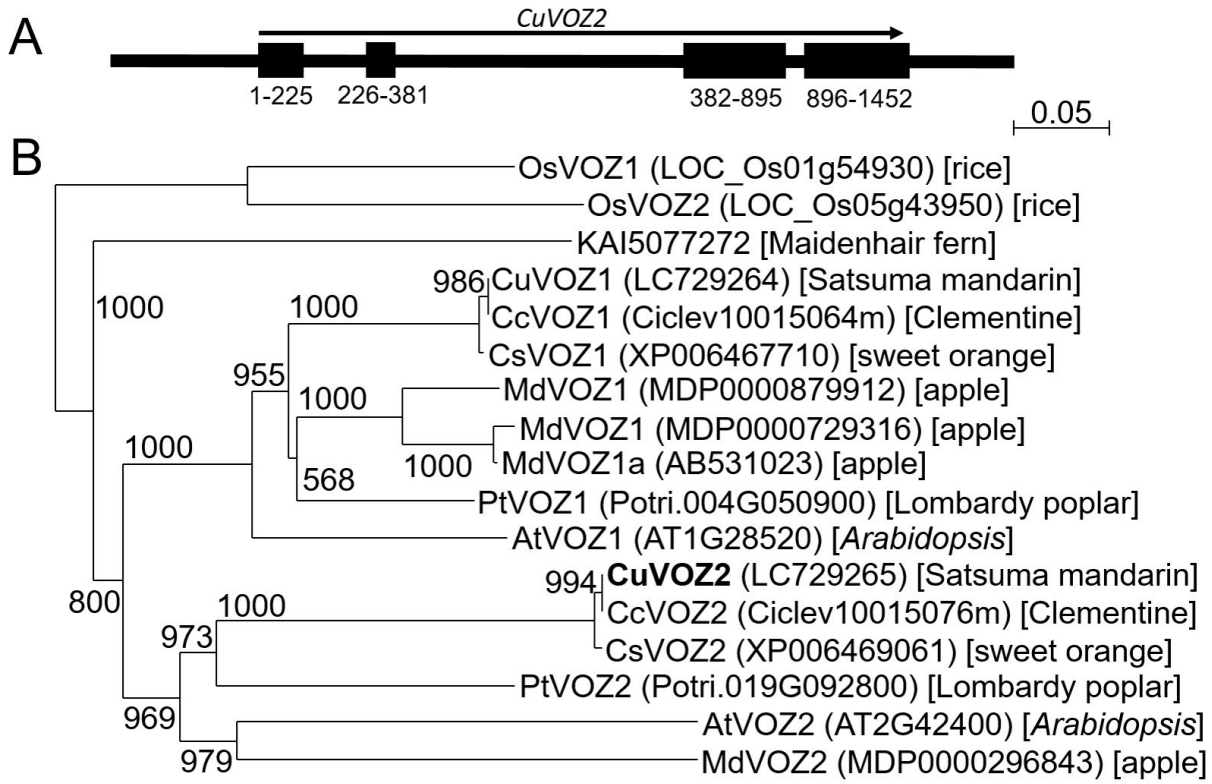

Fig. 3-1. Sequence and phylogenetic analysis of *CuVOZ2*.

(A) Schematic representation of the genomic organization of *CuVOZ2*. The numbers that appear below the exon region are based on the cDNA sequence of *CuVOZ2.* (B) Relationship of the predicted VOZ-family proteins between Satsuma mandarin and other plant species. Phylogenetic tree of VOZ-family proteins of apple, *Arabidopsis*, citrus, maidenhair fern, poplar, rice, and tomato species. The amino acid sequences of *Arabidopsis* VOZ-family proteins were obtained from TAIR, and others were obtained from NCBI, phytozome and Genome Database for Rosaceae (GDR). Numbers along branches are bootstrap values (1000 replicates). The unit for the scale bars indicates branch lengths (0.05 substitutions/site).

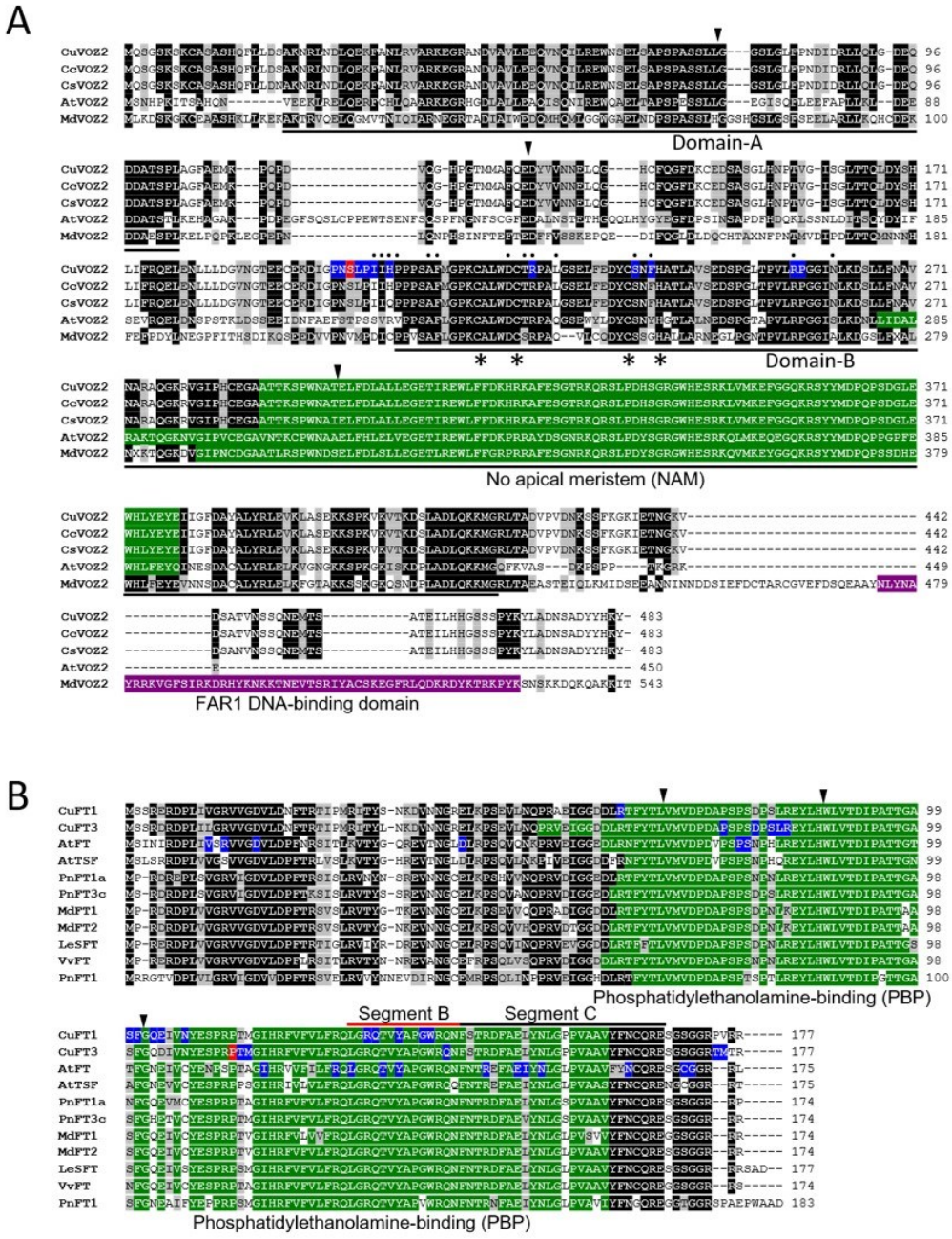

Fig. 3-2. Comparison of the deduced protein sequences of VOZ2 or FT in several plant species. (A) The deduced protein sequence of CuVOZ2 with those of the VOZ2 family proteins from citrus, apple, and *Arabidopsis* species. The genes used for comparison are *CuVOZ2* (LC729264, Satsuma mandarin), *CcVOZ2* (Ciclev10015076m, Clementine), *CsVOZ2* (XP006469061, sweet orange), *MdVOZ2* (MDP0000296843, apple), and *AtVOZ2* (AT2G42400, *Arabidopsis*). Amino acids in black and gray are identical and similar, respectively. The gaps indicated by dashes are attributed to the lack of amino acids. The triangles show the intron positions. The

green and purple regions show the predicted motif regions. Two domains, Domain A and Domain B, were represented by black lines, as defined by Mitsuda et al. (2004). Asterisks represent conserved residues possibly forming a functional zinc-coordinating motif (Mitsuda et al., 2004). Amino acids in blue are in the predicted docking regions when the CuVOZ2 interact with CuFTs. Amino acids with a dot on the top are the residues predicted to bind with AtFT. The amino acids in red are the amino acid residues predicted to have a hydrogen bond. (B) The deduced protein sequences of CuFT1 and CuFT3 with those of the TFL1/FT family from apple, *Arabidopsis*, grapevine, and Lombardy poplar species. The genes used for analysis are as follows: *MdFT1* (AB161112, apple), *MdFT2* (AB458504, apple), *AtFT* (AT1G65480, *Arabidopsis*), *AtTSF* (AT4G20370, *Arabidopsis*), *VvFT* (DQ871590, grapevine), *PnFT1* (AB106111, Lombardy poplar), *PnFT1a* (AB161109, Lombardy poplar), *PnFT3c* (AB110009, Lombardy poplar), *CuFT1* (LC729261, Satsuma mandarin), *CuFT3* (LC729263, Satsuma mandarin), and *LeSFT* (AY186735, tomato). Putative amino acid sequences were aligned using the ClustalX2 multiple-sequence alignment program ver.2.0.5 (Jeanmougin et al., 1998). Red and black lines on the fourth exon of FT family proteins indicate segment B and C regions, respectively, as defined by Ahn et al. (2006).

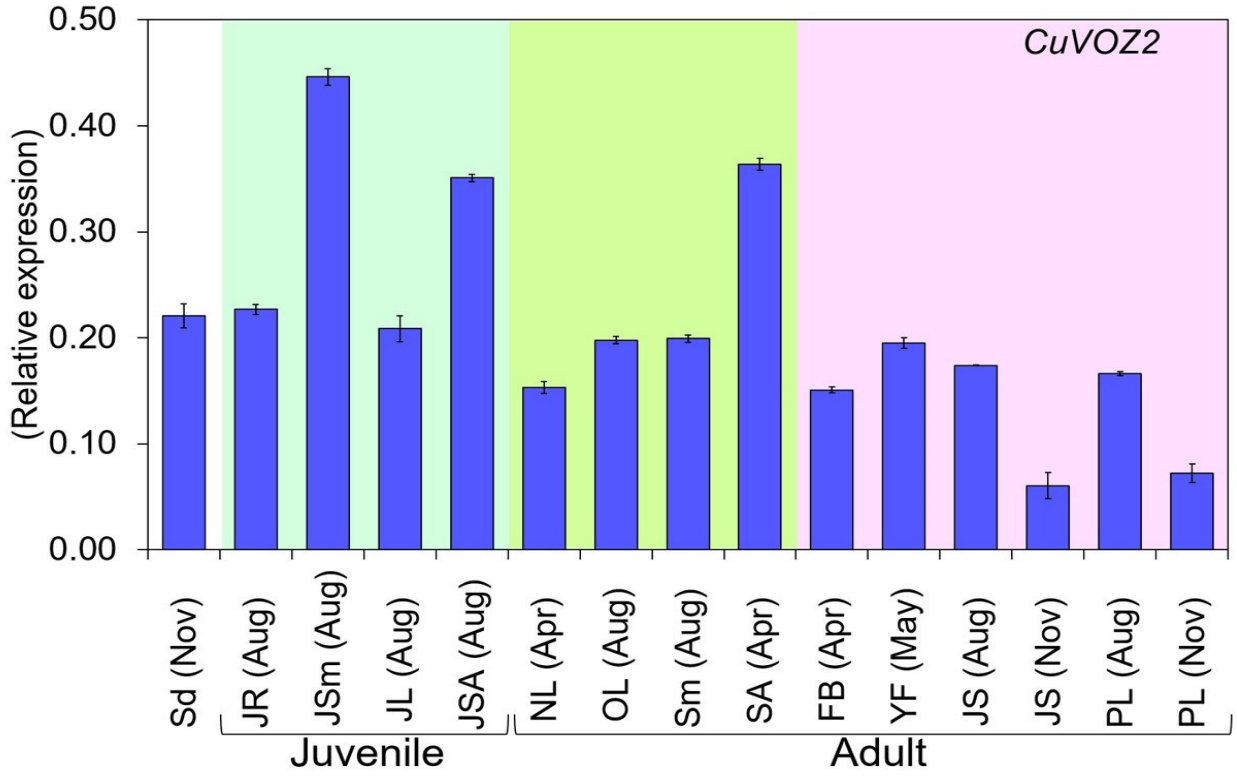

Fig. 3-3. Expression pattern of *CuVOZ2* in various tissues in the Satsuma mandarin 'Aoshima' by quantitative real-time RT-PCR.

The samples (left to right) are as follows: the seeds (Sd), juvenile roots (JR), Juvenile stems (JSm), leaf from the juvenile plant (JL), and Juvenile shoot apices (JSA) of one-year-old seedlings in the juvenile phase; the new leaf (NL), old leaf (OL), stem (Sm), and shoot apices (SA) in the adult phase; and the flower buds (FB), young fruit (YF), juice sack (JS), and peel (PL) in the adult reproductive phase. Expression levels were normalized by citrus actin. Values are the means ± SD of the results from three technical replicates. A column without an error bar indicates that the standard deviation fell within the symbol.

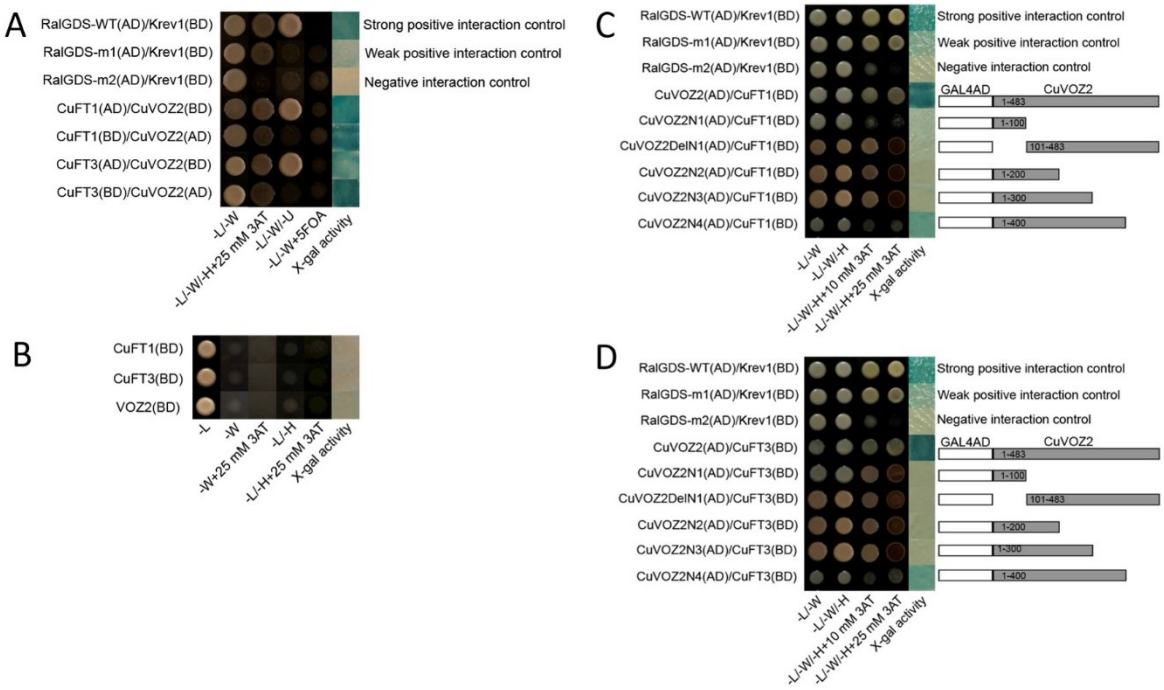

Fig. 3-4. Protein–protein interactions between CuFTs with CuVOZ2 detected in a yeast two-hybrid system.

(A) Yeast competent cell MaV203 was transformed with a pair of bait and prey plasmids, CuFTs(AD)/CuVOZ2(BD) and CuVOZ2(AD)/CuFTs(BD), using the lithium method. The transformants were grown at 30°C for 48 h. The selection test for the *HIS*3 reporter gene of yeast transformants was performed on a selective agar medium with a Minimal SD Base and –L–W–H DO supplement containing 25 mM 3-amino-1,2,4-triazole (3AT) and 2% glucose. The selection test for the *URA*3 reporter gene was performed on an SD –L/–W/–Ura DO supplement containing 0.2% 5-fluoroorotic acid (5FOA). A subsequent X-gal (5-Bromo-4-chloro-3-indolyl-β-D-galactopyranoside) filter lift assay for ß-galactosidase activity was performed using yeast transformant cells to test the *Lac*Z reporter gene. (B) No effect of self-activation was detected in the constructed vector. The interaction between the truncated CuVOZ2 and full-length CuFT1 (C) and CuFT3 (D) in yeast is shown. The left panel shows the growth of the transformed yeast cells on SD/–L–W, SD/–L–W–H, SD/–L–W–H+10 mM 3AT, and SD/–L–W–H+25 mM 3AT and a filter assay for the β-galactosidase activity of the transformants grown on SD/–L–W–H. The right panel illustrates the full-length or truncated version of CuVOZ2 (N1, DelN1, N2-4). An RalGDS-WT(AD)/Krev1(BD) construct was used as a strong positive interaction control, an RalGDS-m1(AD)/Krev1(BD) construct as a weak positive interaction control, and an RalGDS-m2(AD)/Krev1(BD) construct as an negative interaction control.

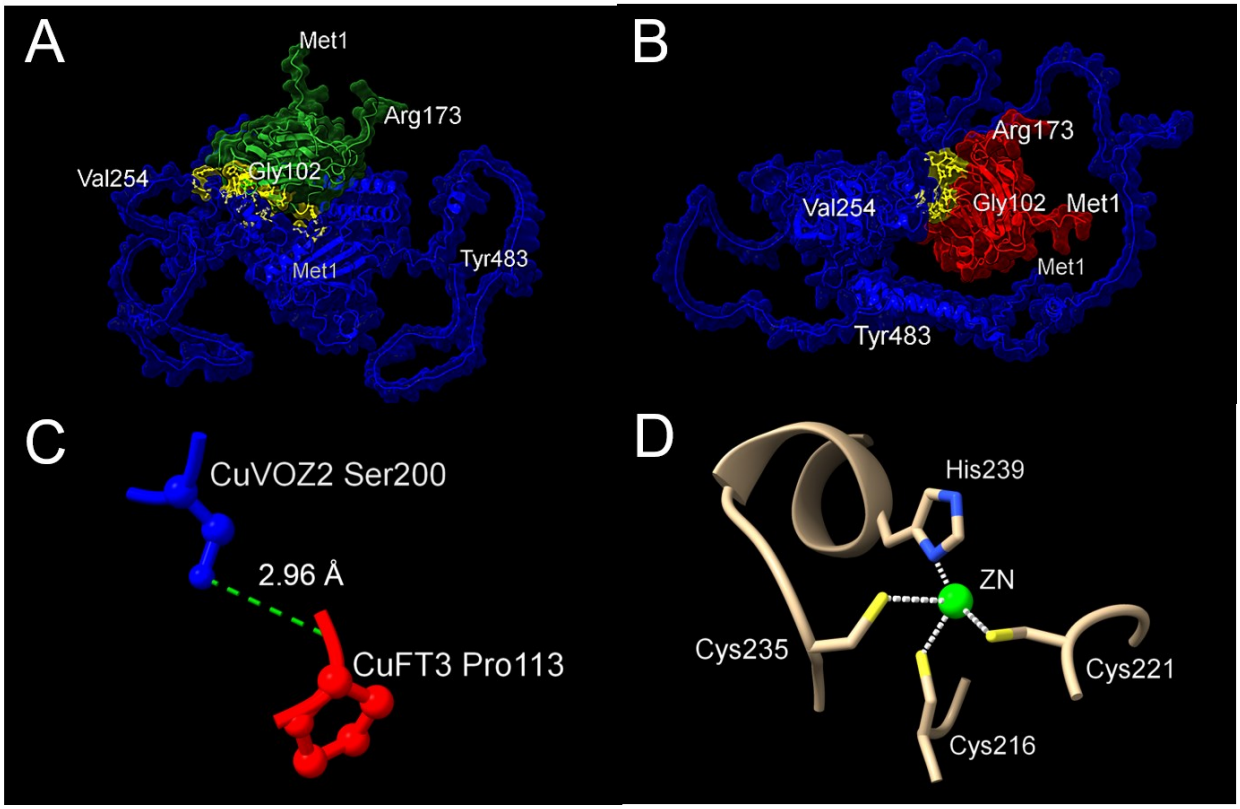

Fig. 3-5: Predicted protein–protein interaction between CuVOZ2 and CuFT1 and between CuVOZ2 and CuFT3.

(A) Green and blue areas indicate CuFT1 and CuVOZ2, respectively. (B) Red and blue areas indicate CuFT3 and CuVOZ2, respectively. The yellow regions in the middle of the two proteins indicate possible docking regions. Met1, Val254, and Tyr483 for CuVOZ2 and Met1, Gly102, and Arg173 for FTs are displayed to confirm the relative position among the complexes. (C) A predicted hydrogen bond between CuVOZ2 and CuFT3 is shown. (D) The predicted Zn^{2+} binding site in the CuVOZ2 protein is shown. The prediction of protein–protein interaction was calculated with AlphaFold.ipnyb (Jumper et al., 2021) and visualized with ChimeraX ver. 1.5 (Pettersen et al., 2021). The Zn^{2+} binding site was predicted using the Metal Ion-Binding site prediction and modeling server (MIB) (Lu et al., 2012)

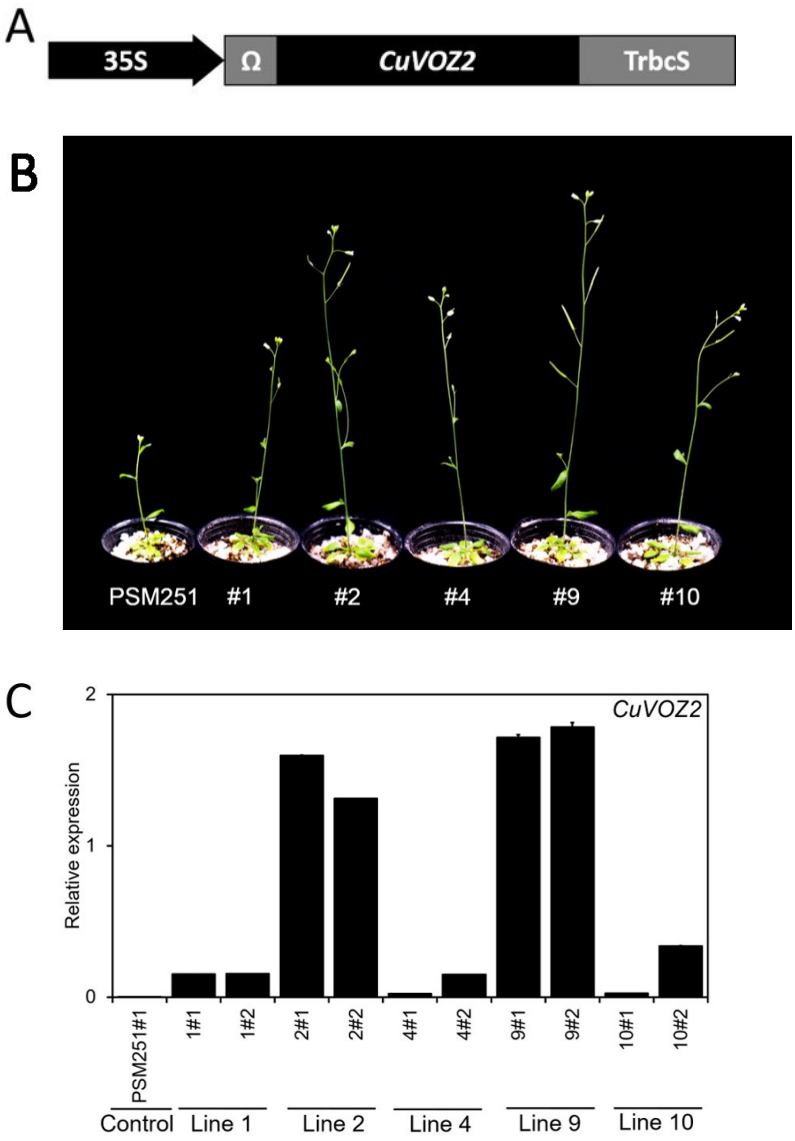

Fig. 3-6. Production of transgenic *Arabidopsis* with *CuVOZ2*.

(A) Schematic representation of a constructed transformation vector. (B) Typical phenotypes of transgenic *Arabidopsis* with *CuVOZ2* lines at flowering time in a growth chamber under LD conditions. (C) Expression analysis for transgenes in whole plants of transgenic *Arabidopsis*. The photo was taken on the 22nd day after the start of incubation. Samples for expression analysis of *CuVOZ2* in transgenic lines were collected 40 DAI. PSM251 was the transgenic control plant with an empty vector. Levels of detected amplicons were normalized by reference to *AtTUB4*. Values are the means ± SD of the results from three technical replicates per line.

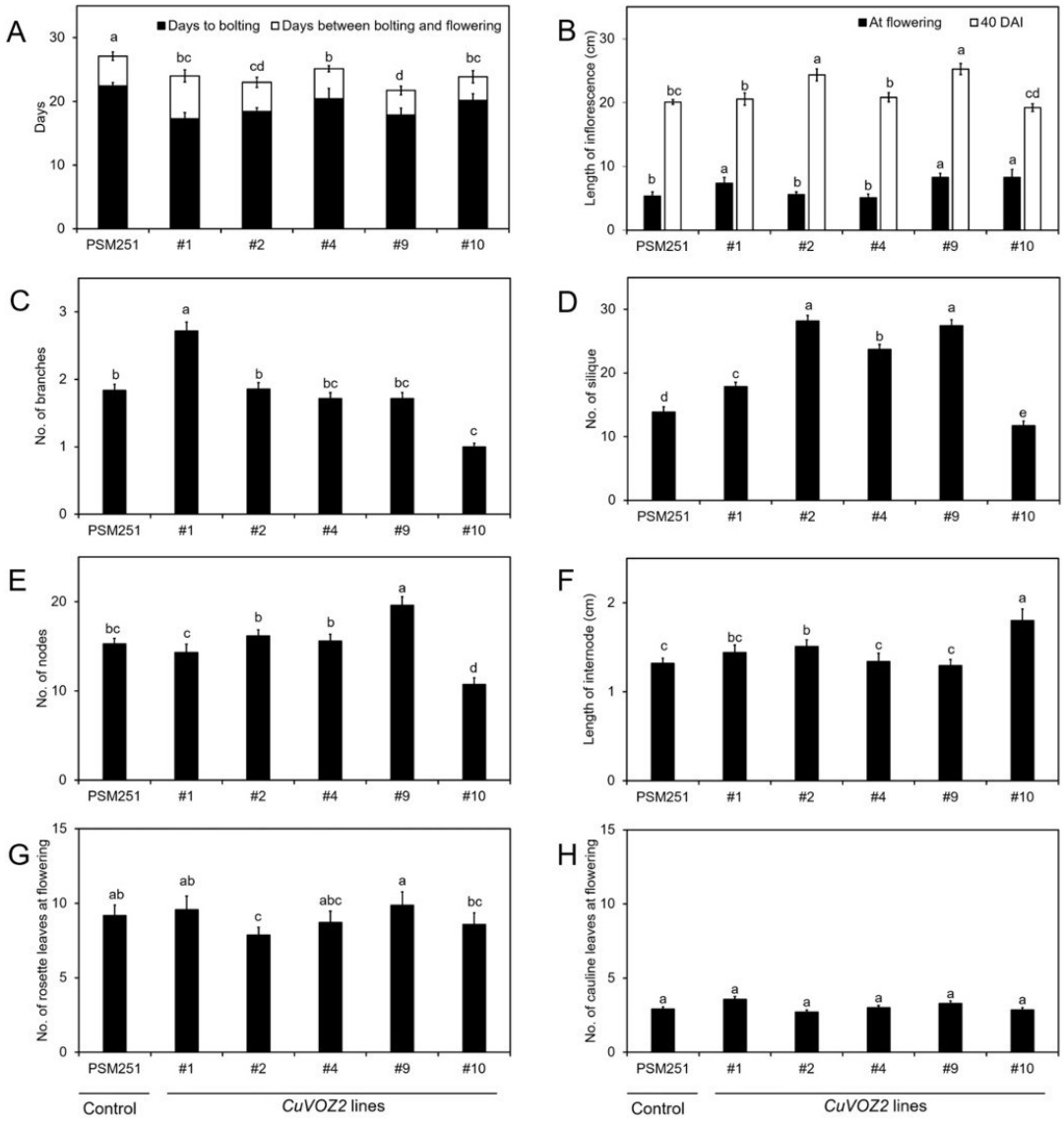

Fig. 3-7. Characteristics of transgenic *Arabidopsis* lines ectopically expressing *CuVOZ2*.
(A) Days to bolting and flowering, (B) length of the first inflorescence, (C) no. of branches, (D) no. of siliques, (E) no. of nodes, (F) length of internodes, (G) no. of rosette leaves, and (H) no. of cauline leaves. The transgenic plants in the third generation (T_3) and the controls were grown under LD conditions. Days to bolting and flowering were counted from the first day of incubation. All the transgenic plants showed early bolting and flowering. The length of the primary inflorescences was measured at flowering and 40 DAI. The rosette and cauline leaves were counted on the day of the first flowering. Different letters at the top of each column indicate significant differences among the lines, contrasted with Tukey's multiple comparison tests ($P < 0.05$).

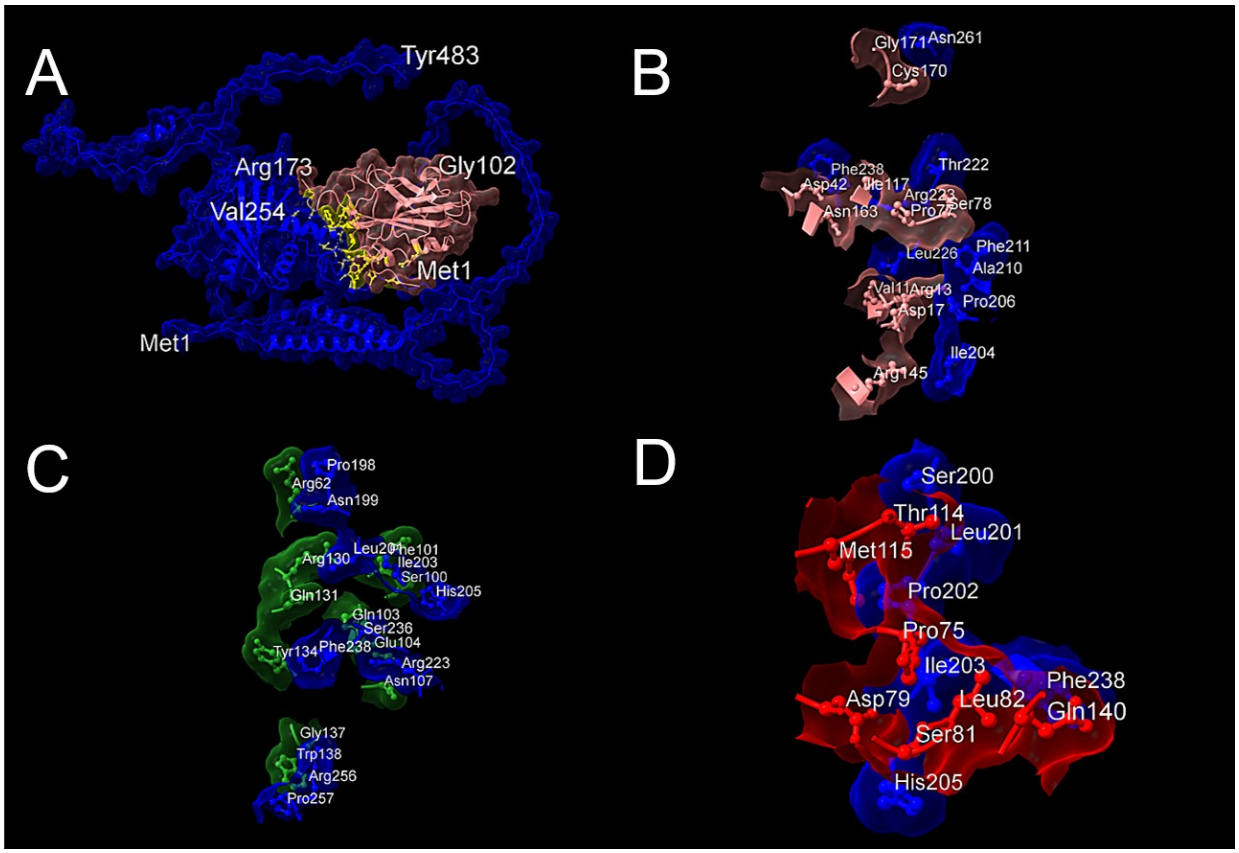

Fig. 3-8 Predicted protein-protein interaction between CuVOZ2 and AtFT and the contact regions between CuVOZ2 and CuFTs.

(A) Blue and pink areas indicate CuVOZ2 and AtFT, respectively. Met1, Val254, and Tyr483 for CuVOZ2 and Met1, Gly102, and Arg173 for FTs are displayed to confirm the relative position among the complexes. (B) The amino acid residues involved in docking in CuVOZ2-AtFT complex (C) The amino acid residues involved in docking in CuVOZ2-CuFT1 complex (D) The amino acid residues involved in docking in CuVOZ2-CuFT3 complex. Some amino acids might be hidden in the background.

Chapter 4

General discussion

4. General Discussion

Transcription factors (TFs) are regulatory proteins that are associated with the development, metabolism, and stress management of plants, and they typically work by regulating gene expression by binding to local or distal *cis*-elements and modulating the local protein concentrations of limiting factors at the target promoters (Latchman, 1993; Lee and Young, 2000; Singh, 1998; Yang et al., 2012; Yuan and Perry, 2011). To activate or inhibit the recruitment of the basic transcriptional machinery to particular genes, TFs function alone or in complexes with other molecules and regulate the transcription of DNA to mRNA. TFs are encoded by around 3-10% of all genes in eukaryotic genomes (Harbison et al., 2004; Levine and Tjian, 2003; Reece-Hoyes et al., 2005). They have a crucial role in controlling plant growth, reproduction, intercellular communication, environmental response, cell cycle, and metabolism. Plant genomes have a large number of TF genes because some TF superfamilies have expanded more quickly than those in other biological kingdoms (Yuan and Perry, 2011). Despite the significance of TFs and the fast proliferation of TF genes identified by genomics and bioinformatics, only a small number of TFs have undergone substantial functional characterization. In this study, two VOZ TFs were screened for interacting with two FT proteins in the Y2H system, and the genes' functions were characterized by transgenic technique.

The characteristic feature of VOZ1 derived from citrus, highlighted by a functionally uncharacterized DUF4749 (PF15936) (Finn et al., 2016) motif, is found in eukaryotes. This region is typically between 121 and 170 amino acids in length, usually found in association with Pfam:PF00595 (PDZ) and Pfam:PF00412 (LIM), and often contains the conserved Zasp-like motif (IPR006643). However, this characteristic feature of CuVOZ1 was not found in CuVOZ2.

VOZ transcription factors were reported to function as transcriptional regulators, repressing abiotic stress tolerance, such as freezing and drought stress tolerance, while increasing biotic stress resistance to a fungal pathogen, *Colletotrichum higginsianum*, in *Arabidopsis* (Nakai et al., 2013a). In contrast, loss-of-function mutations in both *AtVOZ1* and *AtVOZ2* increased cold and drought stress tolerance and hypersensitivity to salt stress, decreasing biotic stress resistance in *Arabidopsis* (Nakai et al., 2013b; Prasad et al., 2018). *voz1voz2* double mutants were tolerant to cold and drought stress but resistant to *C. higginsianum* and another bacterial pathogen, *Pseudomonas syringae*. (Nakai et al., 2013b; Selote et al., 2018). VOZ1 and VOZ2 separately suppress the expression of *DREB2C* or *DREB2A* in *Arabidopsis* to mediate the high-temperature stress response (Koguchi et al., 2017; Song et al., 2018). VOZ transcription factors react to salt stress differently than they do to freezing and drought stress. Salt tolerance in *Arabidopsis* has been demonstrated to be increased by *VOZ*s, which have previously been shown to be able to either directly or indirectly affect the transcriptional level of a large number of stress-responsive genes (Prasad et al., 2018). Additionally, the tolerance to iron deficiency stress was examined in *Arabidopsis*; however, the results revealed that VOZs did not significantly contribute to the physiological response to iron shortage (Selote et al., 2018). However, this study is the first to explain the morphological characteristics of overexpression of citrus *VOZ*s in *Arabidopsis.*

The difference between the phenotypes of 35SΩ:*CuVOZ1* and 35SΩ:*CuVOZ2* transgenic *Arabidopsis* ectopically expressing *CuVOZ1* and *CuVOZ2* was the adventitious flowering. This difference in adventitious flower buds might be due to the absence of the DUF4749 motif in CuVOZ2 in the same region or the difference in the number of α-helices and β-pleated sheets of the VOZ proteins.

It has long been known that many citruses, including Satsuma mandarin, can produce flowers in drought conditions, and the number of flowers, flowering nodes, and flowers per node can be increased (Huang et al., 2021; Inoue, 1989). Recent studies identified SlVOZ1 in tomato as a substrate of OPEN STOMATA 1 (SlOST1). The phosphorylated SlVOZ1 by *SlOST1* binds directly to the promoter region of *SFT* in drought condition and promote flowering (Bürger, 2022; Chong et al., 2022). Through phosphorylation, SlOST1 promotes the stability and nuclear translocation of SlVOZ1, which is additionally enhanced by ABA. The expression of *SFT* is then positively induced by nucleus-localized SlVOZ1, providing a probable explanation for how tomato balances drought responses and flowering (Chong et al., 2022). OST1 is essential for the control of ABA signaling, abiotic stress responses, and stomatal movement in *Arabidopsis* and numerous other plant species (Ali et al., 2020). The *slost1* mutants, which were as well smaller than the WT, displayed delayed flowering, indicating that *SlOST1* may also be involved in the control of tomato growth and development (Chong et al., 2022). Despite mostly accumulating in the cytoplasm, *Arabidopsis* VOZ1's translocation to the nucleus is essential for optimal operation (Schwarzenbacher et al., 2020; Selote et al., 2018). SlVOZ1 is an unstable cytosolic protein in developing seedlings under normal circumstances, but it becomes more stable in the presence of SlOST1 (Chong et al., 2022). The fact that ABA increases SlOST1's kinase activity while simultaneously promoting SlVOZ1's phosphorylation, protein stability, and nuclear translocation suggests that ABA is crucial in controlling SlVOZ1 function through SlOST1. SlVOZ1 and SlOST1 are likely implicated in regulating the ABA-mediated drought tolerance in tomato as evidenced by the fact that *slvoz1* mutants are late flowering, hypersensitive to mannitol, insensitive to ABA, and lose water more quickly than the WT suggesting that the SlOST1–SlVOZ1 module likely plays a key role in drought response and flowering (Chong et al., 2022). CuVOZ1 might also be involved in the branching of the stem because 35SΩ:*CuVOZ1* transgenic lines had phenotypes

showing an increased number of nodes and branches (Fig. 2-6B, D, F), which were not observed in the 35SΩ:*CuVOZ2* transgenic lines. *AtOST1* might be involved in the complex flowering in the transgenic *Arabidopsis* lines. As a result, the number of branching, nodes and flowers could be increased. The presence of *OST1*-related cDNAs were identified through transcriptome analysis in citrus (Quecini et al., 2007). There is a possibility that *OST1* in citrus functions in a similar way in the stabilization and translocation of CuVOZs and controls flowering in drought conditions. The relationship between *CuVOZs, OST1* and ABA remains to be studied.

The expressions of *VOZ*s are downregulated and repressed by PhyB in the dark just after the imbibition stage during seed germination of wild-type *Arabidopsis* seeds. On the contrary, if PhyB was inactivated by far-red light, the *voz1* and *voz2* mutants exhibited increased seed germination percentages than the wild type (Yasui et al., 2012). Both red light irradiation and *voz1voz2* mutation increased *GA3ox1* expression. AtVOZ2 directly represses *GA3ox1* expression in *Arabidopsis* by binding to the promoter and negatively regulating *PHYB*-mediated seed germination (Luo et al., 2020). Similar to *AtVOZ*s, *REVEILLE1* (*RVE1*) and *RVE2*, two additional transcription factor genes associated with seed dormancy in *Arabidopsis*, trigger primary seed dormancy and repress red/far-red-light-reversible germination (Jiang et al., 2016). Following imbibition, *RVE1* and *RVE2* expressions are downregulated by phyB. RVE1 directly binds to the promoter of *GA3ox2*, inhibits its transcription and suppresses the synthesis of bioactive gibberellins(Jiang et al., 2016). In addition, DELAY OF GERMINATION 1 (DOG1) also acts downstream of phyB (Jiang et al., 2016). The phenotype of 35SΩ:*CuVOZ2,* opposite to that of semi-dwarf *ga3ox1* mutant (Mitchum et al., 2006), suggests that *CuVOZ2* did not repress but increased active GAs in transgenic *Arabidopsis*. The possibility of the relationship between *VOZ*s and *RVE*s is yet to

be studied. Future studies should focus on the relationship between GA biosynthesis, RVEs and CuVOZs.

The prediction of distances between the CuVOZs and CuFTs or AtFT residues suggests that the interactions between CuVOZs and CuFTs in CuVOZs-CuFTs complexes or between CuVOZs and AtFT in CuVOs-AtFT complex were weak Van der Waals forces. The amino acids in FTs associated with docking with CuVOZs were localized in segments B and C of CuFT1, CuFT3, and AtFT, suggesting that CuVOZs might interact with the region to function as complexes. The numbers of α helices in CuFT1, CuFT3 and AtFT were 5, 6 and 5, respectively. The number of β pleated sheets in three proteins was 8. These differences in protein structures of CuFTs and AtFT could be another reason for the differences in the structure and docking region in the protein-protein complexes associated with VOZs.

In this research, the protein–protein interactions between CuVOZs and CuFTs were validated with a Y2H system, and the truncation experiment revealed that the N-terminal region of CuVOZs from the first to 400th amino acid would be critical for the protein–protein interaction. Furthermore, a docking simulation was used to anticipate the nature of binding that would occur between two proteins. The 35SΩ:*CuVOZ1* and 35SΩ:*CuVOZ2* transgenic *Arabidopsis* suggested that *CuVOZs* may serve as one of the catalysts for precocious flowering and may also contribute to the elongation of the inflorescence. Unlike *CuVOZ2*, *CuVOZ1* could also be involved in increasing the number of branches. However, how these proteins interact *in vivo* and how CuVOZs-FTs complexes work in citrus or *Arabidopsis* remains a mystery. The response of CuVOZs–CuFTs complexes to environmental stimuli and phytohormones such as ABA and GA synthetic genes concerning flowering remains to be studied further.

The use of the co-immunoprecipitation (Co-IP) assay or bimolecular fluorescence complementation (BiFC) assay is highly recommended to verify interactions within the host

plant. Two practical approaches to comprehending the functioning of *VOZ*s in plant bodies could be complementation experiments using mutant *Arabidopsis* of *voz*s or repression domain experiments in *Arabidopsis*. To gain insight into the functions of *CuVOZ* genes concerning salt tolerance, drought tolerance, or cold tolerance, assays with transgenic or mutant *Arabidopsis* could be helpful, as previous studies have indicated. Additionally, to examine the role of *VOZ* genes in biotic stress responses, it would be beneficial to investigate the responses of transgenic or mutant *Arabidopsis* to plant parasitic pathogens. A promoter GUS analysis can provide valuable information regarding the localization of the genes in *Arabidopsis*. To clarify the function of *CuVOZ1* and *2* in citrus, it is recommended to generate overexpression citrus lines using micropropagation and subsequent transformation of 35SΩ:*CuVOZ1/2*. Gene silencing with RNA interference (RNAi) or CRISPR/Cas-mediated mutagenesis is highly recommended as a cutting-edge tool for producing citrus mutant lines to understand the function of these genes in citrus.

As *VOZ* genes are responsible for various stress responses in plants, another recommendation to understand the function of *CuVOZ* genes is to check the expression of differential genes under different stress conditions in citrus. For example, Satsuma mandarin seedlings can be grown under saline stress conditions, and then the expression levels of *FT*s and other stress-responsive genes can be checked. This way, the stress response mechanism in citrus through *VOZ*s could be elucidated.

5. Summary

Shortening the juvenility is a burning issue in breeding woody fruit trees such as Satsuma mandarin (*Citrus unshiu* Marc.). Decreasing the breeding period requires an inevitable understanding of the flowering process in woody plants for developing methods to shorten the breeding period and regulate the yield of tree fruits. FLOWERING LOCUS T (FT) acts as a transmissible floral inducer and can interact with other transcription factors (TFs) throughout the flowering system in *Arabidopsis*. In this study, two citrus orthologs of the transcription factors (TF) *VASCULAR PLANT ONE-ZINC FINGER1* (*VOZ1*)-like gene, *CuVOZ1* and CuVOZ2, two *FT*-like genes, *CuFT1* and *CuFT3*, were isolated from the Satsuma mandarin 'Aoshima'. *In vitro* Protein-protein interaction was confirmed between CuVOZs and CuFTs in the Y2H system. N-terminal 400 amino acids of CuVOZ1, consisting of three motifs: domain of unknown function 4749 (DUF4749), no apical meristem (NAM), and zinc coordination motif, were assumed to be involved in the CuVOZ1–CuFT1 and CuVOZ1–CuFT3 complexes. NAM and zinc coordination motifs were identified within the N-terminal 400 amino acids of CuVOZ2. DUF4749 was not found in the sequence of CuVOZ2. Docking simulation suggested that three motifs in CuVOZ1 participated in the interaction of the CuVOZ1-CuFT1 complex. Only the zinc coordination motif of CuVOZ1 was possibly involved in the interaction of CuVOZ1-CuFT3, CuVOZ2-CuFT1, and CuVOZ2-CuFT3 protein-protein complexes and the phosphatidylethanolamine-binding protein (PBP) motif in exon 4 of CuFTs was predicted to be crucial for the interaction between CuVOZs and CuFTs. The distance between the amino acid residues involved in docking was varied in CuVOZs-CuFTs complexes. The distances were predicted to be from 2.69 to 3.37 Å in CuVOZ1–CuFTs complexes and from 1.09 to 4.37 Å in CuVOZ2–CuFTs complexes, respectively, suggesting that the forces between CuVOZs and CuFTs in the CuVOZs–CuFTs complexes were weak Van der Waals forces. Cys218, Cys223, Cys237, and His241 in CuVOZ1 and Cys216, Cys221, Cys235, and His239 in

CuVOZ2 were suggested to bond with a Zn^{2+} in the Zn coordination motif region. Ectopic expression of 35SΩ:*CuVOZ1* and 35SΩ:*CuVOZ2* affected the morphology of transgenic *Arabidopsis*. Flowering time, plant size, length of inflorescence, number of flowers and siliques, and formation of flower buds on the elongated stem were observed in the *Arabidopsis* overexpressed with 35SΩ:*CuVOZ1.* Unlike 35SΩ:*CuVOZ1,* overexpression of 35SΩ:*CuVOZ2* in *Arabidopsis* affected the flowering time, length of inflorescence, and the number of siliques. These results indicate that *CuVOZ1* might act as a trigger for early flowering and might be involved in the elongation and branching of the inflorescence. The CuVOZ1–CuFT complexes might regulate cellular proliferation and the formation of new tissues and affect both vegetative and reproductive development. On the other hand, *CuVOZ2* might regulate both vegetative and reproductive development, act as a trigger for early flowering, and be involved in the elongation of inflorescence.

6. Acknowledgments

All praises to the almighty and the kindest 'Allah Rabbul Alamin' who enabled me to pursue my higher studies, complete the research works, and submit the thesis for the degree of **Doctor of Philosophy in Agriculture** from The United Graduate School of Agricultural Sciences, Kagoshima University in association with Saga University, Japan.

It is a proud privilege to express the deepest gratitude, immense indebtedness, and sincere appreciation to my major advisory supervisor, **Prof. Dr. Nobuhiro Kotoda (Laboratory of Fruit Science, Department of Applied Biological Sciences, Faculty of Agriculture, Saga University)**, for his keen interest, scholastic guidance, valuable suggestions, constructive criticisms, continuous inspiration, and constant encouragement, through the entire period of research work and in the preparation of the manuscripts for dissertation and publications.

I express my heartfelt thanks and extreme gratitude to my vice advisory professors, **Dr. Masashi Yamamoto (Kagoshima University) and Dr. Satoshi Watanabe (Saga University),** for their precious advice, instruction, inspiration, and cordial help in completing the research work successfully. I am also grateful to my other two referee professors, **Dr. Kanji Ishimaru (Saga University)** and **Dr. Sho Nishida (Saga University)**, for their valuable comments and judgment of my doctoral research. I feel thankful to **Dr. H. Ichikawa** for providing the binary vectors, pSMAK251 and pSMAK193E, and **Dr. E.E. Hood** for providing Agrobacterium tumefaciens EHA101.

I am highly indebted to my laboratory members **Mr. Naoki Tokuhara**, **Takehiro Kubo,** and **Ryosuke Higo**, for their cordial assistance, critical reading, and constructive suggestion of the manuscript. I also express my warmest thanks to my past and present lab mates for their cordial support and cooperation.

I want to express my heartfelt thanks to my beloved wife, **Dr. Kohinoor Begum**, and my beloved son, **Ahmed Abdullah Hasan Waafi**, for their sacrifices, support, and unlimited patience during my whole period of doctoral studies. They always acted as my stress reliever and inspiration for all my working power. I am grateful to my beloved parents, **Prof. Mohammad Hossain Bhuiyan** and **Nilufar Sultana**, Sisters **Marufa Swati** and **Prof. Dr. Mashura Shammi**, and my nephews and niece (**Asef Jahan Bejoy**, **Tasmia Jahan Urboshi**, and **Areeb Hasan Shah Choudhury**) for their endless patient, continuous inspiration and mental supports during my doctoral studies, and feeling my stress until the successful completion of doctoral studies.

References

Abe, M., Y. Kobayashi, S. Yamamoto, Y. Daimon, A. Yamaguchi, Y. Ikeda, H. Ichinoki, M. Notaguchi, K. Goto and T. Araki. 2005. FD, a bZIP protein mediating signals from the floral pathway integrator FT at the shoot apex. Science 309:1052–1056.

Adrian, J., S. Farrona, J. J. Reimer, M. C. Albani, G. Coupland and F. Turck. 2010. *cis*-regulatory elements and chromatin state coordinately control temporal and spatial expression of *FLOWERING LOCUS T* in *Arabidopsis*. Plant Cell 22:1425–1440.

Ahn, J. H., D. Miller, V. J. Winter, M. J. Banfield, J. H. Lee, S. Y. Yoo, S. R. Henz, R. L. Brady and D. Weigel. 2006. A divergent external loop confers antagonistic activity on floral regulators FT and TFL1. EMBO J. 25:605–614.

Albrigo, L. G., L. L. Stelinski and L. W. Timmer. 2019. Citrus, 2nd edition. CABI, Boston, MA, 1–314 pp.

Ali, A., J. M. Pardo and D.J. Yun. 2020. Desensitization of ABA-Signaling: The swing from Activation to degradation. Frontiers in Plant Science 11:379.

An, H., C. Roussot, P. Suárez-López, L. Corbesier, C. Vincent, M. Piñeiro, S. Hepworth, A. Mouradov, S. Justin, C. Turnbull and G. Coupland. 2004. CONSTANS acts in the phloem to regulate a systemic signal that induces photoperiodic flowering of *Arabidopsis*. Development 131:3615–3626.

Andrés, F. and G. Coupland. 2012. The genetic basis of flowering responses to seasonal cues. Nat. Rev. Genet. 13:627–639.

Balasubramanian, S., S. Sureshkumar, J. Lempe and D. Weigel. 2006. Potent Induction of *Arabidopsis thaliana* flowering by elevated growth temperature. PLOS Genetics 2:0980–0989.

Bent, A. F. and S. J. Clough. 1998. *Agrobacterium* germ-line transformation: Transformation of *Arabidopsis* without tissue culture. *In* S.B. Gelvin, R.A. Schilperoort (eds.). Plant Molecular Biology Manual. Springer Netherlands, Dordrecht. 17–30.

Bernier, G. and C. Périlleux. 2005. A physiological overview of the genetics of flowering time control. Plant Biotechnology Journal 3:3–16.

Blázquez, M. A., J. H. Ahn and D. Weigel. 2003. A thermosensory pathway controlling flowering time in *Arabidopsis thaliana*. Nat. Genet. 33:168–171.

Bradley, D., R. Carpenter, L. Copsey, C. Vincent, S. Rothstein and E. Coen. 1996. Control of inflorescence architecture in *Antirrhinum*. Nature 379:791–797.

Bradley, D., O. Ratcliffe, C. Vincent, R. Carpenter and E. Coen. 1997. Inflorescence commitment and architecture in *Arabidopsis*. Science 275:80–83.

Breeden, L. and K. Nasmyth. 1985. Regulation of the yeast *HO* gene. Cold Spring Harb. Symp. Quant. Biol. 50:643–650.

Bürger, M. 2022. Escaping the drought: The OST1-VOZ1 module regulates early flowering in tomato. Plant Cell 34:1886–1887.

Castillejo, C. and S. Pelaz. 2008. The balance between CONSTANS and TEMPRANILLO activities determines *FT* expression to trigger flowering. Curr. Biol. 18:1338–1343.

Celesnik, H., G. S. Ali, F. M. Robison and A. S. N. Reddy. 2013. *Arabidopsis thaliana* VOZ (Vascular plant One-Zinc finger) transcription factors are required for proper regulation of flowering time. Biology Open 2:424–431.

Chong, L., R. Xu, P. Huang, P. Guo, M. Zhu, H. Du, X. Sun, L. Ku, J.-K. Zhu and Y. Zhu. 2022. The tomato OST1–VOZ1 module regulates drought-mediated flowering. Plant Cell 34:2001–2018.

Clough, S. J. and A. F. Bent. 1998. Floral dip: a simplified method for *Agrobacterium*-mediated transformation of *Arabidopsis thaliana*. Plant J. 16:735–743.

Conklin, P. L., S. R. Norris, G. L. Wheeler, E. H. Williams, N. Smirnoff and R. L. Last. 1999. Genetic evidence for the role of GDP-mannose in plant ascorbic acid (vitamin C) biosynthesis. Proc. Natl. Acad. Sci. U.S.A. 96:4198–4203.

Conklin, P. L., S. Gatzek, G. L. Wheeler, J. Dowdle, M. J. Raymond, S. Rolinski, M. Isupov, J. A. Littlechild and N. Smirnoff. 2006. *Arabidopsis thaliana VTC4* encodes L-Galactose-1-P phosphatase, a plant ascorbic acid biosynthetic enzyme. J. Biol. Chem. 281:15662–15670.

Corbesier, L., C. Vincent, S. Jang, F. Fornara, Q. Fan, I. Searle, A. Giakountis, S. Farrona, L. Gissot, C. Turnbull and G. Coupland. 2007. FT protein movement contributes to long-distance signaling in floral induction of *Arabidopsis*. Science 316:1030–1033.

Endo, T., T. Shimada, H. Fujii, Y. Kobayashi, T. Araki and M. Omura. 2005. Ectopic expression of an *FT* homolog from *Citrus* confers an early flowering phenotype on trifoliate orange (*Poncirus trifoliata* L. Raf.). Transgenic Res. 14:703–712.

FAO. 2021. Citrus fruit fresh and processed statistical bulletin 2020. Food and Agriculture Organization of the United Nations, Rome 48.

Ferrándiz, C., Q. Gu, R. Martienssen and M. F. Yanofsky. 2000. Redundant regulation of meristem identity and plant architecture by *FRUITFULL*, *APETALA1* and *CAULIFLOWER*. Development 127:725–734.

Finn, R. D., P. Coggill, R. Y. Eberhardt, S. R. Eddy, J. Mistry, A. L. Mitchell, S. C. Potter, M. Punta, M. Qureshi, A. Sangrador-Vegas, G. A. Salazar, J. Tate and A. Bateman. 2016. The Pfam protein families database: Towards a more sustainable future. Nucleic Acids Res. 44:D279–D285.

Gallie, D. R. and V. Walbot. 1992. Identification of the motifs within the tobacco mosaic virus 5′-leader responsible for enhancing translation. Nucleic Acids Res. 20:4631–4638.

Gaxiola, R. A., J. Li, S. Undurraga, L. M. Dang, G. J. Allen, S. L. Alper and G. R. Fink. 2001. Drought- and salt-tolerant plants result from overexpression of the AVP1 H^+-pump. Proc. Natl. Acad. Sci. U.S.A. 98:11444–11449.

Gietz, R. D. and R. A. Woods. 2002. Transformation of yeast by lithium acetate/single-stranded carrier DNA/polyethylene glycol method. Methods in enzymology. vol. 350. Elsevier. 87–96.

Hackett, W. P. 1985. Juvenility, maturation, and rejuvenation in woody plants. Horticultural reviews. vol. 7. Wiley-Blackwell. 109–154.

Hall, T. A. 1999. BioEdit: a user-friendly biological sequence alignment editor and analysis program for Windows 95/98/NT. Nucl. Acids Symp. Ser. 41:95–98.

Han, X., D. Wang and G. Song. 2021. Expression of a maize *SOC1* gene enhances soybean yield potential through modulating plant growth and flowering. Sci Rep 11:12758.

Harbison, C. T., D. B. Gordon, T. I. Lee, N. J. Rinaldi, K. D. Macisaac, T. W. Danford, N. M. Hannett, J. B. Tagne, D. B. Reynolds, J. Yoo, E. G. Jennings, J. Zeitlinger, D. K. Pokholok, M. Kellis, P. A. Rolfe, K. T. Takusagawa, E. S. Lander, D. K. Gifford, E. Fraenkel and R. A. Young. 2004. Transcriptional regulatory code of a eukaryotic genome. Nature 431:99–104.

Huang, B., P. Wang, M. Wen, S. Wu and J. Xu. 2021. Effects of different degrees of drought stress on plants and flowering physiology in Satsuma mandarin (*Citrus unshiu* ‘Yura’). Journal of Zhejiang University (Agriculture and Life Sciences) 47:557–565.

Igasaki, T., Y. Watanabe, M. Nishiguchi and N. Kotoda. 2008. The *FLOWERING LOCUS T/TERMINAL FLOWER 1* family in Lombardy poplar. Plant Cell Physiol. 49:291–300.

Iñigo, S., M. J. Alvarez, B. Strasser, A. Califano and P. D. Cerdán. 2012. PFT1, the MED25 subunit of the plant Mediator complex, promotes flowering through CONSTANS dependent and independent mechanisms in *Arabidopsis*. Plant J. 69:601–612.

Inoue H. 1989. Effects of soil drought and temperature on flower bud differentiation of Satsuma mandarin. Engei Gakkai zasshi 58:581–585.

Jaeger, K. E. and P. A. Wigge. 2007. FT protein acts as a long-range signal in *Arabidopsis*. Curr. Biol. 17:1050–1054.

Jeanmougin, F., J. D. Thompson, M. Gouy, D. G. Higgins and T. J. Gibson. 1998. Multiple sequence alignment with Clustal X. Trends Biochem. Sci. 23:403–405.

Jensen, M. K., T. Kjaersgaard, M. M. Nielsen, P. Galberg, K. Petersen, C. O'Shea and K. Skriver. 2010. The *Arabidopsis thaliana* NAC transcription factor family: structure–function relationships and determinants of ANAC019 stress signaling. Biochemical Journal 426:183–196.

Jeong, J. H., H. R. Song, J. H. Ko, Y. M. Jeong, Y. E. Kwon, J. H. Seol, R. M. Amasino, B. Noh and Y. S. Noh. 2009. Repression of *FLOWERING LOCUS T* chromatin by functionally redundant histone H3 lysine 4 demethylases in *Arabidopsis*. PLoS One 4:1–11.

Jiang, D., Y. Wang, Y. Wang and Y. He. 2008. Repression of *FLOWERING LOCUS C* and *FLOWERING LOCUS T* by the *Arabidopsis* Polycomb repressive complex 2 components. PloS One 3:e3404.

Jiang, Z., G. Xu, Y. Jing, W. Tang and R. Lin. 2016. Phytochrome B and REVEILLE1/2-mediated signaling controls seed dormancy and germination in *Arabidopsis*. Nat. Commun. 7:12377.

Jin, J., F. Tian, D. C. Yang, Y. Q. Meng, L. Kong, J. Luo and G. Gao. 2017. PlantTFDB 4.0: toward a central hub for transcription factors and regulatory interactions in plants. Nucleic Acids Res. 45:D1040–D1045.

Jumper, J., R. Evans, A. Pritzel, T. Green, M. Figurnov, O. Ronneberger, K. Tunyasuvunakool, R. Bates, A. Žídek, A. Potapenko, A. Bridgland, C. Meyer, S. A. A. Kohl, A. J. Ballard, A. Cowie, B. Romera-Paredes, S. Nikolov, R. Jain, J. Adler, T. Back, S. Petersen, D. Reiman, E. Clancy, M. Zielinski, M. Steinegger, M. Pacholska, T. Berghammer, S. Bodenstein, D. Silver, O. Vinyals, A. W. Senior, K. Kavukcuoglu, P. Kohli and D. Hassabis. 2021. Highly accurate protein structure prediction with AlphaFold. Nature 596:583–589.

Kardailsky, I., V. K. Shukla, J. H. Ahn, N. Dagenais, S. K. Christensen, J. T. Nguyen, J. Chory, M. J. Harrison and D. Weigel. 1999. Activation tagging of the floral inducer *FT*. Science 286:1962–1965.

Kobayashi, Y., H. Kaya, K. Goto, M. Iwabuchi and T. Araki. 1999. A pair of related genes with antagonistic roles in mediating flowering signals. Science 286:1960–1962.

Koguchi, M., K. Yamasaki, T. Hirano and M. H. Sato. 2017. Vascular plant one-zinc-finger protein 2 is localized both to the nucleus and stress granules under heat stress in *Arabidopsis*. Plant Signal. Behav. 12:e1295907-1-e1295907-7.

Komeda, Y. 2004. Genetic regulation of time to flower in *Arabidopsis thaliana*. Annu. Rev. Plant Biol. 55:521–535.

Koornneef, M., C. J. Hanhart and J. H. van der Veen. 1991. A genetic and physiological analysis of late flowering mutants in *Arabidopsis thaliana*. Molec. Gen. Genet. 229:57–66.

Kotake, T., S. Takada, K. Nakahigashi, M. Ohto and K. Goto. 2003. *Arabidopsis TERMINAL FLOWER* 2 gene encodes a heterochromatin protein 1 homolog and represses both *FLOWERING LOCUS T* to regulate flowering time and several floral homeotic genes. Plant Cell Physiol. 44:555–564.

Kotchoni, S. O., K. E. Larrimore, M. Mukherjee, C. F. Kempinski and C. Barth. 2009. Alterations in the endogenous ascorbic acid content affect flowering time in *Arabidopsis*. Plant Physiol. 149:803–815.

Kotoda, N. and M. Wada. 2005. *MdTFL1*, a *TFL1*-like gene of apple, retards the transition from the vegetative to reproductive phase in transgenic *Arabidopsis*. Plant Sci. 168:95–104.

Kotoda, N., H. Iwanami, S. Takahashi and K. Abe. 2006. Antisense expression of *MdTFL1*, a *TFL1*-like gene, reduces the juvenile phase in apple. J. Am. Soc. Hortic. Sci. 131:74–81.

Kotoda, N., S. Matsuo, I. Honda, K. Yano and T. Shimizu. 2016. Isolation and functional analysis of two gibberellin 20-oxidase genes from satsuma mandarin (*Citrus unshiu* Marc.). Hort. J. 85:128–140.

Kotoda, N., M. Wada, S. Komori, S. Kidou, K. Abe, T. Masuda and J. Soejima. 2000. Expression pattern of homologues of floral meristem identity genes *LFY* and *AP1* during flower development in apple. J. Am. Soc. Hortic. Sci. 125:398–403.

Kotoda, N., H. Hayashi, M. Suzuki, M. Igarashi, Y. Hatsuyama, S. Kidou, T. Igasaki, M. Nishiguchi, K. Yano, T. Shimizu, S. Takahashi, H. Iwanami, S. Moriya and K. Abe. 2010.

Molecular characterization of *FLOWERING LOCUS T*-like genes of apple (*Malus* × *domestica* Borkh.). Plant Cell Physiol. 51:561–575.

Krajewski, A. J. and E. Rabe. 1995. Citrus flowering: a critical evaluation. J. Hortic. Sci. 70:357–374.

Kumar, S., P. Choudhary, M. Gupta and U. Nath. 2018. VASCULAR PLANT ONE-ZINC FINGER1 (VOZ1) and VOZ2 Interact with CONSTANS and promote photoperiodic flowering transition. Plant Physiol. 176:2917–2930.

Kumar, S. V., D. Lucyshyn, K. E. Jaeger, E. Alós, E. Alvey, N. P. Harberd and P. A. Wigge. 2012. Transcription factor PIF4 controls the thermosensory activation of flowering. Nature 484:242–245.

Laing, W. A., M. A. Wright, J. Cooney and S. M. Bulley. 2007. The missing step of the l-galactose pathway of ascorbate biosynthesis in plants, an l-galactose guanyltransferase, increases leaf ascorbate content. Proc. Natl. Acad. Sci. U.S.A. 104:9534–9539.

Laing, W. A., S. Bulley, M. Wright, J. Cooney, D. Jensen, D. Barraclough and E. MacRae. 2004. A highly specific L-galactose-1-phosphate phosphatase on the path to ascorbate biosynthesis. Proc. Natl. Acad. Sci. U.S.A. 101:16976–16981.

Latchman, D. S. 1993. Transcription factors: an overview. Int. J. Exp. Pathol. 74:417–422.

Lee, J. H., H.-S. Ryu, K. S. Chung, D. Posé, S. Kim, M. Schmid and J. H. Ahn. 2013. Regulation of temperature-responsive flowering by MADS-Box transcription factor repressors. Science 342:628–632.

Lee, R., S. Baldwin, F. Kenel, J. McCallum and R. Macknight. 2013. *FLOWERING LOCUS T* genes control onion bulb formation and flowering. Nat. Commun. 4:1–9.

Lee, T. I. and R. A. Young. 2000. Transcription of eukaryotic protein-coding genes. Annu. Rev. Genet. 34:77–137..

Levine, M. and R. Tjian. 2003. Transcription regulation and animal diversity. Nature 424:147–151.

Levy, Y. Y. and C. Dean. 1998. The transition to flowering. Plant Cell 10:1973–1989.

Li, B., J.C. Zheng, T. T. Wang, D. H. Min, W. L. Wei, J. Chen, Y. B. Zhou, M. Chen, Z. S. Xu and Y. Z. Ma. 2020. Expression analyses of soybean VOZ transcription factors and the role of *GmVOZ1G* in drought and salt stress tolerance. Int. J. Mol. Sci. 21:1–17.

Li, D., C. Liu, L. Shen, Y. Wu, H. Chen, M. Robertson, C. A. Helliwell, T. Ito, E. Meyerowitz and H. Yu. 2008. A repressor complex governs the integration of flowering signals in *Arabidopsis*. Dev. Cell 15:110–120.

Li, J., H. Yang, W. Ann Peer, G. Richter, J. Blakeslee, A. Bandyopadhyay, B. Titapiwantakun, S. Undurraga, M. Khodakovskaya, E. L. Richards, B. Krizek, A. S. Murphy, S. Gilroy and R. Gaxiola. 2005. *Arabidopsis* H+-PPase AVP1 regulates auxin-mediated organ development. Science 310:121–125.

Lifschitz, E., T. Eviatar, A. Rozman, A. Shalit, A. Goldshmidt, Z. Amsellem, J. P. Alvarez and Y. Eshed. 2006. The tomato *FT* ortholog triggers systemic signals that regulate growth and flowering and substitute for diverse environmental stimuli. Proc. Natl. Acad. Sci. U.S.A. 103:6398–6403.

Lifschitz, E. and Y. Eshed. 2006. Universal florigenic signals triggered by FT homologues regulate growth and flowering cycles in perennial day-neutral tomato. Journal of Experimental Botany 57:3405–3414

Lin, M. K., H. Belanger, Y. J. Lee, E. Varkonyi-Gasic, K. I. Taoka, E. Miura, B. Xoconostle-Cázares, K. Gendler, R. A. Jorgensen, B. Phinney, T. J. Lough and W. J. Lucas. 2007. FLOWERING LOCUS T protein may act as the long-distance florigenic signal in the cucurbits. Plant Cell 19:1488–1506.

Linster, C. L., T. A. Gomez, K. C. Christensen, L. N. Adler, B. D. Young, C. Brenner and S. G. Clarke. 2007. *Arabidopsis VTC2* encodes a GDP-L-galactose phosphorylase, the last unknown enzyme in the smirnoff-wheeler pathway to ascorbic acid in plants. J. Biol. Chem. 282:18879–18885.

Liu, H., X. Yu, K. Li, J. Klejnot, H. Yang, D. Lisiero and C. Lin. 2008. Photoexcited CRY2 interacts with CIB1 to regulate transcription and floral initiation in *Arabidopsis*. Science 322:1535–1539.

Liu, L., Y. Zhu, L. Shen and H. Yu. 2013. Emerging insights into florigen transport. Curr. Opin. Plant Biol. 16:607–613.

Liu, L., C. Liu, X. Hou, W. Xi, L. Shen, Z. Tao, Y. Wang and H. Yu. 2012. FTIP1 is an essential regulator required for florigen transport. PLoS Biol. 10:e1001313.

Long, M., C. Rosenberg and W. Gilbert. 1995. Intron phase correlations and the evolution of the intron/exon structure of genes. Proc. Natl. Acad. Sci. USA 92:12495–12499.

Lu, C. H., Y. F. Lin, J. J. Lin and C. S. Yu. 2012. Prediction of metal ion–binding sites in proteins using the fragment transformation method. PLOS ONE 7:1–12.

Luo, D., L. Qu, M. Zhong, X. Li, H. Wang, J. Miao, X. Liu and X. Zhao. 2020. Vascular plant one-zinc finger 1 (VOZ1) and VOZ2 negatively regulate phytochrome B-mediated seed germination in *Arabidopsis*. Biosci. Biotechnol. Biochem. 84:1384–1393.

Lutz, U., T. Nussbaumer, M. Spannagl, J. Diener, K. F. Mayer and C. Schwechheimer. 2017. Natural haplotypes of *FLM* non-coding sequences fine-tune flowering time in ambient spring temperatures in *Arabidopsis*. ELife 6:e22114.

Mandel, M. A. and M. F. Yanofsky. 1995. A gene triggering flower formation in *Arabidopsis*. Nature 377:522–524.

Mathieu, J., N. Warthmann, F. Küttner and M. Schmid. 2007. Export of FT protein from phloem companion cells Is sufficient for floral induction in *Arabidopsis*. Curr. Biol. 17:1055–1060.

Mathieu, J., L. J. Yant, F. Mürdter, F. Küttner and M. Schmid. 2009. Repression of flowering by the miR172 target SMZ. PLoS Biol. 7:e1000148.

Michaels, S. D. and R. M. Amasino. 1999. *FLOWERING LOCUS C* encodes a novel MADS domain protein that acts as a repressor of flowering. Plant Cell 11:949–956.

Mimida, N., S. I. Kidou, H. Iwanami, S. Moriya, K. Abe, C. Voogd, E. Varkonyi-Gasic and N. Kotoda. 2011. Apple FLOWERING LOCUS T proteins interact with transcription factors implicated in cell growth and organ development. Tree Physiol. 31:555–566.

Mimida, N., N. Kotoda, T. Ueda, M. Igarashi, Y. Hatsuyama, H. Iwanami, S. Moriya and K. Abe. 2009. Four *TFL1*/*CEN*-Like genes on distinct linkage groups show different expression patterns to regulate vegetative and reproductive development in apple (*Malus×domestica* Borkh.). Plant Cell Physiol. 50:394–412.

Mitchum, M. G., S. Yamaguchi, A. Hanada, A. Kuwahara, Y. Yoshioka, T. Kato, S. Tabata, Y. Kamiya and T. Sun. 2006. Distinct and overlapping roles of two gibberellin 3-oxidases in *Arabidopsis* development. Plant J. 45:804–818.

Mitsuda, N., T. Hisabori, K. Takeyasu and M. H. Sato. 2004. VOZ; isolation and characterization of novel vascular plant transcription factors with a one-zinc finger from *Arabidopsis thaliana*. Plant Cell Physiol. 45:845–854.

Moss, G. I. 1971. Effect of fruit on flowering in relation to biennial bearing in sweet orange *(Citrus sinensis)*. J. Hortic. Sci. 46:177–184.

Mouradov, A., F. Cremer and G. Coupland. 2002. Control of flowering time: interacting pathways as a basis for diversity. Plant Cell 14:S111–S130.

Mulat, M. W. and V. B. Sinha. 2021. VOZS identification from TEF [Eragrostis tef (Zucc.) Trotter] using in silico tools decipher their involvement in abiotic stress. Materials Today: Proceedings 49:S2214785321004363.

Nakai, Y., S. Fujiwara, Y. Kubo and M. H. Sato. 2013a. Overexpression of *VOZ2* confers biotic stress tolerance but decreases abiotic stress resistance in *Arabidopsis*. Plant Signal. Behav. 8:e23358.

Nakai, Y., Y. Nakahira, H. Sumida, K. Takebayashi, Y. Nagasawa, K. Yamasaki, M. Akiyama, M. Ohme-Takagi, S. Fujiwara, T. Shiina, N. Mitsuda, E. Fukusaki, Y. Kubo and M. H. Sato. 2013b. Vascular plant one-zinc-finger protein 1/2 transcription factors regulate abiotic and biotic stress responses in *Arabidopsis*. Plant J. 73:761–775.

Nakamura, S., F. Abe, H. Kawahigashi, K. Nakazono, A. Tagiri, T. Matsumoto, S. Utsugi, T. Ogawa, H. Handa, H. Ishida, M. Mori, K. Kawaura, Y. Ogihara and H. Miura. 2011. A wheat homolog of MOTHER OF FT AND TFL1 acts in the regulation of germination. Plant Cell 23:3215–3229.

Navarro, C., J. A. Abelenda, E. Cruz-Oró, C. A. Cuéllar, S. Tamaki, J. Silva, K. Shimamoto and S. Prat. 2011. Control of flowering and storage organ formation in potato by FLOWERING LOCUS T. Nature 478:119–122.

Nishikawa, F., T. Endo, T. Shimada, H. Fujii, T. Shimizu, M. Omura and Y. Ikoma. 2007. Increased *CiFT* abundance in the stem correlates with floral induction by low temperature in Satsuma mandarin (*Citrus unshiu* Marc.). J. Exp. Bot. 58:3915–3927.

Niwa, M., Y. Daimon, K. Kurotani, A. Higo, J. L. Pruneda-Paz, G. Breton, N. Mitsuda, S. A. Kay, M. Ohme-Takagi, M. Endo and T. Araki. 2013. BRANCHED1 Interacts with FLOWERING LOCUS T to repress the floral transition of the axillary Meristems in *Arabidopsis*. Plant Cell 25:1228–1242.

Notaguchi, M., M. Abe, T. Kimura, Y. Daimon, T. Kobayashi, A. Yamaguchi, Y. Tomita, K. Dohi, M. Mori and T. Araki. 2008. Long-distance, graft-transmissible action of *Arabidopsis* FLOWERING LOCUS T protein to promote flowering. Plant Cell Physiol. 49:1645–1658.

Ohshima, S., M. Murata, W. Sakamoto, Y. Ogura and F. Motoyoshi. 1997. Cloning and molecular analysis of the *Arabidopsis* gene *Terminal Flower 1*. Mol. Gen. Genet. 254:186–194.

Pazhouhandeh, M., J. Molinier, A. Berr and P. Genschik. 2011. MSI4/FVE interacts with CUL4–DDB1 and a PRC2-like complex to control epigenetic regulation of flowering time in *Arabidopsis*. Proc. Natl. Acad. Sci. U.S.A. 108:3430–3435.

Pérez, L. M. and J. Garrido. 1985. Ultrastructure of cells from Citrus sinensis flavedo. Arch. Biol. Med. Exp. 18:41–55.

Pettersen, E. F., T. D. Goddard, C. C. Huang, E. C. Meng, G. S. Couch, T. I. Croll, J. H. Morris and T. E. Ferrin. 2021. UCSF ChimeraX: Structure visualization for researchers, educators, and developers. Protein Sci. 30:70–82.

Pin, P. A. and O. Nilsson. 2012. The multifaceted roles of FLOWERING LOCUS T in plant development. Plant Cell Environ. 35:1742–1755.

Posé, D., L. Verhage, F. Ott, L. Yant, J. Mathieu, G. C. Angenent, R. G. H. Immink and M. Schmid. 2013. Temperature-dependent regulation of flowering by antagonistic FLM variants. Nature 503:414–417.

Prasad, K. V. S. K., D. Xing and A. S. N. Reddy. 2018. Vascular Plant One-Zinc-Finger (VOZ) transcription factors are positive regulators of salt tolerance in *Arabidopsis*. Int. J. Mol. Sci. 19:3731.

Putterill, J. and E. Varkonyi-Gasic. 2016. FT and florigen long-distance flowering control in plants. Curr. Opin. Plant Biol. 33:77–82.

Quecini, V., G. A. M. Torres, V. E. de Rosa Jr, M. A. Gimenes, J. B. de M. Machado, A. V. de O. Figueira, V. Benedito, M. L. P. N. Targon and M. Cristofani-Yaly. 2007. *In silico* analysis of phytohormone metabolism and communication pathways in citrus transcriptome. Genet. Mol. Biol. 30:713–733.

Ratcliffe, O. J., D. J. Bradley and E. S. Coen. 1999. Separation of shoot and floral identity in *Arabidopsis*. Development 126:1109–1120.

Rehman, S. U., G. Qanmber, M. H. N. Tahir, A. Irshad, S. Fiaz, F. Ahmad, Z. Ali, M. Sajjad, M. Shees, M. Usman and Z. Geng. 2021. Characterization of Vascular plant One-Zinc finger (VOZ) in soybean (*Glycine max* and *Glycine soja*) and their expression analyses under drought condition. PLOS ONE 16:1–13.

Reece-Hoyes, J. S., B. Deplancke, J. Shingles, C. A. Grove, I. A. Hope and A. J. Walhout. 2005. A compendium of Caenorhabditis elegans regulatory transcription factors: a resource for mapping transcription regulatory networks. Genome Biol. 6:R110.

Rinne, P. L. H., A. Welling, J. Vahala, L. Ripel, R. Ruonala, J. Kangasjärvi and C. van der Schoot. 2011. Chilling of dormant buds hyperinduces *FLOWERING LOCUS T* and

recruits GA-Inducible 1,3-β-Glucanases to reopen signal conduits and release dormancy in *Populus*. Plant Cell 23:130–146.

RStudio Team. 2020. RStudio: integrated development for R. RStudio, PBC. Boston, MA.

Ryu, J. Y., H. J. Lee, P. J. Seo, J. H. Jung, J. H. Ahn and C. M. Park. 2014. The *Arabidopsis* floral repressor BFT delays flowering by competing with FT for FD binding under high salinity. Mol. Plant 7:377–387.

Samach, A., H. Onouchi, S. E. Gold, G. S. Ditta, Z. Schwarz-Sommer, M. F. Yanofsky and G. Coupland. 2000. Distinct Roles of CONSTANS Target Genes in Reproductive Development of *Arabidopsis*. Science 288:1613–1616.

Sawa, M. and S. A. Kay. 2011. GIGANTEA directly activates *Flowering Locus T* in *Arabidopsis thaliana*. Proc. Natl. Acad. Sci. U.S.A. 108:11698–11703.

Selote, D., A. Matthiadis, J. W. Gillikin, M. H. Sato and T. A. Long. 2018. The E3 ligase BRUTUS facilitates degradation of VOZ1/2 transcription factors. Plant Cell Environ. 41:2463–2474.

Seo, E., J. Yu, K. H. Ryu, M. M. Lee and I. Lee. 2011. *WEREWOLF*, a regulator of root hair pattern formation, controls flowering time through the regulation of *FT* mRNA stability. Plant Physiol. 156:1867–1877.

Shalit, A., A. Rozman, A. Goldshmidt, J. P. Alvarez, J. L. Bowman, Y. Eshed and E. Lifschitz. 2009. The flowering hormone florigen functions as a general systemic regulator of growth and termination. Proc. Natl. Acad. Sci. U.S.A. 106:8392–8397.

Shannon, S. and D. R. Meeks-Wagner. 1993. Genetic interactions that regulate inflorescence development in *Arabidopsis*. Plant Cell 5:639–655.

Shi, P., R. Jiang, B. Li, D. Wang, D. Fang, M. Yin, M. Yin and M. Gu. 2022. Genome-wide analysis and expression profiles of the VOZ gene family in quinoa (*Chenopodium quinoa*). Genes 13:1695.

Shiratake, K., Y. Kanayama, M. Maeshima and S. Yamaki. 1997. Changes in H^+-pumps and a tonoplast intrinsic protein of vacuolar membranes during the development of pear fruit. Plant Cell Physiol. 38:1039–1045.

Simpson, G. G. and C. Dean. 2002. *Arabidopsis*, the rosetta stone of flowering time? Science 296:285–289.

Singh, K. B. 1998. Transcriptional regulation in plants: The importance of combinatorial control. Plant Physiol. 118:1111–1120.

Smirnoff, N., J. Dowdle and T. Ishikawa. 2007. The role of VTC2 in vitamin C biosynthesis in *Arabidopsis* thaliana. Comp. Biochem. Physiol. 4:S250.

Song, C., J. Lee, T. Kim, J. C. Hong and C. O. Lim. 2018. VOZ1, a transcriptional repressor of DREB2C, mediates heat stress responses in *Arabidopsis*. Planta 247:1439–1448.

Sureshkumar, S., C. Dent, A. Seleznev, C. Tasset and S. Balasubramanian. 2016. Nonsense-mediated mRNA decay modulates FLM-dependent thermosensory flowering response in *Arabidopsis*. Nature Plants 2:1–7.

Schwarzenbacher, R. E., G. Wardell, J. Stassen, E. Guest, P. Zhang, E. Luna and J. Ton. 2020. The IBI1 Receptor of β-Aminobutyric Acid Interacts with VOZ Transcription Factors to Regulate Abscisic Acid Signaling and Callose-Associated Defense. Molecular Plant 13:1455–1469.

Takada, S. and K. Goto. 2003. TERMINAL FLOWER2, an *Arabidopsis* Homolog of HETEROCHROMATIN PROTEIN1, Counteracts the Activation of *FLOWERING*

LOCUS T by CONSTANS in the Vascular Tissues of Leaves to Regulate Flowering Time. Plant Cell 15:2856–2865.

Tamaki, S., S. Matsuo, H. L. Wong, S. Yokoi and K. Shimamoto. 2007. Hd3a protein is a mobile flowering signal in rice. Science 316:1033–1036.

Taoka, K., I. Ohki, H. Tsuji, K. Furuita, K. Hayashi, T. Yanase, M. Yamaguchi, C. Nakashima, Y. A. Purwestri, S. Tamaki, Y. Ogaki, C. Shimada, A. Nakagawa, C. Kojima and K. Shimamoto. 2011. 14-3-3 proteins act as intracellular receptors for rice Hd3a florigen. Nature 476:332–335.

Tian, F., D. C. Yang, Y. Q. Meng, J. Jin and G. Gao. 2020. PlantRegMap: charting functional regulatory maps in plants. Nucleic Acids Res. 48:D1104–D1113.

Tiwari, S. B., Y. Shen, H.-C. Chang, Y. Hou, A. Harris, S. F. Ma, M. McPartland, G. J. Hymus, L. Adam and C. Marion. 2010. The flowering time regulator CONSTANS is recruited to the *FLOWERING LOCUS T* promoter via a unique *cis*-element. New Phytol. 187:57–66.

Trakul, N. and M. R. Rosner. 2005. Modulation of the MAP kinase signaling cascade by Raf kinase inhibitory protein. Cell Res. 15:19–23.

USDA. 2022. Citrus: World Markets and Trade. Foreign Agricultural Service/USDA.

Vidal, M. 1997. The reverse two-hybrid system. The yeast two-hybrid system. Oxford University Press. 109–147.

Wang, J., R. Wang, H. Fang, C. Zhang, F. Zhang, Z. Hao, X. You, X. Shi, C. H. Park, K. Hua, F. He, M. Bellizzi, K. T. Xuan Vo, J.-S. Jeon, Y. Ning and G.-L. Wang. 2021. Two VOZ transcription factors link an E3 ligase and an NLR immune receptor to modulate immunity in rice. Mol. Plant 14:253–266.

Wang, R., P. Xu, Z. Chen, X. Zhou and T. Wang. 2019. Complexation of rice proteins and whey protein isolates by structural interactions to prepare soluble protein composites. LWT 101:207–213.

Weigel, D. and O. Nilsson. 1995. A developmental switch sufficient for flower initiation in diverse plants. Nature 377:495–500.

Weigel, D., J. Alvarez, D. R. Smyth, M. F. Yanofsky and E. M. Meyerowitz. 1992. *LEAFY* controls floral meristem identity in *Arabidopsis*. Cell 69:843–859.

Wigge, P. A. 2011. FT, a mobile developmental signal in plants. Curr. Biol. 21:R374–R378.

Wigge, P. A., M. C. Kim, K. E. Jaeger, W. Busch, M. Schmid, J. U. Lohmann and D. Weigel. 2005. Integration of spatial and temporal information during floral induction in *Arabidopsis*. Science 309:1056–1059.

Wilkie, J. D., M. Sedgley and T. Olesen. 2008. Regulation of floral initiation in horticultural trees. J. Exp. Bot. 59:3215–3228.

Wolfe, S. A., L. Nekludova and C. O. Pabo. 1999. DNA recognition by (Cys2His2) zinc finger proteins. Annu. Rev. Biophys. Biomol. Struct. 29:183.

Xu, G., C. Guo, H. Shan and H. Kong. 2012. Divergence of duplicate genes in exon–intron structure. Proc. Natl. Acad. Sci. U.S.A. 109:1187–1192.

Yabuta, Y., T. Mieda, M. Rapolu, A. Nakamura, T. Motoki, T. Maruta, K. Yoshimura, T. Ishikawa and S. Shigeoka. 2007. Light regulation of ascorbate biosynthesis is dependent on the photosynthetic electron transport chain but independent of sugars in *Arabidopsis*. J. Exp. Bot. 58:2661–2671.

Yang, C. Q., X. Fang, X. M. Wu, Y. B. Mao, L. J. Wang and X. Y. Chen. 2012. Transcriptional regulation of plant secondary metabolism. J. Integr. Plant Biol. 54:703–712.

Yasui, Y. and T. Kohchi. 2014. *VASCULAR PLANT ONE-ZINC FINGER1* and *VOZ2* repress the *FLOWERING LOCUS C* clade members to control flowering time in *Arabidopsis*. Biosci. Biotechnol. Biochem. 78:1850–1855.

Yasui, Y., K. Mukougawa, M. Uemoto, A. Yokofuji, R. Suzuri, A. Nishitani and T. Kohchi. 2012. The Phytochrome-Interacting VASCULAR PLANT ONE–ZINC FINGER1 and VOZ2 Redundantly Regulate Flowering in *Arabidopsis*. Plant Cell 24:3248–3263.

Yoo, S. J., K. S. Chung, S. H. Jung, S. Y. Yoo, J. S. Lee and J. H. Ahn. 2010. *BROTHER OF FT AND TFL1* (*BFT*) has *TFL1*-like activity and functions redundantly with *TFL1* in inflorescence meristem development in *Arabidopsis*. Plant J. 63:241–253.

Yoo, S. Y., I. Kardailsky, J. S. Lee, D. Weigel and J. H. Ahn. 2004. Acceleration of flowering by overexpression of *MFT* (*MOTHER OF FT AND TFL1*). Mol. Cells 17:95–101.

Yuan, L. and S. E. Perry, editors. 2011. Plant Transcription Factors. Humana Press, Totowa, NJ, pp. v-vi

Zeevaart, J. A. D. 2008. Leaf-produced floral signals. Curr. Opin. Plant Biol. 11:541–547.

Zeevaart, J. A. D. 1976. Physiology of flower formation. Ann. Rev. Plant. Physiol. 27:321–348.

Zhu, Y., L. Liu, L. Shen and H. Yu. 2016. NaKR1 regulates long-distance movement of FLOWERING LOCUS T in *Arabidopsis*. Nat. Plants 2:1–10.